THESIS

DIRECT MEASUREMENT OF LNAPL FLOW IN POROUS MEDIA USING TRACER DILUTION TECHNIQUES

Submitted by

Geoffrey Ryan Taylor

Department of Civil Engineering

In partial fulfillment of the requirements

For the Degree of Master of Science

Colorado State University

Fort Collins, Colorado

Spring 2004

Colorado State University

February 20, 2004

WE HEREBY RECOMMEND THAT THE THESIS PREPARED UNDER OUR SUPERVISION BY GEOFFREY RYAN TAYLOR ENTITLED "DIRECT MEASUREMENT OF LNAPL FLOW IN POROUS MEDIA USING TRACER DILUTION TECHNIQUES" BE ACCEPTED AS FULFILLING, IN PART, REQUIREMENTS FOR THE DEGREE OF MASTER OF SCIENCE.

Committee on Graduate Work

Committee member: Dr. David McWhorter

Committee member: Dr. James Warner

Advisor: Dr. Thomas Sale

Department Head: Dr. Sandra Woods

ABSTRACT OF THESIS

DIRECT MEASUREMENT OF LNAPL FLOW IN POROUS MEDIA USING TRACER DILUTION TECHNIQUES

Petroleum liquids, commonly referred to as LNAPL's, have become a basic building block of modern society. Used as fuels, lubricants, solvents and chemical feed stocks, petroleum liquids have brought many conveniences to our lives. However, a small fraction of these liquids have been inadvertently released into the subsurface forming contiguous bodies of separate phase liquids. Resolving how to manage these releases hinges largely on the rate at which these bodies are moving. To that end, a number of techniques have been developed in an effort to measure the migration, or flow rate, of LNAPL in the subsurface. Many of the current methods require challenging and costly indirect measurements to estimate this migration.

The purpose of this thesis is to explore a promising new method that directly measures the flow rate of LNAPL's, a method that builds on the tracer dilution technique used to measure the flow of groundwater. Traditional tracer dilution techniques measures the dilution of a tracer, placed into a well, to determine the flow rate of water through the well. The flow rate through the well is then used to calculate the flow rate of groundwater. The same theory applies to LNAPL's flowing through a well.

Determining the potential of the tracer dilution technique to measure LNAPL flow through a well requires investigating the mathematics governing the tracer dilution technique. A first order dilution equation was adapted for LNAPL. A method to analyze

the results in a dimensionless format was also developed because it provides a technique to determine when the data conforms to the assumptions of the dilution equation. The mathematics necessary to convert the flow rate of LNAPL through a well into common measures is also derived.

Laboratory studies were conducted to verify the mathematics and to determine the applicability of the tracer dilution technique to measure LNAPL flow. At first, small scale experiments were used to visualize the dilution process and develop the technology necessary to conduct tracer dilution tests in LNAPL. A fluorescent dye, BSL 715, was selected as a tracer. A spectrometer and computer were used to measure and log the fluorescent intensity, which is a measure of the tracer concentration. A device to mix the tracer in the well without causing adverse dilution was also developed.

A large tank study explored the tracer dilution technique using a typical range of LNAPL thicknesses and flow rates. The flow rates varied from 7.2 $m^3/m/yr$ to 0.035 $m^3/m/yr$ and the LNAPL thicknesses varied from 9cm to 24cm. The results of the large tank study demonstrated that the tracer dilution technique is an accurate and reliable method to measure the migration of petroleum liquids in the subsurface. The measured error tends to increase at lower flow rates but is insensitive to the LNAPL thickness.

The results of the large tank study led to a field test at the former ChevronTexaco Refinery in Casper, WY. The tracer dilution method was deployed in two locations. The first location was near an active recovery well where the flow rate was expected to be high. The second test was conducted in a quiescent area where the flow rate was low. The first test, near the recovery well, measured a flow rate of 0.1 $m^3/m/yr$ to 0.3 $m^3/m/yr$. The second test, in a quiescent area, indicated a flow rate of less then 0.005 $m^3/m/yr$. In

addition, opportunities for improving sensitivity and increasing the usefulness of the method were discovered. In all, the experiments have shown the tracer dilution technique to be an effective method to directly measure the *in situ* migration of petroleum liquids in the subsurface.

Geoffrey Ryan Taylor
Civil Engineering Department
Colorado State University
Fort Collins, CO 80523
Spring 2004

0.2 Acknowledgments

A number of people extended help and technical support in the preparation of this thesis. They include:

- Dr. Sale, for serving the advisor for this work and contributing his guidance, advice and expertise from the initial experiments to the final draft of this thesis.
- Dr. McWhorter and Dr. Warner for serving on the advisory committee.
- Dr. Fontane for his advice on interpreting the results and helping to develop the error analysis algorithm.
- Dr. A. T. Corey for his continual interest in the project and providing a number of useful insights.
- Dr. Vivienne Perkins for editing this document
- Shaun Harshman and Stephanie Whitfield of Tri Hydro for their help leading up to and during the field study.
- G.D. Beckett, of Aqui-Ver, Inc. for his interest in the project and assistance during the field study.
- Pamela and Geoffrey Taylor, this author's parents, for their encouragement and support.

Funding for this research was provided by:

- Mark Lyverse, of ChevronTexaco
- University Solvents-in-Groundwater Research Consortium
- National Science Foundation and A.T. Corey through personal scholarships given to this author and greatly appreciated.

Table of Contents

List of Figures

1.0 Introduction

During the past century large volumes of non-aqueous phase liquids (NAPL) including fuels, lubricants, solvents, and chemical feed stocks have been inadvertently released into the environment. A common method of addressing these releases is direct pumping of the separate phase liquids. This is commonly referred to as free product recovery. Due to immobile residual NAPL, limited sweep efficiencies, limited target efficiencies, and an asymptotic decay of NAPL recovery rates, only a small fraction of the total NAPL is typically recovered. The primary benefit of free product recovery is a reduced potential for the NAPL to migrate. The key issue in determining when to initiate, and when to end recovery operations, is the rate at which the NAPL's are moving. To determine the rate of LNAPL migration a number of techniques have been developed. Unfortunately, these techniques require parameters which can be hard to estimate. This thesis explores a promising new method, involving tracer dilution techniques. Potential advantages include: direct measurement of the parameter of interest, and simplicity.

In more detail, the objectives are to:

- Resolve the applicability of tracer dilution techniques for measurement of NAPL flow.
- Develop the technology necessary to apply tracer dilution techniques
- Test the methods and technology at a laboratory scale and in the field.

Content and organization of this thesis is as follows: Section 2 provides the reader with the necessary background information about NAPL releases, current technologies, and the development of tracer dilution tests. Section 3, presents the reader with an

understanding of the mathematics of dilution, and lays out the assumptions employed in deriving the governing equation. Section 4 presents the results from the laboratory studies and discusses the importance of the findings. Section 5 describes the two field tests conducted in Casper, WY. Section 6 provides an overview of the work completed for this thesis and suggests areas of future work.

2.0 Theoretical Foundation

The purpose of this section is to provide the reader with relevant background information. Specifically, this section includes a review of multiphase flow in porous media. Metrics for LNAPL flow, current methods for measuring LNAPL flow, and a summary of past work with the tracer dilution technique.

2.1 Non-Aqueous Phase Liquids

The phrase 'non-aqueous liquids' is a convenient label to describe a wide variety of liquid hydrocarbons. Two common classifications of NAPL are light non-aqueous liquids (LNAPL) and dense non-aqueous liquids (DNAPL). The light and dense prefixes denote the fluid density compared to that of water. LNAPL will float in water, while DNAPL will sink. The term 'non-aqueous' is used to indicate that these fluids are immiscible (will not mix) with water. The focus of this thesis is LNAPL. However, many of the same principles can be applied to DNAPL. Examples of LNAPL include gasoline, diesel fuel, and crude oil.

As a first step, it is important to understand the complexities of what happens when LNAPL is released into the subsurface. Following Sale, 2003, Figure 1 depicts a typical scenario where LNAPL has been released into the ground forming a contiguous body of LNAPL on a sloping water table.

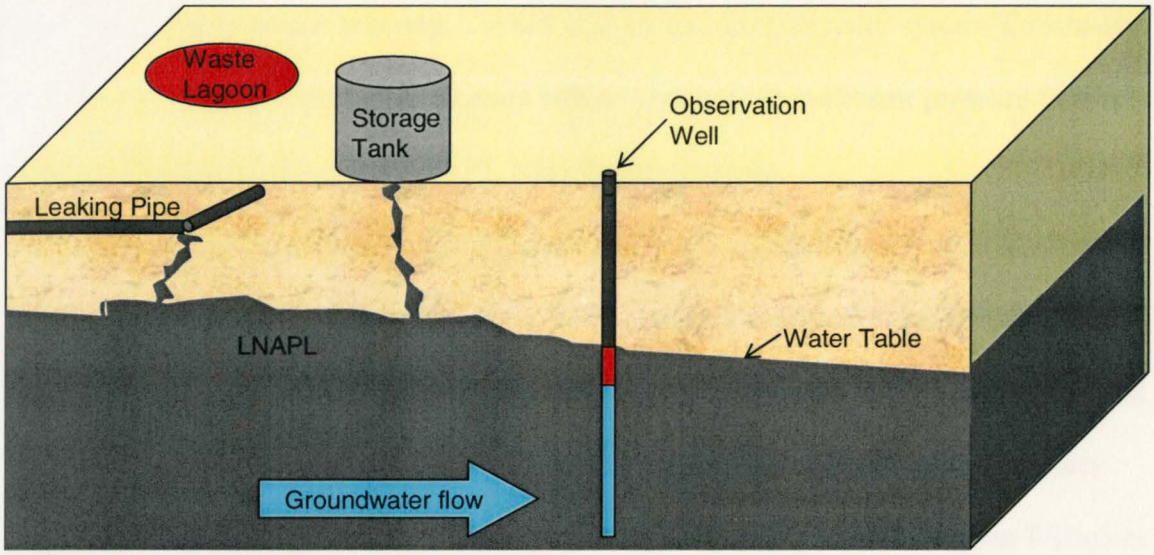

Figure 1: Conceptual Model of an LNAPL Release

The sediment below grade, the formation, is a porous media consisting of solids and interconnected voids. Below the water table, the void spaces are filled with water. Above the water table, the voids are filled with both air and water. Wherever air and water exist in the same pore space, the water is preferentially attracted to the soil grain and forms a continuous film around the granule; this is known as the wetting fluid. The air is then called the non-wetting fluid and exists in the void space surrounded by water.

When a LNAPL is released, it migrates downward, under the influence of gravity, as an intermediate wetting fluid and displaces some of the air in the pore space. Eventually, if a sufficient quantity of LNAPL is released, the LNAPL will continue downward and encounter the water table. Since there is no substantial volume of air below the water table, the LNAPL must displace water. Because water is held in the pore space via capillary forces, the LNAPL must have a sufficient pressure to displace the water from the pore; this is known as the bubbling or displacement pressure (Brook and Corey, 1966). The pressure difference between the LNAPL and water (capillary pressure) increases with the overlying height of LNAPL. When the capillary pressure

exceeds the displacement pressure, LNAPL moves into adjacent pore spaces. Eventually a continuous LNAPL body of fixed mass will no longer have sufficient pressure to enter additional pore spaces and the LNAPL body becomes stable.

Subsequent depletion of a continuous LNAPL body via weathering, water table fluctuations, or pumping will reduce the LNAPL saturation. Ultimately, the LNAPL becomes discontinuous; this is commonly referred to as residual LNAPL. At this residual saturation, the relative permeability to LNAPL is zero and the LNAPL globules under typical hydraulic gradients are no longer mobile as a separate phase. Following Wilson et al. (1990), Figure 2 illustrates where continuous and residual LNAPL reside in an idealized pore network.

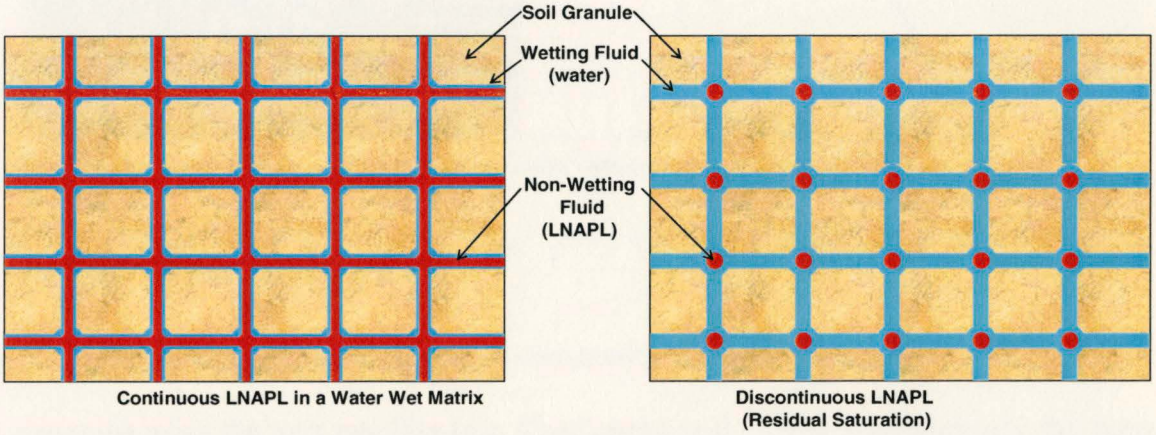

Figure 2: Continuous and Residual LNAPL in a Soil Matrix

In the formation, the two fluids co-exist at different pressures. In the absence of the formation (e.g. an observation well) the capillary forces are effectively zero. For this reason, the LNAPL thickness in an observation well is greater then the LNAPL thickness in the formation as shown in Figure 3 (Farr et al., 1989). Moreover, the presence of LNAPL in a well does not indicate that the LNAPL in the formation is moving. Nonetheless, when LNAPL accumulates in wells there is often a concern that migration is occurring. This concern is a common driver for LNAPL depletion measures.

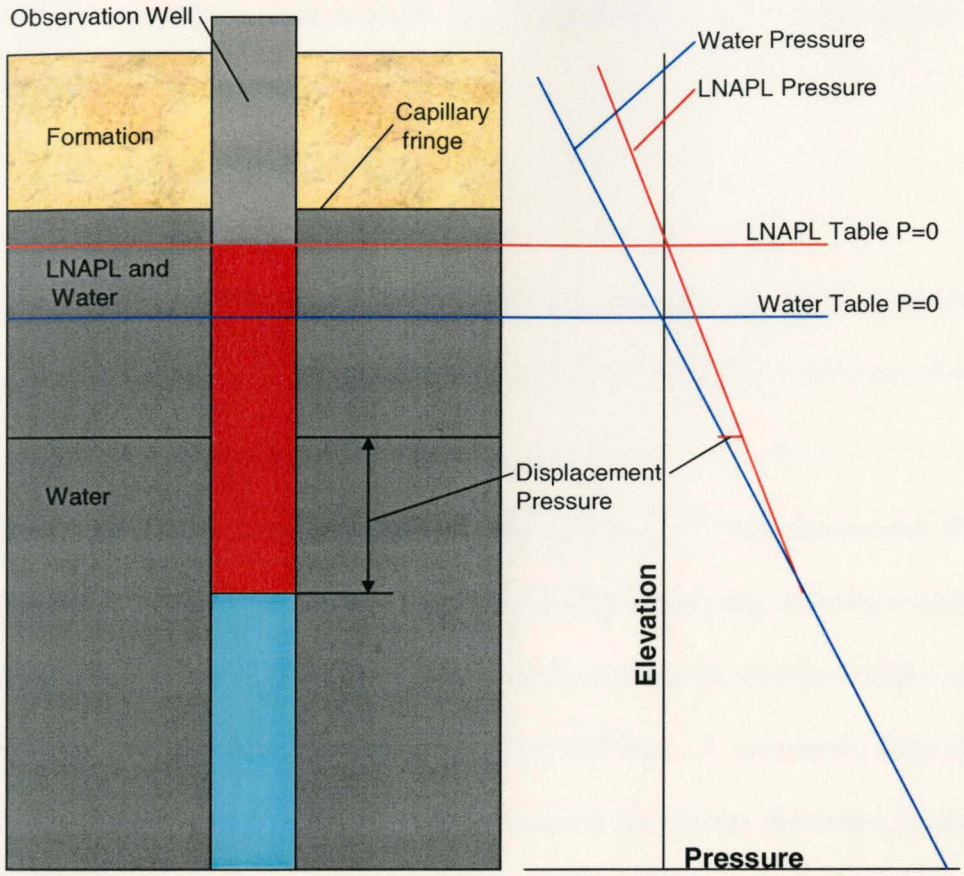

Figure 3: Pressure diagram of LNAPL and water (after Farr et al., 1989)

2.2 Metrics for LNAPL Flow

In recent years the professional community has been discussing LNAPL migration using the term mobility (e.g. Charbeneau et al., 1999). Unfortunately, this term is used in many different contexts, and its meaning is ambiguous. For the purposes of quantifying the risk associated with LNAPL migration, it is necessary to be more specific and describe LNAPL migration more rigorously. A common measure of migration is volumetric LNAPL flux, or a Darcy flux. The volumetric flux is defined as the rate at which fluid moves through a cross sectional area, perpendicular to flow, and with units of volume per time per area ($L^3/L^2/T$) or length per time (L/T). The volumetric flux provides

a way to report how much LNAPL is moving through a given plane and can be expressed as Equation (1).

$$q_n = -K_{ne} \cdot \nabla h_n \quad (1)$$

Where:

q_n= Volume of LNAPL passing through a unit area per unit time

K_{ne}= effective LNAPL conductivity (which is a function of saturation)

∇h_n = LNAPL gradient

Seepage velocity can also be used to describe LNAPL movement. The seepage velocity is the flow rate divided by the area of flow. Seepage velocity is also measured by units of length per time (L/T). It is important to note that volumetric flux and seepage velocity although dimensionally similar, are different. A volumetric flux can be related to a seepage velocity by dividing the volumetric flux by the formation porosity and the LNAPL saturation. The seepage velocity, a measure of how fast the LNAPL is traveling in the average direction of flow, can be expressed mathematically as Equation (2)

$$v_n = \frac{-q_n}{\phi S_n} \quad (2)$$

Where:

v_n= The rate of migration of the LNAPL front

q_n= Volume of LNAPL passing through a unit area per unit time

ϕ= Porosity of the media

S_n= LNAPL saturation or percent of the void space containing LNAPL

It is important to note that even under ideal conditions, the flux and velocity of the LNAPL will vary vertically in the formation as a function of the saturation. The volumetric flux and seepage velocities can be point values, or they can be vertically

integrated average values over the height of continuous LNAPL in the formation. To determine the velocity at any given point, or the maximum velocity, requires knowledge of the relationship between the saturation and the relative permeability. These parameters can be estimated by collecting soil cores, measuring capillary pressure as a function of saturation, and employing the Brooks and Corey equations (Brooks and Corey, 1966) or the VanGenuchton model (VanGenuchton, 1980).

Mobility is another measure of the potential for LNAPL to migrate. In the environmental field, mobility is generally used to describe the ability of LNAPL to move. The petroleum industry defines mobility mathematically as the permeability to LNAPL divided by the LNAPL viscosity. Per prior discussion, this thesis avoids the term mobility.

Tracer dilution techniques described herein directly measure a flow rate (L^3/T) attributed to a given width of LNAPL body. This value can be expressed as a $L^3/T/L$ or a flow rate per unit width of LNAPL body, perpendicular to flow. Reporting this measure is a direct method to report LNAPL movement and can be easily used to calculate total discharge for a given LNAPL body. When necessary, this measure can also be converted to a volumetric flux or seepage velocity. The detailed mathematics for the conversions are presented in a later section.

2.3 Current Methods for Measuring LNAPL Flow

Determining how quickly and how much LNAPL is moving through a given site is vital to determine the risk posed by the LNAPL body and thus the relative need to take corrective action. A large amount of work has been conducted on methods to determine the stability of LNAPL in porous media. Many recommendations and tools designed to

determine the risk posed by migrating LNAPL and predict the "success" of recovery methods have been developed. A brief review of common methods is presented in this section.

Determining the properties of the formation porosity and hydraulic conductivity as well as methods of obtaining the fluid properties of viscosity and density are well known (Sale, 2001). The effective LNAPL conductivity, saturation, and driving force are less typical properties; common methods of obtaining these parameters are summarized in this section.

2.3.1 Tests for Effective Conductivity

Three methods to determine the effective conductivity are presented in this section. The first two methods--bail down tests and pumping tests--are conducted on a field scale and integrate the heterogeneity in the formation. Methods which integrate heterogeneity are typically preferred (McWhorter and Sale, 2000).

2.3.1.1 Bail-down Test for Effective Conductivity

One method to determine the effective conductivity is the bail down test (e.g. Huntley, 2000). Some or all of the LNAPL is removed (bailed out) from a well. LNAPL from the formation then begins to fill the well. By measuring the thickness and elevation of LNAPL in the well through time, the conductivity can be determined. McWhorter and Sale, 2000, provide the following approach to calculate LNAPL conductivity from a bail down test via Equation (3).

$$K_{ne} = \left[\phi_{gp} r_w^2 + \left(1-\phi_{gp}\right) r_c^2\right] \left(\frac{1}{2 b_w t}\right) \int_{B_o}^{B} \frac{1}{F_1 + F_2 + F_3} dB \cdot \ln\left(\frac{R}{r_w}\right) \qquad (3)$$

Where:

K_{oe}= Effective LNAPL conductivity

ϕ_{gp}= Porosity of the gravel pack (1 if no gravel pack)

r_w= Radius of wellbore

r_c= Radius of the well casing

R= Radius of influence ($R \sim 100 r_w$)

b_w= Equilibrium thickness of LNAPL column in well

b= Thickness of LNAPL

$B = b/b_w$

B_o= Value of B at the start of recovery

T= Time

$$F_1 = (1 - B) \cdot \frac{w}{b_o} - \left(1 + \frac{\Delta p}{3 \cdot p_o}\right)\left(\frac{w}{b_o}\right)^3 \quad (4)$$

$$F_2 = \frac{a}{b_o} \cdot \left[\left(1 - \frac{a}{b_o}\right)^2 - \left(1 - \frac{a}{b_o} - \frac{b}{b_o}\right)^2\right] \quad (5)$$

$$F_3 = \frac{1}{3} - \left(1 - \frac{a}{b_o}\right)^2 + \frac{2}{3} \cdot \left(1 - \frac{a}{b_o}\right)^3 \quad (6)$$

The Equations (4), (5), and (6) for each value of b(t) are defined by the recovery data. Polynomial functions are fitted to the data and the integration performed.

2.3.2.2 Pumping Tests for Effective Conductivity

Pumping tests can also be used to determine the effective conductivity. A pumping test involves removing (pumping) LNAPL from a well over a long period of time; this causes a drawdown in the LNAPL table. If the LNAPL-water interface is maintained at equilibrium, the LNAPL conductivity can be estimated by Equation (7).

$$K_{ne} = \frac{Q_n \cdot \ln\left(R/r_w\right)}{2\pi \cdot b_o \cdot \Delta h} \tag{7}$$

Where:

K_{oe}= Effective LNAPL conductivity

Q_n= Steady LNAPL pumping rate

r_w= Radius of the well

R= Radius of influence

b_o= Equilibrium thickness of LNAPL column

Δh= Water level drawdown

2.3.2.3 Indirect Calculation of Effective Conductivity

It is possible to determine the effective LNAPL conductivity by indirectly determining the capillary and displacement pressures. Due to the density difference between the LNAPL and water, there is a pressure gradient above the LNAPL water interface, thus the capillary pressure increases above the LNAPL water interface. Brooks and Corey (1966) relate the LNAPL relative permeability to the capillary pressure through Equation (8).

$$k_{rn} = \left[1 - \left(\frac{P_c}{P_e}\right)^{-\lambda}\right]^2 \left[1 - \left(\frac{P_c}{P_e}\right)^{-(2+\lambda)}\right] P_c \geq P_e, \qquad K_{rn} = 0 \; P_c \leq P_e \tag{8}$$

Where:

k_{rn}= Relative permeability

P_c= Capillary pressure

P_e= Entry or displacement pressure

λ= Pore size distribution index

According to the above equation, the relative permeability varies with elevation; it is therefore necessary to integrate the equation over the thickness of LNAPL in order to obtain an average value. The entry pressure is a function of interfacial tension and size of the pore openings. McWhorter (1996) propose the entry pressure can be correlated to the hydraulic conductivity via Equation (9).

$$h_e = \frac{P_e}{\Delta\rho \cdot g} = 9.6\left(\frac{\rho_w}{\Delta\rho}\right)\left(\frac{\sigma_g}{\sigma_n}\right)\left(\frac{K}{\phi}\right)^{-0.403} \tag{9}$$

Where:

h_e= Entry head (cm)

σ_w= Interfacial tension between water and air

σ_n= Interfacial tension between water and LNAPL

K= Hydraulic conductivity (cm/s)

ϕ= Porosity

Finally, the effective conductivity can be calculated by Equation (10).

$$K_{ne} = K\left(\frac{\mu_w \cdot \rho_n}{\mu_n \cdot \rho_w}\right)\bar{k}_{rn} \tag{10}$$

Where:

K_{ne}= Effective LNAPL conductivity

μ_w= Viscosity of water

μ_n= Viscosity of LNAPL

ρ_w= Density of water

ρ_n= Density of LNAPL

$\bar{k}_{rn}$= Vertically integrated LNAPL permeability

2.3.2 Saturation Measurements

Following Farr et al. (1989) the saturation of the LNAPL in the formation varies with elevation; however, McWhorter and Sale (2000) propose that the average saturation can be determined via Equation (11).

$$S_n = k_{rn}^{1/2} \tag{11}$$

Where k_{rn} is the relative permeability and can be determined from any number of methods. By testing sample cores, it is also possible to determine the saturation at a point. However, since the saturation can vary widely from point to point, a large number of samples may be required to characterize the bulk capacity of the formation to conduct LNAPL.

2.3.3 Determination of the Driving Force

The driving force (gradient) is also necessary to determine the velocity or flux of LNAPL. This force is similar to hydraulic head, and can be determined by the slope of the LNAPL table, assuming there is sufficient data to determine the LNAPL table. If there is insufficient data to determine the LNAPL table, McWhorter and Sale (2000) propose that the slope of the water table can be used. Doing so neglects the gradient imposed by the capillary pressure; however, this error is usually small relative to other uncertainties.

2.3.4 Summary of Current Methods

Current methods to determine the migration rates of LNAPL are complex. This section describes methods to determine only some of the parameters necessary in calculating LNAPL migration rates. In many cases, these methods can be time

consuming, costly and potentially inaccurate. Results often depend on a number of parameters that vary widely from point to point and are estimated and/or averaged.

2.4 Well Dilution Method

This thesis explores the use of tracer dilution techniques to measure *in situ* flow of LNAPL. This is a direct measurement method that avoids many of the complexities associated with multiphase flow described in the previous section. The underlying premise is to introduce a tracer into a well and keep the tracer concentration, in the well, uniform through time via mixing. The rate at which the tracer is depleted from the well is proportional to the flow rate of LNAPL through the well.

2.4.1 History of the Well Dilution Method

The well known concept of the mixing cell can be found in most differential equation texts (e.g. Edwards and Penny, 2000). The concept of applying the mixing cell solution to groundwater velocities is credited to Kocherin, 1916 (HALEVY et al., 1967). Little was done with the technique until the 1950's when, due to ease of detection, radioisotopes became a popular tracer. A number of scientists began to develop the dilution method to determine groundwater velocities. Since the late 1960's, when the side effects of radioisotopes were better understood, research on tracer dilution studies slowed. More recently scientists have adopted the earlier methods and are using the dilutions of salt solutions to estimate groundwater flows (Freeze and Cherry, 1979).

In 1958 an equation was derived to account for the presence of the well in the formation, based on the change in conductivity. This is equation is commonly referred to as Ogilvi's equation (Drost, 1968). Because a well is generally more conductive then the

formation, flow tends to converge toward the well, increasing the flow through the well relative to the formation. Ogilvi's formula, as it is commonly referred to, determines the extent of this convergence via Equation (12).

$$\alpha_o = \frac{4}{\left[1 + \left(\frac{r_1}{r_2}\right)^2\right] + \frac{k_2}{k_1}\left[1 - \left(\frac{r_1}{r_2}\right)^2\right]} \quad (12)$$

Where:

α_o= Convergence factor (observed flow / actual flow)

r_1= Radius of the well screen

k_1= Hydraulic conductivity of the gravel pack

r_2= Radius of the gravel pack

k_2= Native hydraulic conductivity

Halevy et al., (1967) summarized a conference held in 1966 on the uses of tracer dilutions. By this time, dilution of radioactive isotopes was being used, with limited success, to determine the groundwater flow rates, directions, and vertical gradients. Ogilvi's formula had been refined to account for the presence of the well screen as Equation (13)

$$\alpha_o = \frac{8}{\left(1 + \frac{k_3}{k_2}\right)\left[1 + \left(\frac{r_1}{r_2}\right)^2\right] + \frac{k_2}{k_1}\left[1 - \left(\frac{r_1}{r_2}\right)^2\right] + \left(1 - \frac{k_3}{k_2}\right)\left[\left(\frac{r_1}{r_3}\right)^2 + \left(\frac{r_2}{r_3}\right)^2\right] + \frac{k_2}{k_1}\left[\left(\frac{r_1}{r_3}\right)^2 - \left(\frac{r_2}{r_3}\right)^2\right]} \quad (13)$$

Where:

α_o= Convergence factor

k_1= Hydraulic conductivity of the well screen

k_2= Hydraulic conductivity of the gravel pack

k_3= Hydraulic conductivity of the formation

r_1= Inner radius of the well screen

r_2= Outer radius of the well screen

r_3= Outer radius of the gravel pack

Halevy et al., (1967) also describe the limitations of the method and factors that complicated the results: mainly, that tracer decay through time is a result of a number of processes. These processes can be summarized in Equation (14).

$$\frac{dC}{dt} = f(\alpha_o v_a, t, s, m, d) \tag{14}$$

Where:

v_a= The measured or "apparent" velocity

t= Losses caused by density and temperature gradients

s= Losses due to vertical currents

m= Losses caused by the mixing device

d= Losses via molecular diffusion

Tracer adsorption and biodegrading can also potentially cause the tracer concentration to decay through time. Clearly, there are many unknowns and only one equation, which can make determination of any single parameter a challenging task. Fortunately, many of these other loss mechanisms can, under certain conditions, be neglected. These conditions are addressed in subsequent sections of this thesis.

Drost et al., (1967) presents a similar summary of past tracer dilution work and suggests methods to best calculate some of the necessary parameters. Drost et al., (1967) also presents methods to calculate the hydraulic conductivity of the well screen. Direct

experimentation proved to be the most accurate method. When necessary, the well screen hydraulic conductivity can be calculated via Poiseuille's Law.

Drost et al., (1967) also investigated different ways to calculate the convergence factors comparing Ogilvi's equation, the modified Ogilvi's equation, and experimentally obtained results. The comparison concluded that the modified Ogilvi's equation more closely agreed with the experimental findings; however, all three methods were within 17% of each other, and modern references cite both forms Ogilvi's equation.

Work continued with different tracers; today tracer dilution of salt solutions is a generally accepted method to estimate the groundwater flow. However, the problem of other mechanisms causing tracer loss has not been completely resolved. Gaspar (1987), recommends concentration for a variety of tracers, and attempts to quantify when the results are likely to be valid, and at what point the other loss mechanisms become large factors in the analysis.

Lamontagne et al., (2002) presented "Estimation of groundwater velocities in riparian zones using point dilution tests." The tests used a simple vertical gradient mixer and potassium salt solution to estimate the groundwater flow in riparian zones. The dilution data was then fit, via type curves, to the velocity. The tests were considered successful; however, like their predecessors, the mixing technique likely caused adverse migration, and initial mixing of the tracer proved to be challenging.

2.4.2 Well Dilution Theory

This thesis begins with the observation that a well at steady state can be thought of as a simple mixing cell. If a tracer is present in the LNAPL, the concentration of the tracer will be diluted by the inflowing LNAPL. Provided the tracer remains well mixed,

the rate at which the tracer is diluted is related to the flow through the well via Equation (15)

$$C\ (t) = C_o e^{\frac{-Q}{V}t} \tag{15}$$

Where:

C(t)= Tracer concentration as a function of time

C_o= Initial concentration at time zero

Q= Flow rate through the well

V= Volume of the well

t= Time

A derivation of this equation is presented in the following section. By measuring the tracer concentration through time and fitting the exponential expression, Equation (15), to the data, it is possible to calculate the flow rate through the well.

2.4.3 Summary of Well Dilution Studies

As first proposed in 1919 (Halevy et al., 1967), the dilution of a tracer has been developed to determine the flow of groundwater. In the 1950's the potential of radioactive tracers fueled further development of the theory and led to the development of Ogilvi's equation, which determines a correction factor to account for the presence of the well. The research of the 1950's and 60's also revealed the dilution method's limitations, mainly that tracer losses were due to a number of processes, not just the flow of water through the well. Under some conditions these other loss mechanism interfered with the results.

By the 1970's the side effects of radioisotopes were better understood, and the idea of placing isotopes in groundwater was abandoned. In the late 1970's and early 1980's the idea again became popular, this time using a more benign salt solution as a tracer. Today the tracer dilution method is a generally accepted technique to estimate local groundwater flows although many of the original problems of mixing and diffusion still remain.

2.5 Summary of Theoretical Foundation

This section has presented relevant background information. First, explaining what NAPL is, and the complexities associated with LNAPL releases into the subsurface. This section has defined some of the common measures used to quantify LNAPL movement, and has reviewed typical methods to estimate the parameters required in calculating LNAPL flow rates. This section also introduced the concept, and development of tracer dilution techniques, that subsequent sections of this thesis build upon.

3.0 Mathematics

This section presents a derivation of the primary governing equation. It begins with a mass balance and discusses the assumptions employed in the derivation. A dimensionless analysis is also developed. The dimensionless analysis allows for different experiments to be compared on a single graph and provides a basis to determine when the data is consistent with the employed assumptions. This section also introduces mathematical conversions to calculate the mean seepage velocity, and volumetric flux, from the measured flow rate through a well.

3.1 Mathematics of a Mixing Cell Applied to a Well

A conceptualization of a mixing cell is shown in Figure 4.

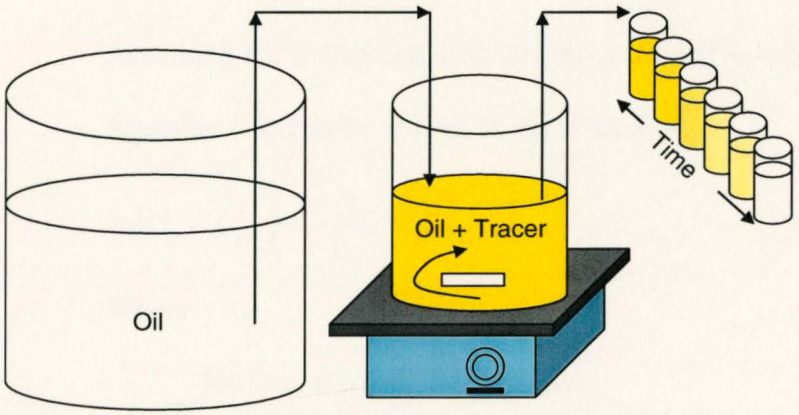

Figure 4: Concept of a Mixing Cell

Beginning with a mass balance, and assuming the tracer is well mixed, Equation (16) presents a suitable starting point for the derivation.

$$\frac{dC^*V}{dt} = Q_{in}C_{in} - Q_{out}C^*_{out} \tag{16}$$

Where:

C*= Concentration in the cell (M/L^3)

C_{in}= Influent concentration (M/L^3)

C^*_{out}= effluent concentration (M/L^3)

V= Volume of the cell (L^3)

Q_{in}= Flow rate into the cell (L^3/T)

Q_{out}= Flow rate from the cell (L^3/T)

Assuming steady flow condtions, Equation (16) reduces to Equation (17).

$$\frac{dC^*}{dt} = \frac{Q_w}{V}\left(C_{in} - C^*_{out}\right) \tag{17}$$

Where:

Q_w= Is the flow rate through the well

Separating variables and integrating results in Equations (18) and (19).

$$\int \frac{dC^*}{C_{in} - C^*_{out}} = \frac{Q_w}{V}\int dt \tag{18}$$

Assuming C_{in} is constant, and assuming the cell is well mixed $C^*=C^*_{out}$

Equation (18) can be written as Equation (19).

$$\ln\left(C_{in} - C^*_{out}\right) = \frac{-Q_w}{V}\ t + K \tag{19}$$

Where:

K= Is a constant of integration.

Equation (19) can then be solved for C*

$$C^*(t) = -Ke^{\frac{-Q_w}{V}t} + C_{in} \tag{20}$$

Application of the initial condition: at results $C^*(0) = C^*_o$ in Equation (21).

$$C^*(t) = (C^*_o - C_{in})e^{\frac{-Q_w}{V}t} + C_{in} \tag{21}$$

Where:

C^*_o= Is the initial concentration in the cell at time zero

Equation (21) can then be simplified to Equation (22).

$$C(t) = C_o e^{\frac{-Q_w}{V}t} \tag{22}$$

Where:

$C_o = C_o^* - C_{in}$

$C = C^* - C_{in}$

Lastly the active volume (V) can be defined for a well as Equation (23).

$$V = \pi\left(\frac{D}{2}\right)^2 b_w - V_{mixer} \tag{23}$$

Where:

D= Well diameter (L)

V_{mixer}= Displacement of the mixing device (L^3)

Substituting Equation (23) into Equation (22) results in Equation (24), which is the final governing equation for tracer dilutions.

$$C(t) = C_o \cdot e^{\frac{-Q_w}{\pi\left(\frac{D}{2}\right)^2 b_w - V_{mixer}}t} \tag{24}$$

3.2 Calculations of the Flow in the Formation

This section presents methods to transform the measured flow rate through a well into other metrics of interest in describing LNAPL movement.

3.2.1 Unit Flow Rate Calculations

The first step is to convert a volumetric flow rate through a well to a volumetric flow rate per unit width of LNAPL body, perpendicular to flow, through the formation. This metric has units of volume per length per time ($L^3/L/T$). Equation (25) relates the

volumetric flow rate through the well to a unit volumetric flow rate per unit width, perpendicular to flow, in the surrounding formation.

$$Q'_F = \frac{Q_w}{\alpha_o \cdot D} \tag{25}$$

The convergence factor is necessary to account for the permeability contrast between the well and the formation. This factor is described by Ogilvi's formula (1958) for water, and is typically two times the well diameter (Freeze and Cherry, 1979). However, for LNAPL flow, no documentation is available. The tank experiments conducted for this thesis conclude that the convergence is equal to approximately one tracer diameter, or 1.5 times the well screen diameter, under the experimental conditions. Ogilvi's formula estimated a convergence of 2.1 diameters for the experimental conditions. The discrepancy is likely a result of the relative permeability to the LNAPL. Ogilvi's equation is derived for homogenous, isotropic media where the conductivity is uniform. In multiphase flow the LNAPL conductivity is not uniform; even under ideal condition the conductivity varies vertically (Farr et al, 1989). When other compelling data are not available, using a range of convergence factors from 1 to 2 will produce a range of reasonable values. Compared to other sources of error, the error imposed by this approximation is small.

3.2.2 Darcy Flux

When necessary, the Darcy flux can be calculated using Equation (26).

$$\overline{q}_n = \frac{Q'_F}{b_f} \tag{26}$$

Where

b_f= Height of continuous LNAPL in the formation

The height of continuous LNAPL in the formation can be estimated following Farr et al. (1989). A first order approximation for the height of continuous LNAPL in the formation is to simply use the height in the well. This approximation neglects the capillary and displacement pressures and will typically overestimate the thickness of continuous LNAPL in the formation. This approximation can be improved by accounting for the displacement pressure through Equation (27).

$$b_f = b_w - h_d \tag{27}$$

Where:

h_d= Displacement head

The displacement head can be measured via soil cores or can be estimated by Equation (28) (McWhorter, 1996).

$$h_d = 9.6\left(\frac{\rho_w}{\Delta\rho}\right)\left(\frac{\sigma_w}{\sigma_n}\right)\left(\frac{K}{\phi}\right)^{-0.403} \tag{28}$$

Where:

h_d= Displacement head (cm)

K= Saturated hydraulic conductivity (cm/s)

ρ_w= Density of water (M/L^3)

$\Delta\rho$= Density difference of water and NAPL (M/L^3)

σ_w= Interfacial tension between water and air (F/L)

σ_n= Interfacial tension between water and LNAPL (F/L)

3.2.3 Vertically Averaged Seepage Velocity Calculation

The mean seepage velocity of LNAPL can also be calculated from a Darcy flux, or from a unit volumetric flow rate in the formation, via Equation (29).

$$\overline{v}_n = \frac{\overline{q}_l}{\phi \overline{S}_n} = \frac{Q'_f}{\phi \overline{S}_n b_f} \tag{29}$$

Where:

$\overline{S}_n$ = Average LNAPL saturation in the formation

3.2.4 Vertically Averaged LNAPL Conductivity Calculation

The transmissivity to LNAPL can be determined from the volumetric flow rate per unit width, perpendicular to flow, and the LNAPL gradient via Equation (30).

$$\overline{T}_n = -Q'_f \left(\frac{dh_n}{dx} \right)^{-1} \tag{30}$$

Where:

Q'_f= Unit volumetric flow rate

h_n= Height of LNAPL above a datum

x= Direction of flow

The average LNAPL conductivity can then be determined by Equation (31).

$$\overline{K}_n = \frac{\overline{T}_n}{b_f} \tag{31}$$

3.2.5 Estimation of the Maximum Seepage Velocity

Another parameter of potential interest is the maximum LNAPL seepage velocity. This occurs at the LNAPL-air interface, where the LNAPL saturation and thus the LNAPL conductivity are at a maximum. Using Brooks and Corey (1966) or Van

Genuchten (1980) models, an estimate of the maximum seepage velocity can be obtained for homogenous settings. At first glance, the maximum seepage velocity seems to have relevance to the rate of advancement of the LNAPL body. In fact, care must be taken as the processes governing the movement of a leading edge can be substantially different from the processes within the LNAPL body. For this reason, a more useful measure to determine LNAPL stability is the volumetric flow rate per unit width, perpendicular to flow, described previously. Consequently, this thesis does not go further with the application of Brooks and Corey (1966) or VanGenuchten (1980) models.

3.2.6 Summary of LNAPL Flow Metric Calculations

The equations presented in this section provide a means to transform the measured flow rate through a well into a variety of metrics of interest. This development illustrates how tracer dilution techniques can be used to determine stability within LNAPL bodies.

3.3 Dimensionless Analysis

A dimensionless analysis of data collected during tracer dilution tests provides a number of useful insights into how well the data fits the model, and into other processes that may affect the results. The developments of the equations necessary for the dimensionless analysis are presented below, beginning with the equation for the mixing cell, which can be written as Equation (32).

$$C\ (t) = C_o e^{-\alpha \cdot t} \tag{32}$$

Where:

α= has been substituted for the term Q/V

Dimensionless parameters for the concentration, time and rate constant are introduced in Equations (33), (34) and (35)

$$C'(t) = \frac{C(t)}{C_o} \quad (33) \qquad t' = \frac{t}{t_{1/2}} \quad (34) \qquad \alpha' = \alpha t_{1/2} \quad (35)$$

Where:

C'(t)= Normalized concentration

t'= Dimensionless time, normalized to $t_{½}$

$t_{½}$= Time to dilute the tracer concentration by a factor of 2

α'= Dimensionless rate constant

Solving for C(t), t, and α leads to Equations (36), (37) and (38)

$$C(t) = C'(t) C_o \quad (36) \qquad t = t' t_{1/2} \quad (37) \qquad \alpha = \frac{\alpha'}{t_{1/2}} \quad (38)$$

Substitution of Equations (36), (37) and (38) into Equation (32) and simplifying results in Equation (39)

$$\log(C'(t')) = \frac{-\alpha}{2.303} \tag{39}$$

Applying the boundary condition when t'=1 C'(t') = ½, substituting into Equation (39) and solving for α' becomes Equation (40).

$$\alpha' = 0.693 \tag{40}$$

Solving Equation (35) and (40) for $t_{½}$ becomes Equation (41)

$$t_{½} = \frac{0.693}{\alpha} \tag{41}$$

This dimensionless analysis provides a number of useful insights into the equations. First, note that for all data sets α' is a constant. By plotting the data in this dimensionless format, the slope should always be ~0.693 regardless of the LNAPL flow rate. When α' is not the expected slope, or varies with respect to t', it suggests that other mechanisms maybe affecting the tracer dilution.

3.4 Critical Assumptions

Lastly, a discussion as to the critical assumptions employed in the process of deriving the mixing cell is presented. These assumptions, which are easy to overlook, can greatly influence the results of the experiments.

The first important assumption was that of steady flow ($Q_{in}=Q_{out}=Q_w$), which requires the volume in the well to be constant. For the mixing cell in Figure 4, this is a good assumption, as it is easy to keep the volume constant. However, in a well the LNAPL thickness, and thus the LNAPL volume, will vary greatly with movement of the water table (Marinelli and Durnford, 1996). It is important that the water table be stable in order to maintain a constant volume of LNAPL in the well and thus obtain accurate

results. If the water table were to rise during a tracer dilution test, the volume of the well would decrease as more LNAPL and tracer flowed from the well than entered. In fact, during a rising water table, the LNAPL inflow rate would likely be very small or zero. With no inflowing LNAPL, the tracer concentration would not dilute, and the test would predict a very low or zero flow through the well when, in fact, a large volume of LNAPL maybe flowing. Conversely, if the water table were to fall, the LNAPL thickness in the well would increase, diluting the tracer and would predict a high flow rate.

A second important assumption is complete mixing of the tracer in the well. Without some form of mechanical mixing, the tracer will not stay well mixed under most conditions. When the tracer is not well mixed, the tracer dilution does not follow the governing equation, making a good fit impossible. At the same time, mixing too vigorously may induce tracer losses which are not associated with the natural flow through the well. Due to the importance of mixing, the development of a mixing system was a primary challenge of this research; it is discussed further in subsequent sections.

The construction of the well is also vital to obtaining accurate results. Some well completion techniques leave a layer of fine material about the annulus of the wellbore, either bentonite slurry or naturally occurring fine materials. This layer of fine material can prevent LNAPL flow through the well.

Selecting the well screen is also important. First, the well must be screened over the entire layer of continuous LNAPL. Partially screened wells inhibit flow and will likely result in underestimating the LNAPL flow in the formation. The well screen must also be made from non-reactive materials. Well screens constructed from PVC material

can swell shut in the presence of LNAPL. Proper design and construction of the test well is vital to obtaining accurate results from a tracer dilution test.

Another important assumption is that the only source of tracer dilution is the flow through the wellbore. There are a number of loss mechanisms that can affect the rate at which the tracer dilutes (Halevy et al., 1967). If these other loss mechanisms are large compared to the flow through the well then the tracer will disappear faster; thus, a higher flow than actually exists will be predicted. Other potentially significant loss mechanisms that can affect the results include:

Diffusion: by introducing the tracer in the well there is a concentration gradient between the LNAPL in the well and that in the formation, resulting in a diffusive flux from the well into the formation. A preliminary analysis of this process is presented in Appendix B. This analysis uses an analog to the slug test which was developed by Cooper et al., (1967). These calculations indicate that the tracer losses are not significant relative to the advection from flow through the well. Therefore, for the purposes of this thesis, it is possible to neglect the diffusive losses.

Volatilization: If the tracer contains volatile constituents at high concentrations, it is possible that some of the tracer could volatize from the LNAPL, resulting in a decreased concentration. However, at low concentrations the effects of volatilization are minimal.

Adverse Mixing: If the flow were small and the mixing rate high, it would be possible that poor mixing techniques could cause a gradient from the well into the formation, or vice-versa, resulting in an artificially high flow rate prediction. By using the

diffusive style mixer described in Appendix E, the effects of adverse advection are minimized.

Heating: If LNAPL is heated its volume changes: if the mixing or monitoring of the concentration adds energy, it is possible the LNAPL in the well could expand, migrate outward and remove tracer from the well, without causing a volume change. By minimizing the amount of energy used in the well, the heating effects can be neglected.

Density Differences: If the addition of the tracer to the LNAPL affects the density of the LNAPL, this will induce a gradient in the well and cause the tracer to dilute at an artificially high rate. Using small concentrations of a tracer, and a tracer that has a similar density to the LNAPL, prevents these gradients.

Most of these loss mechanisms will occur early in the process when the tracer concentration is at its maximum. By allowing some time between the tracer introduction and the beginning of the test, the effects of these other loss mechanism can be reduced further.

3.5 Summary of Mathematics

This section has presented a derivation for the primary governing equation, and a dimensionless analysis for data gathered during a tracer dilution test. This section has also provided a method to calculate a volumetric flow per unit width of LNAPL body, perpendicular to flow, as well as mathematical transforms to calculate Darcy flux, mean seepage velocity, and mean LNAPL conductivity from the results from a tracer dilution test. This section has described the importance of the assumptions employed in deriving the governing equation, and suggested methods to ensure the assumptions are not violated.

4.0 Laboratory Experiments

This section describes the laboratory experiments that were conducted to:

- Demonstrate the use of the tracer dilution technique to measure LNAPL flow.
- Develop the technology needed to conduct LNAPL tracer dilution tests.
- Measure the accuracy of the tracer dilution test through a representative range of flow rates and LNAPL thicknesses.

Preliminary experiments were conducted on a small scale to test tracers, mixing devices, and detection methods. Next, large scale tank experiments were conducted at a variety of LNAPL flow rates and thicknesses. The methods, procedures, and results for the experiments are discussed in detail below.

4.1 Preliminary Investigation

The following describes the preliminary experiments.

4.1.1 Mixing Cell Experiment

The first effort was a simple mixing cell experiment, shown in Figure 5. The experiment used Soltrol 220 as LNAPL and 2,5 Diphenyloxazole commonly known as PPO as a tracer. PPO, a fluorescing compound, was selected for this initial experiment due to its availability in the laboratory.

Fluorescence is a phenomenon where electrons in certain molecules jump orbits when excited by a specific wavelength of light energy. When the electrons fall back to a lower orbit, they emit light, usually at a higher wavelength the]that at which they were

excited. By measuring the intensity of the light emitted from the fluorescent molecules, the concentration of the tracer can be determined. Fluorescence measurements can be made in real time, without affecting the volume or concentration of the tracer. This type of real time, unobtrusive measuring technique is required to apply the tracer dilution technique to LNAPL flow.

4.1.1.1 Simple Mixing Cell Methods

A mixture of LNAPL and tracer was placed in a flask, and pure LNAPL was pumped through the flask via a peristaltic pump (Ismatec[tm] reglo analog MS-4/8) at 3.00ml/min. The effluent from the flask was collected and the fluorescent intensity measured through time, using a spectrometer in the chemistry department at Colorado State University. By measuring the fluorescence of a series of known concentration, a linear calibration between fluorescence readings and concentration was developed. Using the calibration and the florescence measurements from the mixing cell experiment, the concentration of the tracer was determined. The concentration vs. time data was then fitted to the model for a mixing cell, via least squares regression, to determine the flow rate.

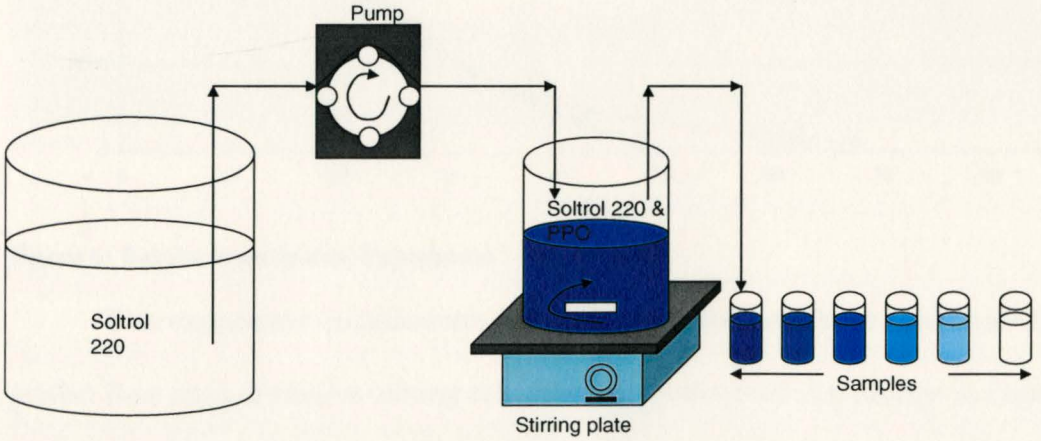

Figure 5: Setup for the Beaker Experiment

4.1.1.2 Results

Figure 6 plots the tracer concentration vs. time. A least squares regression was used to fit Equation (22) to the concentration data. The least squares regression estimated a flow rate of 2.98ml/min, while the measured flow rate was 3.00ml/min.

In the process of this analysis, it was observed that the tracer dilution method is based only on the change in concentration through time. It was also noted that the fluorescence intensity is linearly proportional to the concentration. Therefore, it should be possible to substitute the fluorescent intensity for the tracer concentration. In future experiments the least squares regression can be used to fit the fluorescence intensity vs. time data to the Equation (22) .

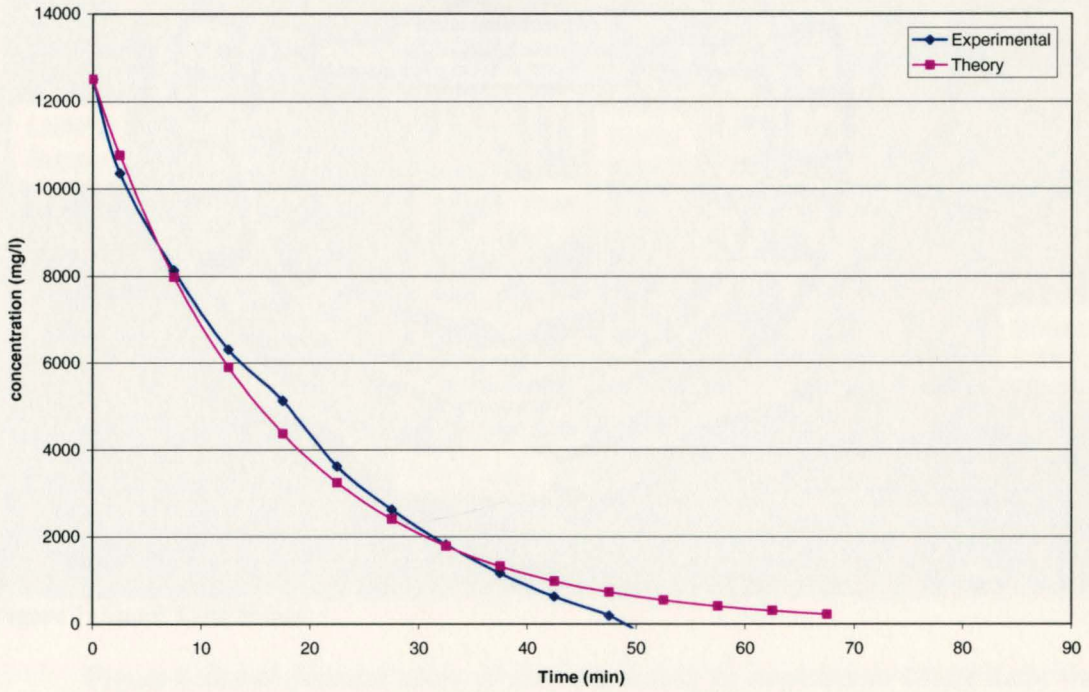

Figure 6: Results from Beaker Experiment

This experiment demonstrates that fluorescent tracers can be used to accurately predict flow rates through a mixing cell. It was also observed that change in fluorescent

intensity can be used in place of tracer concentration. This observation reduced the steps required and simplified the analysis of future experiments.

4.1.2 Small Tank Studies

Next, a small tank glass tank was employed to test different fluorescent tracers and a variety of mixers (see Figure 7). Time lapse photography was used to visually observe different tracers, and tracer movement, under different mixing conditions.

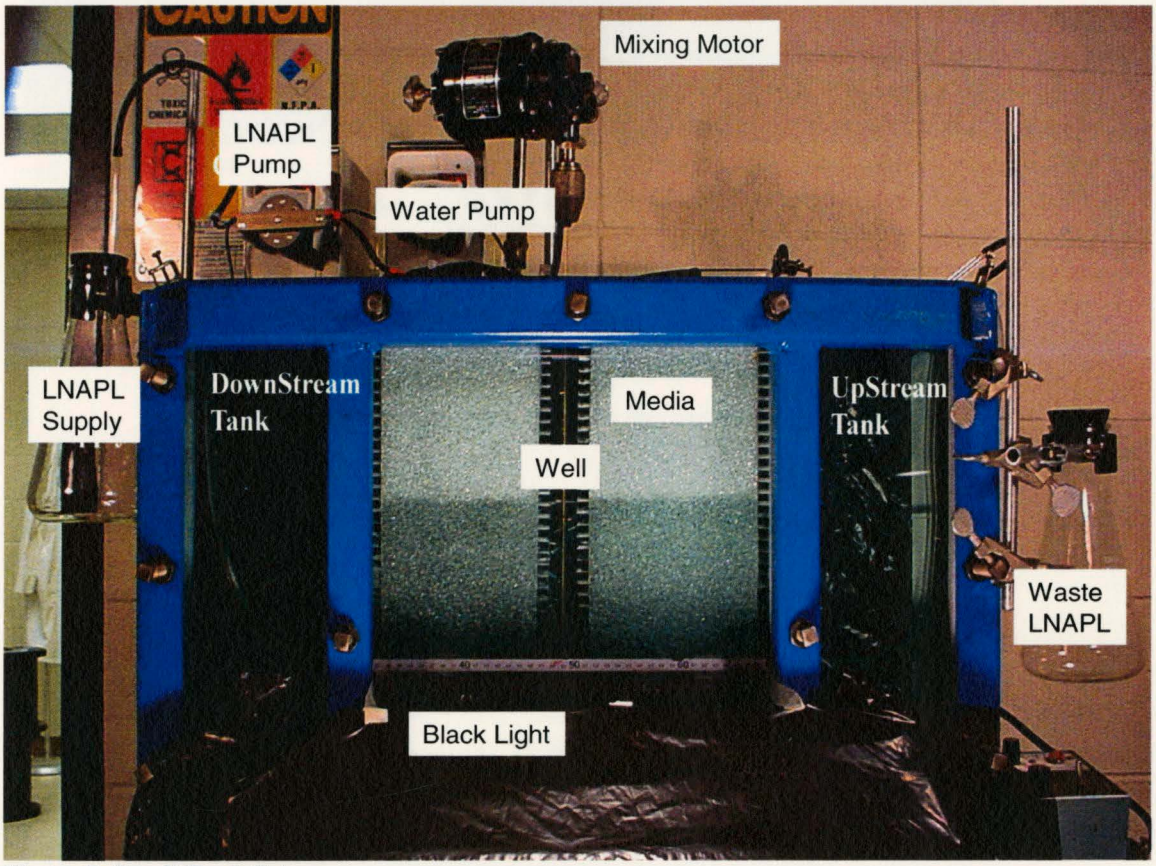

Figure 7: Small Tank Setup

Figure 8 shows pictures taken of the tank during an experiment where there was a high flow rate through the well. The tracer, yellow, is clearly visible both in the well and down gradient. As time goes on, the well becomes poorly mixed. Ultimately, results from these experiments led to the development of a diffusive mixer. When the flow rate

through the well is high, the diffusive mixer is capable of maintaining a uniform tracer concentration. When the flow rate through the well is small, the diffusive mixer does not contribute to the dilution of the tracer.

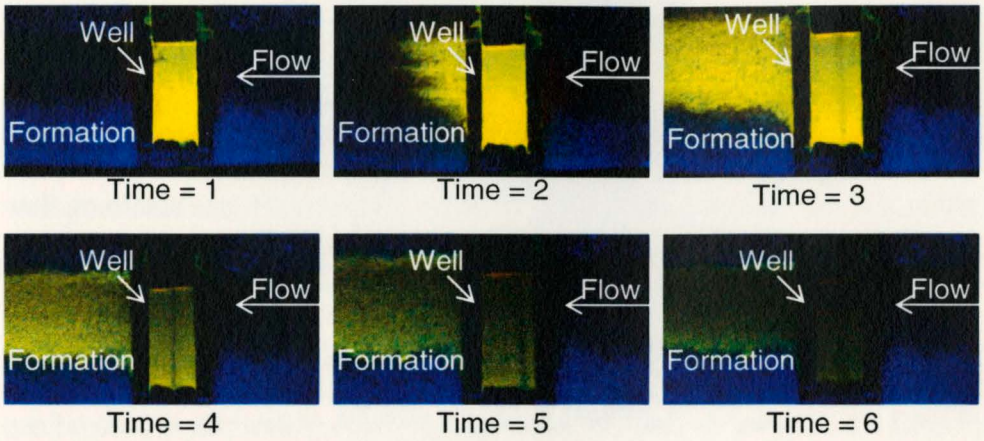

Figure 8: Tracer Visualization Photographs

Key criteria for the tracer include:

- No effect on LNAPL fluid properties (density, viscosity, LNAPL-water interfacial tension, and LNAPL- air interfacial tension)
- Readily detectable
- Low toxicity
- Insoluble in water
- Chemically stable
- Non-sorbing to well materials

Through research and testing, the tracer which most closely met the criteria for an ideal tracer was determined to be BSL 715, a concentrated fluorescent dye used in the automotive industry to detect oil leaks. BSL 715 fluoresces in the yellow (580nm) range. This makes the tracer easy to detect and to distinguish from other fluorescent signals commonly encountered in LNAPL. The tracer is detectable at concentrations of less than

one part per million, is insoluble in water, and has a relatively low toxicity compared to the compounds commonly encountered in LNAPL bodies.

4.1.3 Summary of Preliminary Experiments

Through the preliminary experiments, BSL 715 was identified as a promising tracer. The best mixing device was determined to be a diffusive mixer that minimized in well gradients and thus minimized tracer losses from mixing. Initially, using small scale experiments minimized the time and expense required to study a wide variety of mixers and tracers. The preliminary experiments also verified that fluorescence measurements can be used to accurately determine the concentration of tracer in the LNAPL.

4.2 Large Tank Study

The large tank experiment was designed to test the LNAPL tracer dilution technique on a scale similar to that found in the field. The experiment tested LNAPL flows of 0 .035 m^3/m/yr to 7.2 m^3/m/yr and LNAPL thicknesses in the formation of 9 to 24cm.

4.2.1 Objective

The objectives of the large tank experiments were to:

- Demonstrate that the tracer dilution technique can be applied to LNAPL to predict flow rate through a well.
- Determine the accuracy of the tracer dilution method to predict LNAPL flow rates.
- Investigate the range of flow rates for which the method can be applied.

- Obtain a basic understanding of how LNAPL flow converges about an observation well.
- Refine the necessary technology for subsequent experiments.

4.2.2 Methods

This section provides detail about the construction for the large tank experiments as well as information about the equipment used. This section also discusses the procedures used for each experiment, and the method by which the data was analyzed.

4.2.2.1 Large Tank Setup

The large tank consisted of a steel tank 1.22 meters tall (4ft), 2.44 meters wide (8ft) and 0.15 meters thick (0.5ft) with a single glass face. Head tanks were installed at either end. The head tanks were used to introduce, recover and monitor fluid levels. The tank was filled with uniform sand, Unium 4095 (95% of the sand is retained on a #40 sieve). An analog to a well was constructed at the midpoint of the tank by inserting a semi-circular section of well screen against the glass face. The well screen was installed against the glass so the LNAPL could be observed in the well and in the formation. The well screen is a stainless steel 5cm (2in) ID well with 0.5mm (0.020 in) slots cut in half longitudinally. A gravel pack was constructed about the well screen by filling the annulus between the well screen and a piece of 7.6 cm (3in) PVC pipe with 2095 Unium sand (95% of the sand was retained on the #20 sieve). After the tank was filled with sand, the PVC pipe was carefully removed, leaving a uniform layer of course sand approximately a quarter inch thick surrounding the well screen.

The tank was fully filled with water to wet the media. Subsequently it was drained to create a water table in approximately the middle of the tank. LNAPL (Soltrol 220 dyed red with Sudan IV) was then pumped into the tank to form a body of continuous LNAPL between the head tanks. LNAPL was then circulated using a peristaltic pump (Ismatec[tm] reglo analog MS-4/8). All plumbing was constructed of glass or Viton[tm] tubing. As shown in Figure 9 and Figure 10, two pump circuits were constructed such that LNAPL could be pumped into the upstream head tank, and pumped out of the downstream head tank at the same rate. The two pump circuits prevent any tracer from being introduced into the upstream head tank. If the tracer were introduced to the upstream head tank, it would create a false signal during future tests.

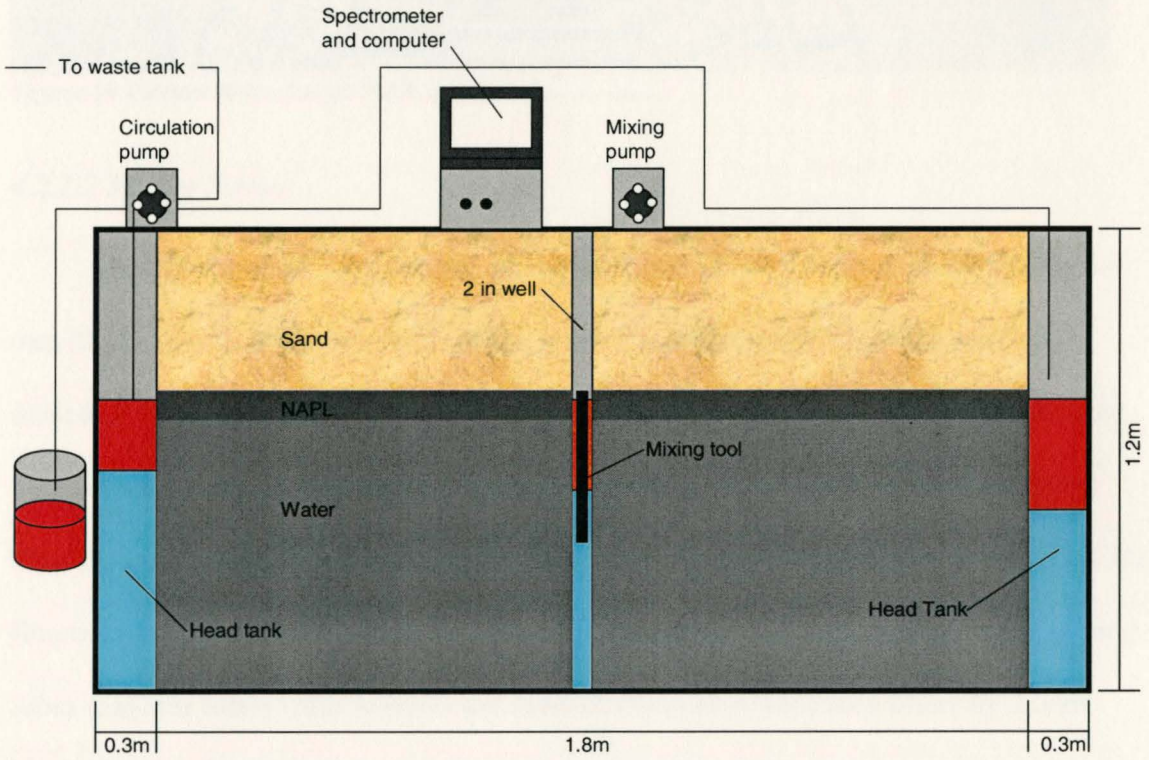

Figure 9: Large Tank Setup

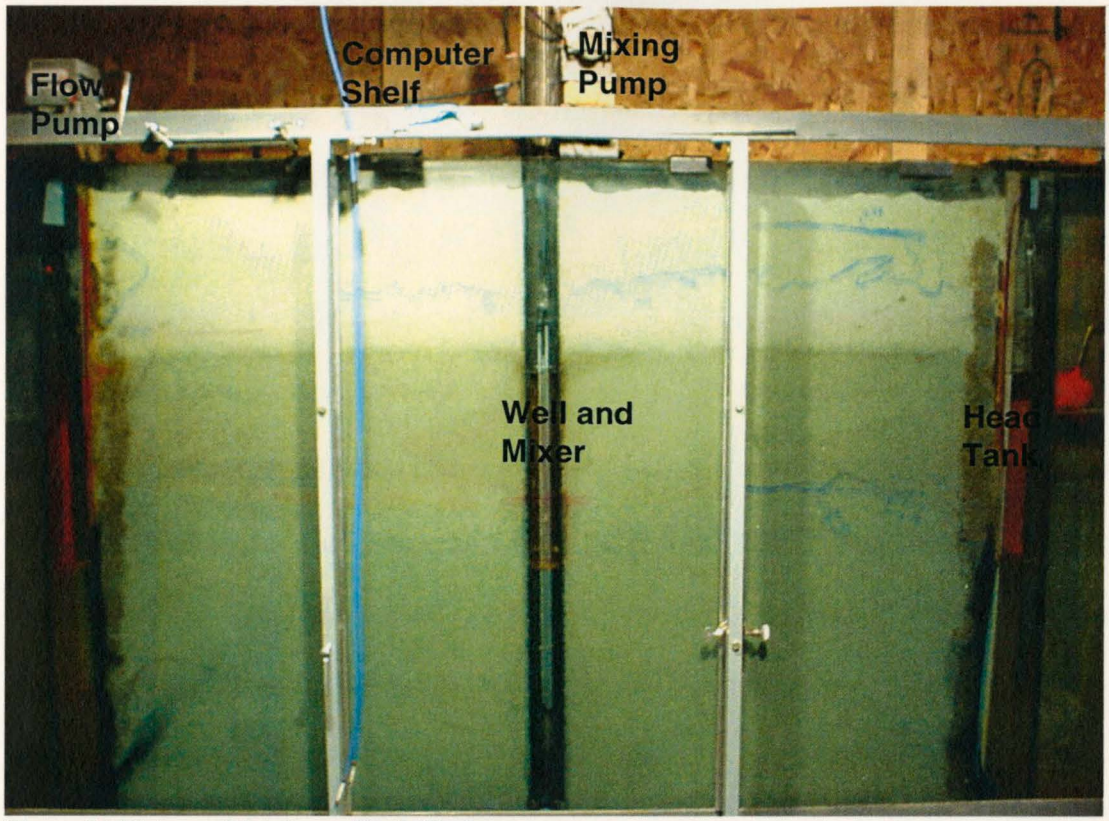

Figure 10 Picture of the Large Tank Study

4.2.2.2 Mixing Device

A diffuser mixer was constructed out of four thin wall, 0.5mm (0.020in), by 6.4 mm (0.25in), stainless steel tubes with two rows of 0.6mm (0.024in) diameter holes drilled on 5cm (2in) centers 180 degrees apart. All four tubes were then attached to the four sides of a solid 1.3cm (0.5in) square metal rod. A pump was then used to extract fluid through two of the tubes, on opposite sides of the square rod (intake tubes), past the fluorescence detector (end of fiber optic cable), and back to the remaining two opposing tubes (exhaust tubes). The holes in the exhaust tubes were vertically offset by 2.5cm (1in). This device is similar to the field mixer described in the following section and in Appendix E. The pumping rate for the mixer was controlled to ensure the well remained mixed, but not excessively high, in order to prevent tracer losses.

4.2.2.3 Measurements of Fluorescent Intensity

To measure the fluorescent intensity, a custom Ocean Optics spectrometer was used. The spectrometer consists of an R-LS-450 light source with a 470nm LED to excite the tracer. The light source was fed into one of the two fibers in a bifurcated 2m fiber optic cable. The light is emitted from the end of the fiber optic cable which is immersed in the LNAPL. The second fiber, located adjacent to the first fiber, transmits the fluorescence emissions through the other fiber to a thermo-regulated S2000 spectrometer which is equipped with a #9 grading centered at 580nm, 200micro slit and a L2 collection lens. The output from the spectrometer is then converted to a digital signal via ADC1000-USB-S 1Mhz A to D converter. The digital signal was then transmitted to a laptop via a USB 1.1 connection. A Pentium 200MHz laptop, equipped with OOiBase32 software program (from Ocean Optics), which controls the spectrometer and displays a graph of the spectrum (intensity vs. wavelength), recorded the output. The software is capable of recording the intensity of up to eight wavelengths at specified intervals.

For the large tank experiment, readings were recorded at four different wavelengths every one to five minutes depending on the experimental conditions. The first wavelength recorded was 480nm, approximately the incident wavelength of the spectrometer. If an air bubble enters the detector, the bubble will act as a mirror and the incident wavelength will spike. A spike in the 480nm wavelength is an indication that the fiber is not immersed and the readings are not valid. The second wavelength recorded was 580nm. This is one of two wavelengths where the tracer's emission is intense. The recordings from the 580nm were used to determine the flow rate through the well.

The remaining channels (582nm and 584nm) were used to verify the measurements of 580nm. In later experiments, it was found that recording 545nm and 700nm provided a better indication as to the accuracy of the readings.

The accuracy of the 580nm readings was determined by the relationship between the four recorded wavelengths. If an external light source, such as a bright light, was turned on, or pointed at the end of the fiber optic cable during the experiment, the relationship between the wavelengths changed. This indicated that the readings were a result of the light source, not the tracer's fluorescence. While 580nm was selected to determine the flow rate, any wavelength within the tracer's emission band that can be readily detected should produce similar results.

4.2.2.4 Large Tank Study Procedure

The experimental design was to make flow measurements over a representative range of known flow rates using three different LNAPL thicknesses. The first step in each experiment was to establish a steady LNAPL flow. This was accomplished by setting the desired LNAPL flow rate and monitoring the fluid levels in the head tanks. Steady-state was defined by stable LNAPL levels in the head tanks. To resolve background readings, data logging began at the four wavelengths prior to the tracer introduction. A dilute mixture of the tracer (BSL 715) and LNAPL (10% tracer) was then injected into the diffuser system to achieve approximately twenty parts per million tracer in the LNAPL.

Initially, data logging continued recording until the fluorescent intensity was too low for the spectrometer to resolve. Analyzing the results from the first few experimental

runs showed that only a portion of the dilution curve was necessary to determine the flow rate. This greatly expedited later experiments.

In an attempt to determine the lower detection limit of the tracer dilution technique, a test was conducted after the circulation pump had been turned off for a long period of time. It was thought that the flow in the tank was zero; as such the test was designed to evaluate the magnitude of the other loss mechanisms discussed previously.

4.2.2.5 Data Analysis

At the conclusion of each experiment the data was downloaded, copied into a spreadsheet, and graphed. The period of invalid, early time data where mixing and other loss mechanisms were occurring, was determined visually. A starting point was then selected after the initial mixing occurred, yet early enough in the experiment to maximize the number of readings. This point varied from 3 to 30 hours depending on the rate of dilution, and mixing. In several experiments a number of start points (after the initial mixing had occurred) were selected to verify that the flow rate prediction is independent of the selected starting point.

The data recorded after the starting point was then isolated and normalized to the initial reading. To calculate the flow rate, a least squares regression was performed to fit the data to the governing equation, Equation (24).

Next, a dimensionless analysis was performed on the selected data. First, the data was normalized to the maximum reading (C'). Then, the dimensionless time was calculated for each data point using a half-life time predicted from the best fit regression (t'). A graph of C' on the Y-axis vs. t' on the X-axis was generated, and an exponential equation was fitted to the data via least squares. From the derivation of the dimensionless

analysis, presented in the previous section, the slope of the exponential best fit should be ~0.693. If the slope of the best fit exponential equation was not close to the expected value, a new start point was selected, later in the data set, and the analysis was repeated.

To quantify the error associated with each experiment, a number of algorithms were explored including log transforms and random sampling. A standard procedure which utilized a direct measure of the data to quantify the uncertainty in flow rate prediction was not found. Some of the procedures explored produced results that were uncertain, not reproducible, or otherwise determined to be inadequate measures of the error.

Eventually, an algorithm was developed that is repeatable, certain, and an adequate measure of the error. This method uses confidence limits of the data to determine maximum and minimum flow rates based on a given confidence level (e.g. 95%). The results from this procedure are dependent only on the error between the data and the governing equation which best fits the data.

The algorithm first bounds the best fit governing equation (which was fitted to the data via least squares regression) with upper and lower confidence limits. Next, two additional curves are defined by fitting the model to the maximum and minimum flow rates for which the generated curve remains within the bounds of the confidence limits. These curves are defined by fitting the model through the y-intercept of the best fit curve (which is the initial condition) and the last point of the upper and lower confidence limits, for which the generated curve remains within the bounds of the confidence limits. Unlike the other methods explored, this procedure is dependent only on the error between the

model and the actual data to produce a measure of the uncertainty in the flow rate measurement. Figure 11 shows the process graphically.

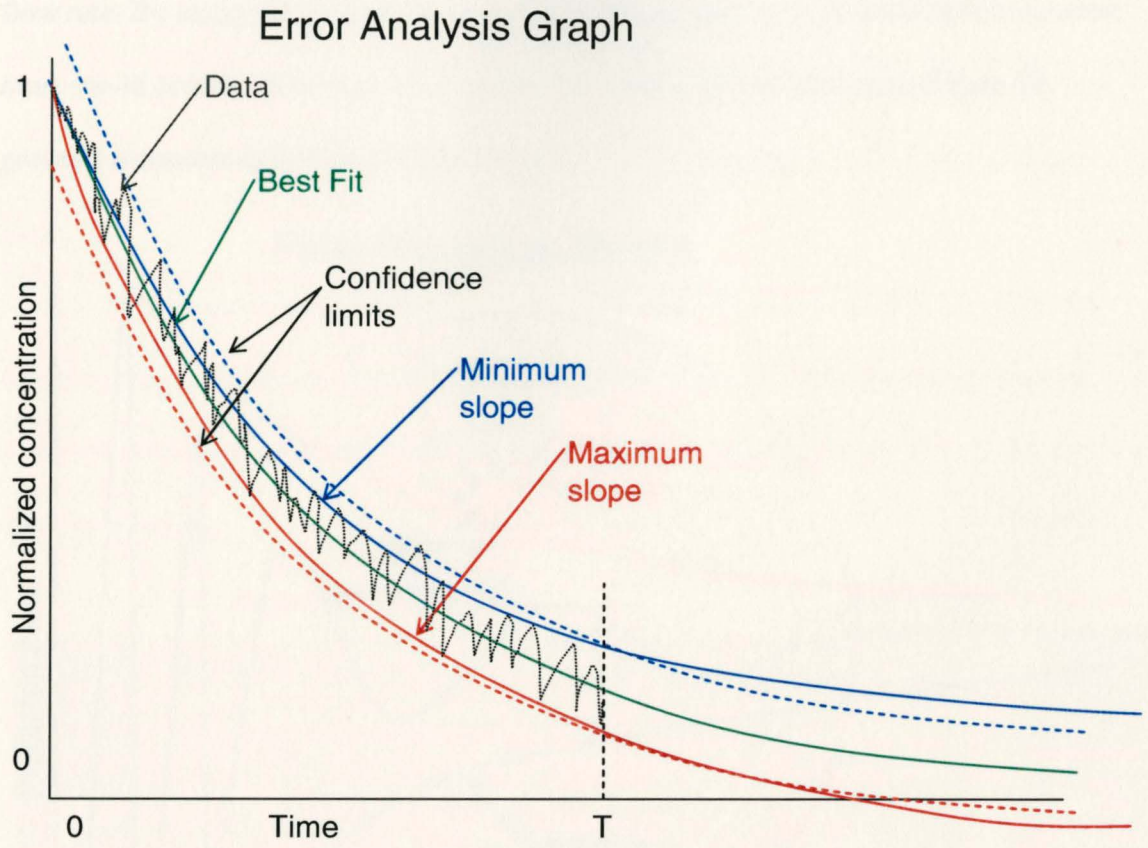

Figure 11: Conceptualization of the Error Analysis

To minimize the time required for future tests, the error analysis was performed on only the first few minutes of selected data. The amount of data was then increased and the process repeated until all of the selected data was analyzed. At each time step, the maximum, minimum and best fit flow predictions were recorded and graphed as the predicted flow on the Y-axis vs. the amount of data used on the X-axis.

Initially, the flow predictions oscillate with very little data, but eventually reach a steady solution, as more data is used for the analysis. The point where the predicted flow

rate becomes steady is the minimum amount of data required to accurately obtain the flow rate through the well. After that point, if more data is gathered, the maximum and minimum flows converge toward the best fit flow rate, reducing the uncertainty in the flow rate. By using this type of error analysis, it is possible to determine how long a test must run in order to determine the flow rate to within a given tolerance. Figure 12 presents a conceptualization of this process.

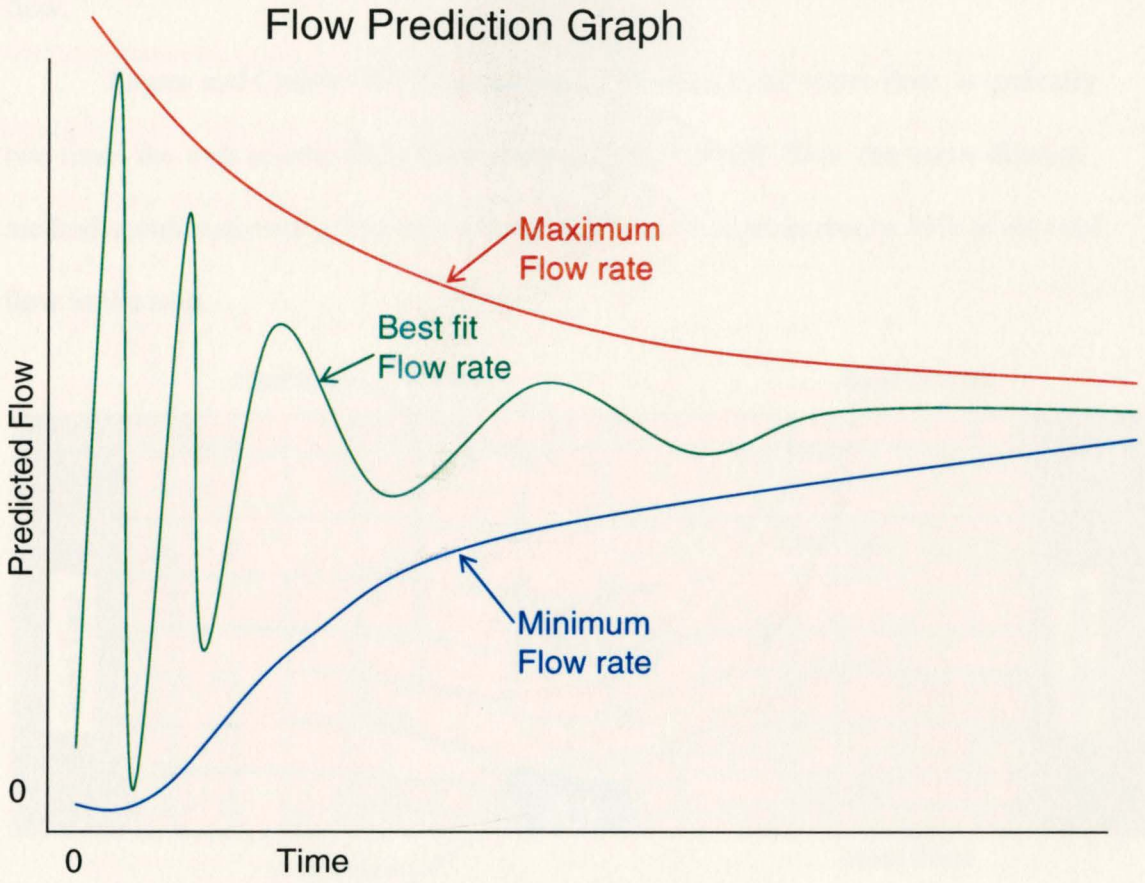

Figure 12: Conceptualization of the Time Step Analysis

4.2.2.6 Expected Results

During the experiments, the flow rate in the tank was varied from 0.013L/day to 3.9 L/day at product thicknesses of 9cm, 13cm, and 24cm. The measured flow rate

through the well was compared to the flow rate in the tank for each run. If the well screen had the same conductivity as the formation, then the flow rate measured through the well should be 17% (1/6) of the total flow through the tank. Because the well is more conductive than the formation, the flow lines will tend to converge about the well as shown in Figure 13, increasing the flow through the well. Therefore, the tracer dilution method should predict a flow rate through the well of more than 17% of the total tank flow.

Freeze and Cherry (1979) found this convergence, for water flow, is typically two times the well screen. If the same holds true for LNAPL flow, the tracer dilution method should estimate a flow rate through the well of approximately 34% of the total flow in the tank.

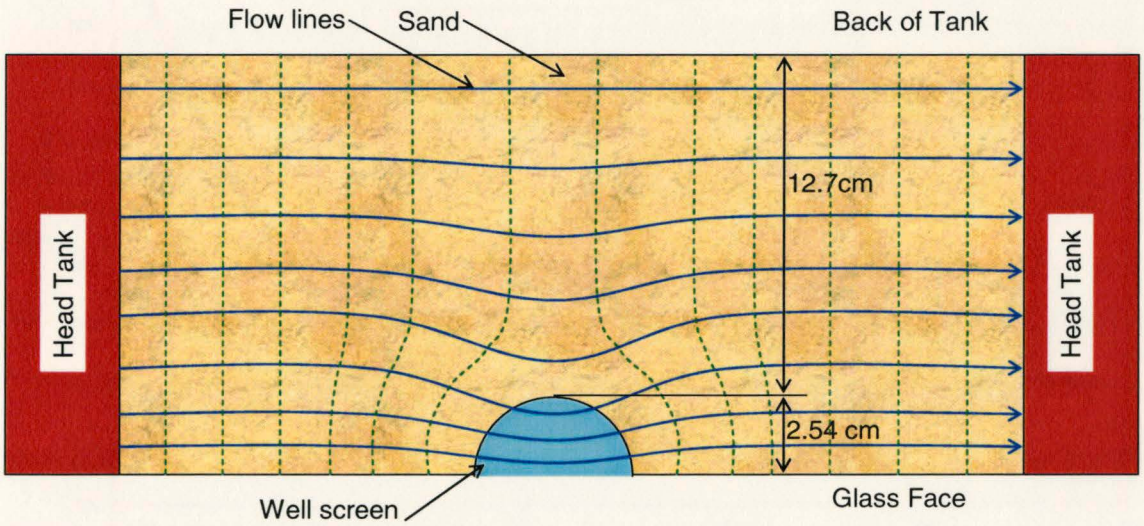

Figure 13: Large Tank Plan View Flow Net

4.2.3 Results

The first experiments conducted used a 9cm thick layer of LNAPL, and a LNAPL flow rate of 3.0 L/day, which corresponds to a volumetric flow rate per unit width of 6.9 $m^3/m/yr$ ($75ft^3/ft/yr$). This was selected as the starting point because the time required for each experimental run was minimal, and the flow rate was already high as a result of the LNAPL introduction. The data set, best fit curve, and 95% confidence intervals for the first experimental run are plotted in Figure 14. The data fits the model (governing equation) quite well and calculates a flow rate of 1.020± 0.01L/day or 34% of the 3 L/day of total flow in the tank. This result is consistent with the expected result.

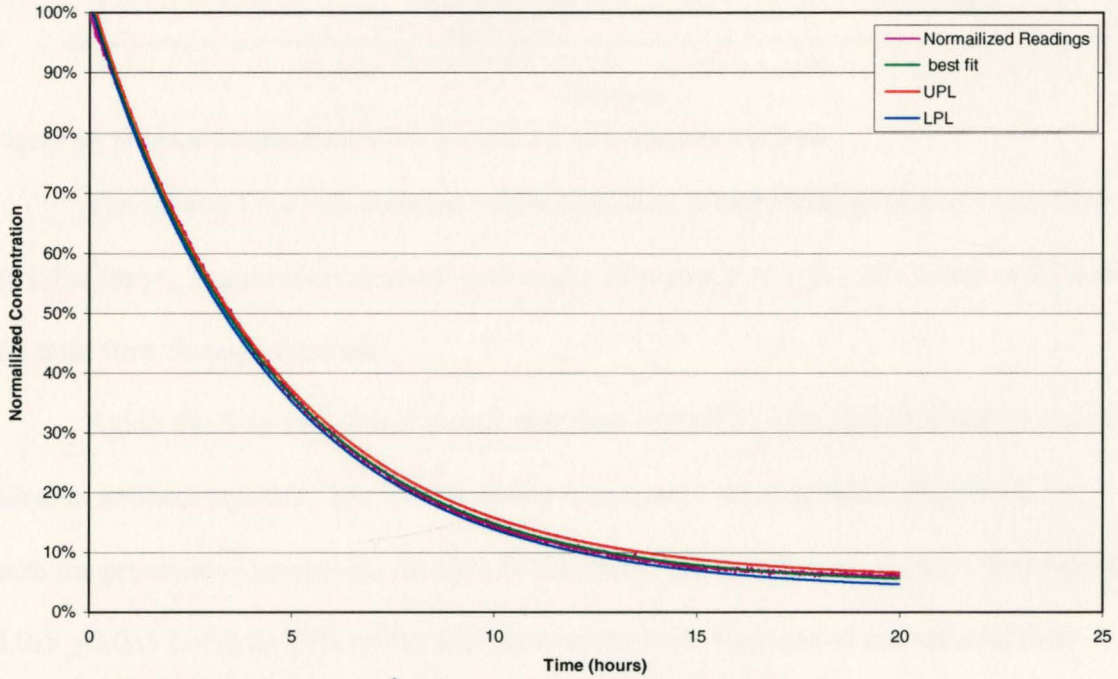

Figure 14: Dilution Results for 6.9 $m^3/m/yr$ and LNAPL Thickness of 9cm

To test the repeatability of the results, a second experiment was conducted at a similar flow rate (2.9L/day). The results of the duplicate experiment are presented in Figure 15. Once again, the data fits the model quite well and predicts the flow rate through the well to be 0.980±0.01L/day or 34% of the 2.9 L/day of flow through the tank.

The results of these first two experiments fit the model well, predict reasonable flow rates through the well, and indicates that the measurements are repeatable.

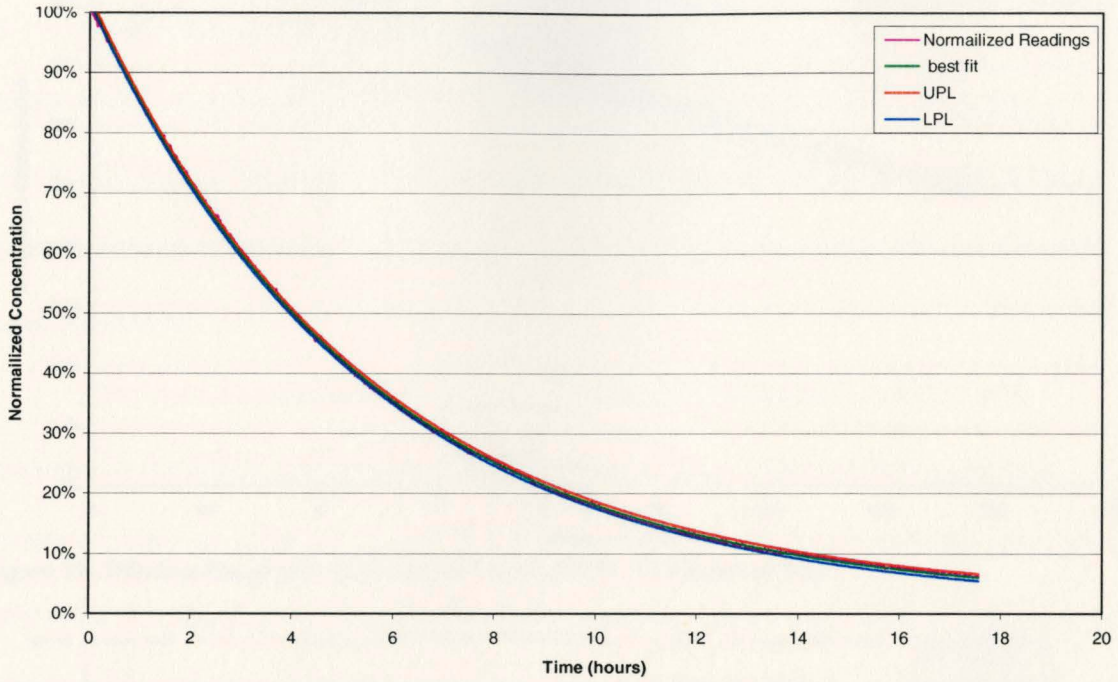

Figure 15: Dilution Results for 6.8 m^3/m/yr and LNAPL Thickness of 9cm

The second flow rate selected was 0.720L/day, which corresponds to a unit flow of 1.7m^3/m/yr. The dilution method predicted a flow rate of 0.180$\pm$.003 L/day or 25% of the total flow through the tank.

Again the flow rate was lowered, this time to 0.072 L/day (0.173m^3/m/yr) and the dilution method repeated. The results of this experiment are graphed in Figure 16. As with the previous experiments, the data fit the model quite well and predict a flow rate of 0.019 $\pm$0.001 L/day or 25% of the total flow in the tank. Because of the reduced flow rate, it is impractical to record the entire dilution curve, as was done with the initial experiments. To determine if enough data had been collected, the data were run through the time step analysis process described previously. The results of this time step analysis are shown in Figure 17 and are typical of subsequent experimental runs.

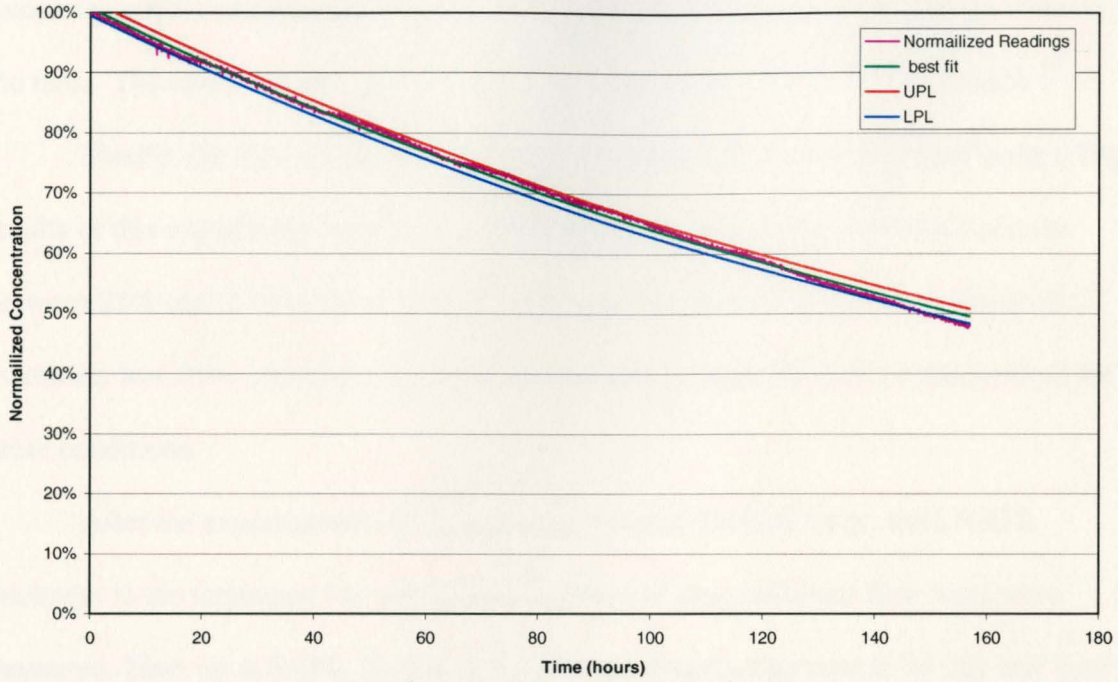

Figure 16: Dilution Results for 0.17 m^3/m/yr and LNAPL Thickness of 9cm

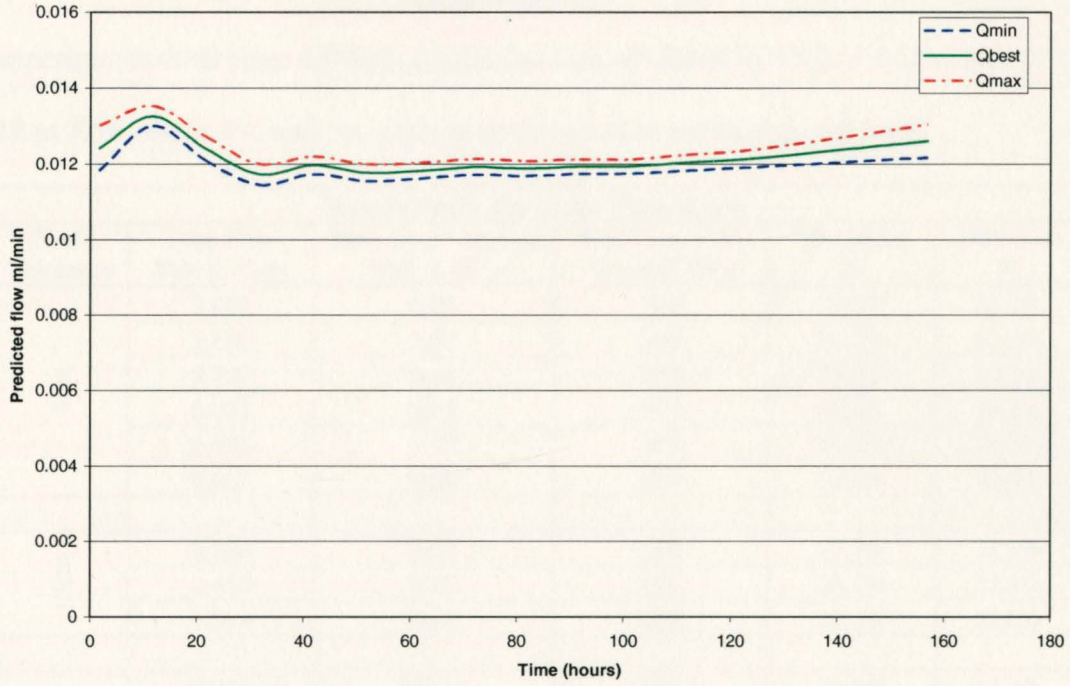

Figure 17: Time Step Analysis Results for 0.17 m^3/m/yr and LNAPL Thickness of 9cm

Again, to determine the reliability of these measurements, the experiment was repeated with a flow rate of 0.086L/day. The results of this duplicate experiment

calculated a flow rate through the well of 0.023±0.001 L/day or 26% of the total flow in the tank. The results of this duplicate show some deviation, but the error is small.

Finally, the flow rate in the tank was lowered to 0.013 L/day ($0.031 m^3/m/yr$). The results of this experiment calculated a flow through the well of 0.003+0.001 L/day or between 23% and 27% of the tank flow. This experiment had a larger error due to the extremely low flow, and maybe approaching the lower detection limit of this method for these conditions.

After the experimental run at a unit flow rate of $0.031 m^3/m/yr$, the LNAPL thickness in the formation was increased to 14cm and three different flow rates were measured. Then the LNAPL thickness was increased again, this time to 25 cm, and three flow rates were measured, all using the same procedure. The results from all the experiments at all three LNAPL thicknesses are tabulated in Table 1 and plotted in Figure 18 as flow rate in the tank vs. percent of flow measured through the well.

Results From The Large Tank Study					
LNAPL Thickness	Tank Flow Rate (L/day)	Flow Rate Through Well (L/day)	% of Tank Flow Through Well	Maximum %	Minimum %
9cm	3.024	1.01	33%	34.0%	32.7%
	2.880	0.97	34%	34.3%	33.3%
	0.720	0.18	25%	25.3%	24.8%
	0.072	0.02	25%	26.1%	24.3%
	0.086	0.02	26%	27.0%	25.7%
	0.013	0.00	25%	27.2%	23.4%
13cm	0.020	0.00	25%	27.3%	21.8%
	0.432	0.10	23%	23.1%	22.5%
	3.888	0.85	22%	22.2%	21.8%
24cm	0.100	0.037	37%	38.3%	35.4%
	0.792	0.23	29%	30.2%	27.6%
	2.880	0.81	28%	28.9%	27.5%

Table 1: Results of the Large Tank Study

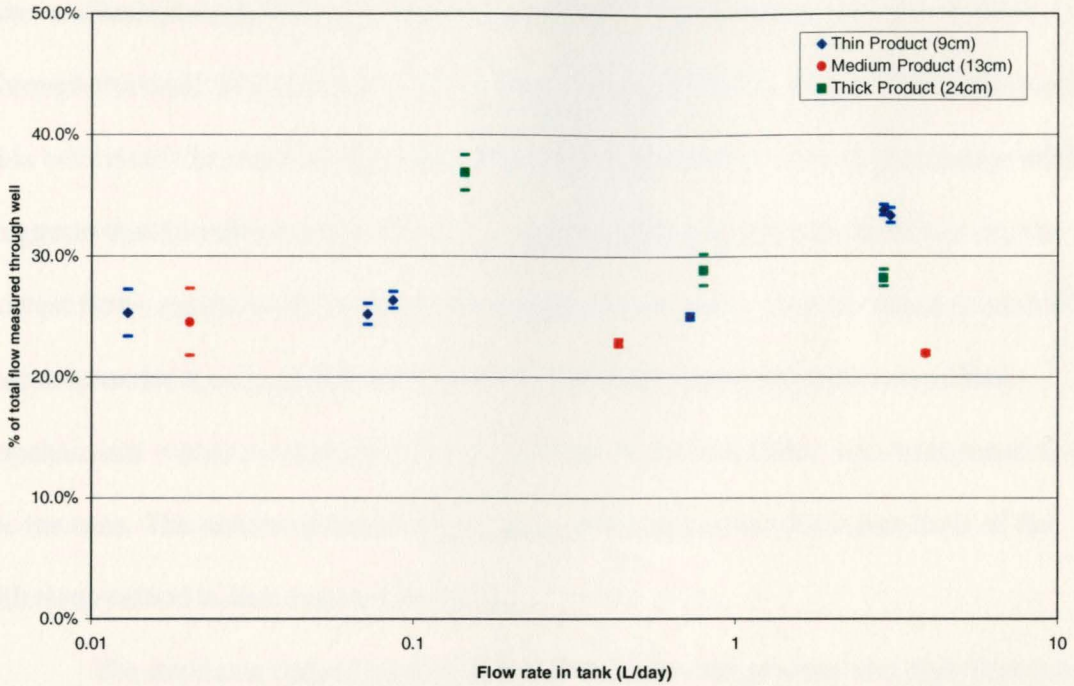

Figure 18: Results of Large Tank Study

Plotting all of the experimental runs in this format suggests that no distinct trend exists between flow rate and percent of flow measured through the well. All of the results are between 22% and 34% of the total tank flow, which corresponds to a convergence factor of between 1 and 2 times the well radius (or diameter if the tank has used a full well).

It was expected that the results would predict flow rates of greater than 17%. A range of 22% to 34% certainly satisfies that criteria. Moreover, the data collected fits the model very well, as shown in Figure 14, Figure 15, and Figure 16. The results from these experiments have demonstrated that the tracer dilution technique can be applied to LNAPL to successfully predict the LNAPL flow rate through a well.

Figure 18 does show a diminishing trend in the accuracy as the flow rate changes. At medium to high flow rates the error associated with the experiments is small. As the flow rate decreases the error increases. At the low flow rates, it was expected that other

loss mechanisms might start to affect the results by increasing the calculated flow through the well. The thin and medium thickness experiments, at low flows, do not show this behavior. The fact that the flow predictions do not show a higher percentage of flow suggests that the effects of the other loss mechanism are small compared to even the lowest flows explored. These experimental runs have shown that the dilution method is accurate under a wide variety of flow rates. The hypothesis that other tracer loss mechanisms would increase the flow predictions at the low flows was determined to not be the case. The results of these experiments demonstrate that the lower limit of the dilution method is less then $0.03 m^3/m/yr$.

The duplicate experiments conducted with the thin product and high flow rate represent an unusually high velocity that is very uncommon under natural conditions. It is possible that under extremely high LNAPL velocities, the well convergence factor increases as a result of a greater difference in head loss through the well and the formation. These experiments also ran quickly, making it difficult to mix the tracer before the tracer had been significantly diluted, which increased the error of these tests.

The error presented in Table 1 and Figure 18 is the measured error in the tracer dilution method; however, other sources of error also affected the results. Setting the flow rate in the tank (the dependent variable) was not a simple task. Small changes to the pump settings caused large changes in the flow rate. Moreover the flow rate was often not constant, and the large volume of LNAPL in the tank required a long period of time to respond to changes. This made establishing a known, steady-state LNAPL flow through the tank a challenging task. These errors were minimized by carefully measuring the flow

rate over long periods of time (24 hour averages) and allowing the tank to equilibrate for extended periods of time between flow rate changes.

The range of flow rates for which the dilution method has been shown to be accurate varies from 0 .035 m^3/m/yr to more then 7.2 m^3/m/yr. The results of these experiments also demonstrate that the extent that flow converges about a well, for the experimental conditions, is between 1 and 2 times the well screen diameter. More significantly, the convergence is not a strong function of the flow rate. While different formations and well screen types may produce a variety of convergence factors, the convergence factor is not a function of the LNAPL flow rate.

The results of the no flow (static) test were not as successful. The test was conducted at the start of the medium product studies with 13cm of LNAPL in the formation (medium LNAPL thickness). The tank had been allowed to sit for approximately four weeks after increasing the LNAPL thickness. Based on fluid levels in the head tanks, it was thought the LNAPL flow rate was zero. The full results from this test are graphed below in Figure 19 as normalized tracer concentration (fluorescent intensity) vs. time.

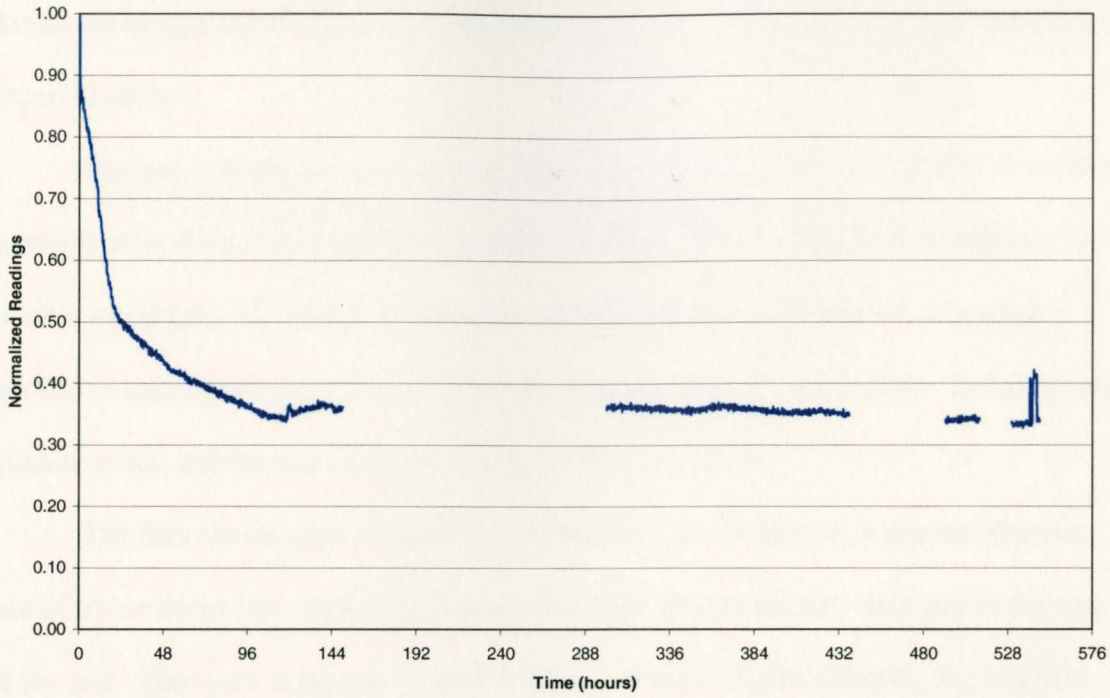

Figure 19: Results of the "Static Test"

The initial concentration was slightly greater then the other tank studies to ensure the concentration would initially decay. As can be seen in Figure 19, the tracer did initially decline very quickly, primarily due to mixing taking place. Initially, the tracer in the mixing system was intense relative to the concentration in the well. After approximately eight hours, the well volume appeared well mixed so the mixing pumping rate was slowed. When the mixing rate was decreased, a sharp change in the tracer decay could be observed. This abrupt change in tracer decay demonstrates that the high mixing rate was contributing to the tracer dilution. 24 hours later, one day into the experiment, the mixing rate was again lowered; this time there was no change in the rate of tracer decay.

The results of the first day show that the mixing device can contribute to tracer migration at low flow rates. However, when the mixing rate is moderate to low, the effects of mixing are minimal, clearly demonstrating that the mixing rate during the test

should not be any higher than necessary, to ensure the mixing does not contribute to tracer dilution.

The tracer decayed at a relatively high, but decreasing rate, for the first three days, at which point the tracer concentration spiked slightly. This spike could be due to a number of factors, including a temperature variation in the spectrometer, or a small amount of tracer from the injection syringe being released into the system. In either case, spike is small, and the rate of decay returns to the same slope.

The data shows gaps caused by computer glitches; however, it appears that the rate of tracer decay was relatively constant from just before the first data gap to the end of the test. The spike at the end of the record is a result of lights affecting the readings.

The middle portion of the curve--hours 288 through 432--was isolated and a regression performed to determine what flow rate the steady portion of the curve would represent if fitted to the governing equation for flow through a well. The data was normalized and fitted to the model using the same procedures as the other large tank experiments. The best fit and confidence limits of the analysis are shown in Figure 20.

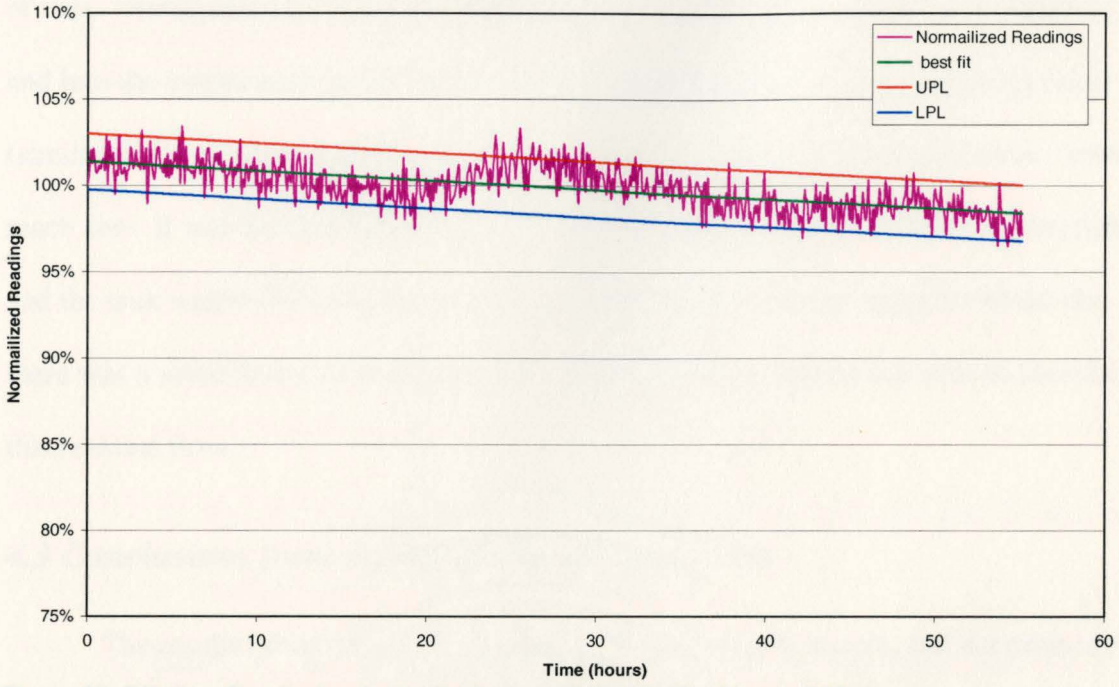

Figure 20: Dilution Results for the Static Test and LNAPL Thickness of 13cm

The results of the analysis calculate a flow of 0.003 $\pm$ 0.001 L/day (~0.03m^3/m/yr). Analysis shows that when the data is compared to the expected result in the dimensionless format, the data has a slope of 0.695 while the expected slope is 0.693, a very similar slope. If the tracer losses were, in fact, due to other loss mechanisms, the results would not fit the model for flow as closely. Moreover, the estimated flow rate from the static test is almost identical to the low flows explored. If the other loss mechanism were this high during the other tests, the results of low flow tests should have indicated a much higher flow rate.

While it is possible that the other loss mechanism contributed to a flow rate of 0.003L/day, it is unlikely. Other experimental runs which were conducted at flow rates similar to 0.003L/day and did not indicate that other loss mechanisms were important factors. Leading up to the static test, LNAPL was added to the head (upstream) tank at a high flow rate. The tank was then allowed to sit with no pumping for an extended period

of time. During that time, LNAPL migrated from the head tank, through the formation, and into the downstream tank. Theoretically, this process follows an exponential curve (similar to the dilution curve) so the flow through the formation will approach but never reach zero. It was thought with the coarse, uniform sand this process would occur quickly and the tank would stabilize. However, the results of the static test suggest instead that there was a small flow of LNAPL present, and the dilution method was able to measure this residual flow.

4.3 Conclusions from the Laboratory Experiments

The results of the laboratory studies explored different tracers, and determined that BSL 715 most closely met the criteria of an ideal tracer. A number of mixing methods were also explored through visual observation. The observations led to the development of a diffusive mixer, which was found to adequately mix the tracer while not causing tracer losses.

Twelve experiments were conducted in the large tank study. The large tank study explored a representative range of LNAPL flow rates from 0 .035 $m^3/m/yr$ to 7.2 $m^3/m/yr$ over three LNAPL thicknesses ranging from 10cm to 25cm. All twelve tests predicted a flow rate through the well which was within the range of expected values. Overall, the large tank study met the objectives of the experiment:

- The results show that the tracer dilution method can be applied to LNAPL to predict flow rate through an observation well.
- The data collected fits the model very closely and produces accurate results.

- The current application of the tracer dilution tests have been shown to work under a wide range of flow rates, including flow rates that are extremely small, representing almost stagnant LNAPL pools.
- It was demonstrated that the convergence about a well is not a strong function of the flow rate, and current methods of predicting the convergence slightly over estimated the measured values for the conditions used in the large tank experiment.
- The technology necessary to conduct tracer dilution tests was developed and refined.

In addition to the 12 tests at known flow rates, an additional experiment was conducted for the large tank study to quantify the other loss mechanisms. To do this, a tracer dilution test was conducted under what were thought to be stagnant conditions. Analysis of the static test results indicate that the tank was not at a completely static state. Moreover, the tracer dilution method was able to measure this low flow rate. Future tests should be conducted to quantify the other loss mechanisms under more controlled conditions. However, the tests thus far indicate the dilution method accurately measures flow rates as low as 0.014L/day. The results from each experiment in the large tank study are presented in Appendix A.

5.0 Field Study

This section describes the field experiments conducted to explore the feasibility of using tracer dilution techniques to measure LNAPL flow in the field. The studies were conducted at the former ChevronTexaco Refinery located northeast of Casper, WY along the south bank of the North Platte River. The refinery, constructed in the early 1920's, actively processed crude oil until 1982. During the sixty plus years of operation, many areas of the site were impacted by LNAPL releases. To contain and clean up these contaminated areas, recovery wells and interceptor trenches have been installed; in total, more then one million gallons of LNAPL has been recovered from the North Platte Alluvium. There is presently a discussion underway to determine an end point for the recovery operations. One of the possible end points being discussed is to stop recovery operations when the remaining LNAPL has reached an inconsequential flow rate. Based on the laboratory experiments in the previous section, tracer dilution tests are a potentially cost effective means to measure *in situ* LNAPL flow rates.

To better understand the potential for tracer dilution tests to measure LNAPL flow, the technique was deployed in two locations. The first was in an area near a recovery well where the LNAPL flow was anticipated to be high. The second test was conducted in a stable region where the LNAPL flow was likely to be low.

5.1 Objectives

The objectives of the field study include:

- Identify any field scale problems or limitations of the procedure, methodology, or equipment employed.

- Determine if tracer dilution techniques can be used to estimate LNAPL flow rates in the field.

5.2 Methods

Twelve wells had previously been selected as possible candidates for the field tests, based on LNAPL thickness, LNAPL properties, and potential for migration. The selected wells were then monitored weekly in an attempt to resolve the stability of the fluid levels. The final locations for the tests were determined based on fluid level stability and proximity to active recovery systems. The detailed setup procedure used to conduct the well dilution tests is presented in Appendix C.

5.2.1 Equipment

The equipment used in the field study is described below. Where possible the filed equipment was the same, or modeled after the equipment used in the laboratory studies.

5.2.1.1 Mixing Device

Building on the laboratory studies, a prototype diffusive style mixer, shown in Figure 21, was constructed to keep the tracer concentration uniform in the well. The prototype mixer consisted of six 0.64cm (0.25in) diameter by 91cm (36in) long, thin wall stainless steel tubes with two rows of 0.6mm (0.024in) diameter pinholes drilled 5cm (2in) on center, 180 degrees apart. The diffuser tubes were mounted, equally spaced, around a 2.54cm (1in) diameter thin wall stainless steel tube and connected, via manifolds, to a miniature peristaltic pump. The peristaltic pump head and rotor (Instech P625 miniature pump) were modified to fit inside the pump housing. A bearing set and

drive connection were constructed from stainless steel. The pump is driven from the surface via a flexible drive cable which was custom built from heavy duty speedometer cable. The manifolds were constructed out of 3.8cm (1.5in) solid stainless steel rod, cut to ~0.64cm (0.25in) thick. Holes were then drilled in the lower face to receive the diffuser tubes; the holes were connected to a custom hose barb in the top of the manifold by drilling holes through the side. The diffuser tubes, and outside edges of the manifolds were then soldered to connect the diffusers and seal the holes in the side of the manifold.

To measure the fluorescence of the tracer, the hose barbs in the intake manifold employed a tee connection with the end of a 10m (33ft) fiber optic cable inserted in the top of the tee. The intake to the pump was then located on the side of the tee. The tee connection on the exhaust diffuser is an "L" shaped connecter. The manifold hose barbs were connected to the pump via a Viton^{tm} 0.045cm ID hose.

Above the pump, a 0.3cm (0.125in) wire rope (cable) was attached for the mixer to hang from. The Viton^{tm} tube, pump and fiber optic cable were then enclosed in a cover constructed from a 3.8cm (1.5in) stainless steel tube. The top of the tube was tapered at 30^{o} to allow the mixer to slide up through the well casing easily. A second cap, also tapered, was installed at the bottom of the device to hold the diffuser tubes in place and allow the device to slide down the well casing. Finally, a small tube (0.15cm ID) ran from the surface down past the outside of the pump cover into the LNAPL zone so the tracer could be injected from the surface.

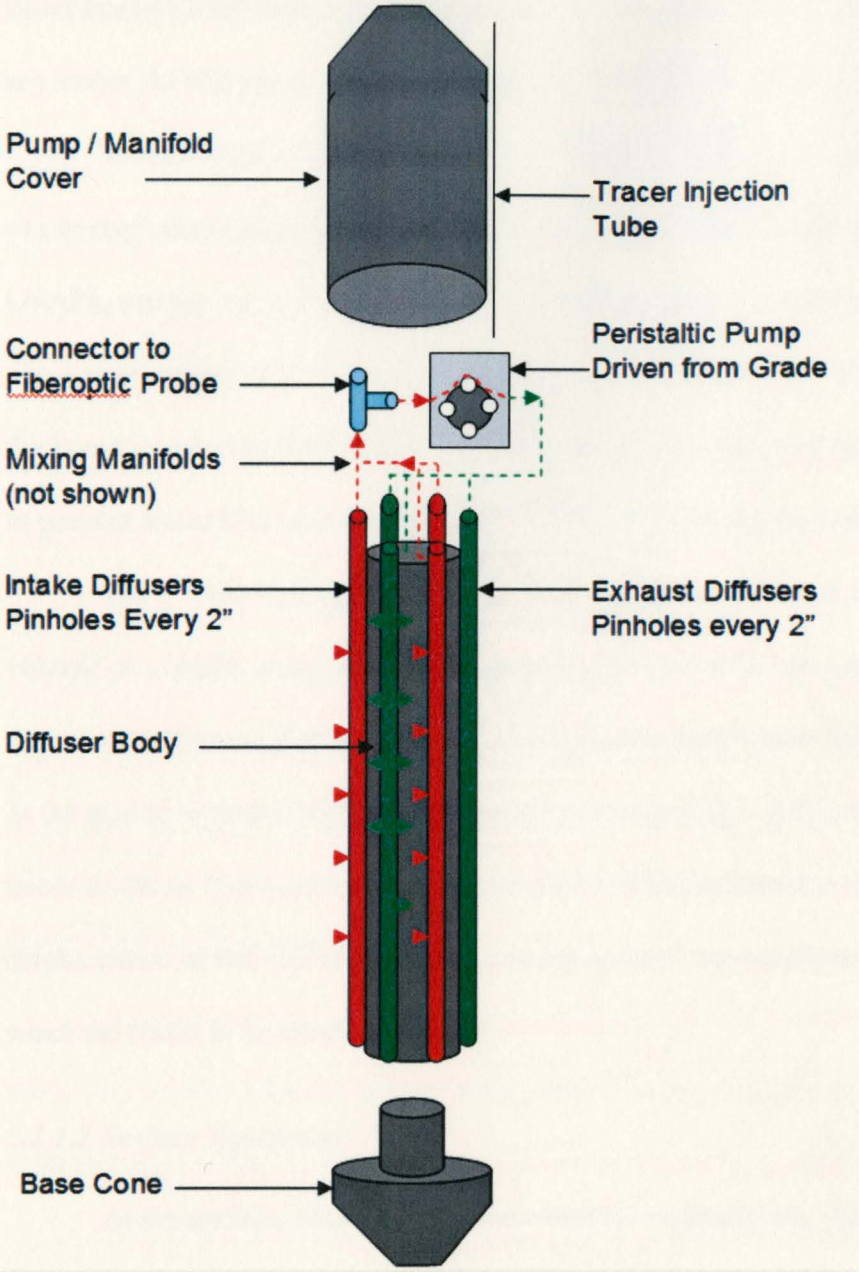

Figure 21: Downhole Diffusive Mixer Design

The mixer works by drawing LNAPL into three opposing diffuser tubes via the small holes. The diffusers mix the tracer without disturbing the equilibrium in the well. The mixed flow then passes into the sampling tee and past the fiber optic cable, so the concentration readings represent the entire well contents. After flowing through the pump, the mixed flow is then separated into three streams via the exhaust manifold and

flows back into the well through the other three diffuser tubes. This process eliminates any major in-well gradients by mixing the tracer in the manifolds of the mixing device.

The diffusers extend past the water LNAPL interface so the same mixing device can be used in a variety of LNAPL thicknesses. The density difference between the LNAPL and the water prevents water from being pulled through the diffuser tubes (much like a straw with a hole at the top will draw in air before water). When the LNAPL thickness is very small relative to the mixer length, the pumping speed must be decreased to prevent water from mixing with the LNAPL and forming an emulsion.

The 1" hollow body provides a solid base for the diffusers as well as isolating a volume of LNAPL in the well. Isolating part of the LNAPL has a number of benefits: 1) the amount of tracer required is reduced; 2) the time required to mix the tracer is reduced; 3) the active volume of LNAPL in the well (mixing cell) is reduced, which causes the tracer to decay faster, increasing the sensitivity of the measurements. And 4) the displacement of the tool is minimized, which reduces any gradients surrounding the well when the mixer is inserted.

5.2.1.2 Surface Equipment

At the surface, enclosed in a steel weather resistant box, the spectrometer and computer from the laboratory experiments are used to record the tracer concentration. An electric motor (GHK GT21-18 reversible drive motor) drives the downhole pump via the drive cable. A battery backup prevented the computer from rebooting in the event of a power failure. Finally, the wire rope was attached to the top of the well casing to hold the mixer at a fixed elevation.

5.2.2 Data Acquisition

During the test, the spectrometer and computer recorded data at four wavelengths. The first was 480nm, which is approximately the incident wavelength of the spectrometer. This wavelength remains fairly constant unless the pump fails or an air bubble forms at the detector. The second and third channels recorded are 545nm and 580nm respectively. These channels record the two peak values associated with the fluorescence of the tracer; both of these channels are representative of the tracer concentration and follow a similar trend. The fourth wavelength monitored, 700nm, was used to resolve any changes in the background readings during the test. Readings were recorded every one minute. At the conclusion of the test, data from the 580nm wavelength was fitted to the exponential model via a least squares regression (as was done with the laboratory experiments) to predict the flow through the well.

5.2.3 Well Construction

The wells selected for the field demonstration were constructed of 10cm (4in) PVC well screens with 0.5mm (0.020in) slots. The observation wells were installed using a 20cm (8in) hollow stem auger and have a 5cm (2in) gravel pack of 10-20 silica sand.

The first test was conducted in well SS-146, which is located approximately 12 meters (40ft) away from an active recovery well on the north side of the former refinery, near the North Platte River. The well is screened from 0.9 to 9 meters (3ft to 30ft) below the ground surface. During the dilution test, the LNAPL thickness in the well was approximately 30cm (12in). The depth to LNAPL from grade was 2.7meters (9ft) feet.

The second test was conducted in well SS-115 which is located in the southwest corner of the property. SS-115, constructed in 1994 as an observation well, was later

used to recover product for a short time in 2000. The well is screened from 4.8 to 7.9 meters (16 ft to 26 ft) below grade, and during the test there was approximately 23cm (9in) of product located 5.4 meters (18ft) below grade.

Unfortunately, the selected wells are both 10cm (4in) in diameter, while our downhole mixing device was designed to fit into a 5cm (2in) well. While the mixer works in larger diameter wells, the greater active volume (5 times that of a 5cm (2in) well with the mixer inserted), will greatly reduce the sensitivity. The reduction in sensitivity can be overcome, in part, by running the tests for a longer time period.

5.3 Results

Overall, the prototype performed well, meeting the objectives of the experiment. The prototype worked sufficiently well to demonstrate that dilution techniques can be used to predict LNAPL flow rates through a well. However, there are a number of improvements that can be made to increase the accuracy of future results.

A number of challenges encountered during the study increased our understanding of subsurface LNAPL migration, and highlighted technical limitations in the equipment, and methodology. Fortunately, it was possible to correct, or work around, the technical limitations. With additional equipment it will be possible to correct many of these limitations and improve the usefulness and accuracy of the method. The challenges are described in more detail in the following sections.

5.3.1 High Flow Test

The first test was conducted in well SS-146, which is located approximately 40 feet from an active recovery system. Data collected prior to the experiment indicated

stable fluid levels for the two months prior to testing. The first test in the field study was started on the afternoon of September 16th, 2003. The test was concluded on September 23rd.

5.3.1.1 Data Analysis

Analyses of the results indicate a flow of 0.07 $\pm$ 0.01 L/day through the well. Depending on the well convergence factor, which most likely varies from 1 to 2 times the well diameter (based on results from laboratory studies), the flow rate in the formation, per unit width of LNAPL body, is 0.1 to 0.3 $m^3/m/yr$ (~1 to 3 $ft^3/ft/yr$). While ultimately successful, the test was not without challenges; these included:

1) Adjustments to the nearby recovery system during the test resulted in falling fluid levels, causing technical problems with the equipment. For the diffusers to function properly, the highest diffuser hole must be set just below the LNAPL air interface. When the fluid levels fell, the diffuser began to pump air instead of LNAPL, preventing the tracer from being mixed and the computer from recording useful readings. Running the pump without fluid for an extended time also caused the pump hose to bind and break. Falling fluid levels also altered the LNAPL thickness in the well. When the LNAPL thickness in the well is changing, the assumptions of steady state are violated and the governing equation should not be applied.

2) The spectrometer is temperature sensitive; to compensate for the varying temperatures experienced in the field, the spectrometer is equipped with a thermo-regulator. During the first test, it became obvious the thermo regulator was not sufficient to compensate adequately. This introduced a cyclical pattern to the readings as the temperature varied.

Due to these complications, the data analysis was limited to a period of ~70 hours of contiguous data. Figure 22 shows the tracer concentration vs. time for the 70 hours of data. The cyclical pattern from temperature variation is clearly visible. However, there is a distinct decreasing trend. Using a least squares regression, the model was fitted to the data and a flow prediction calculated.

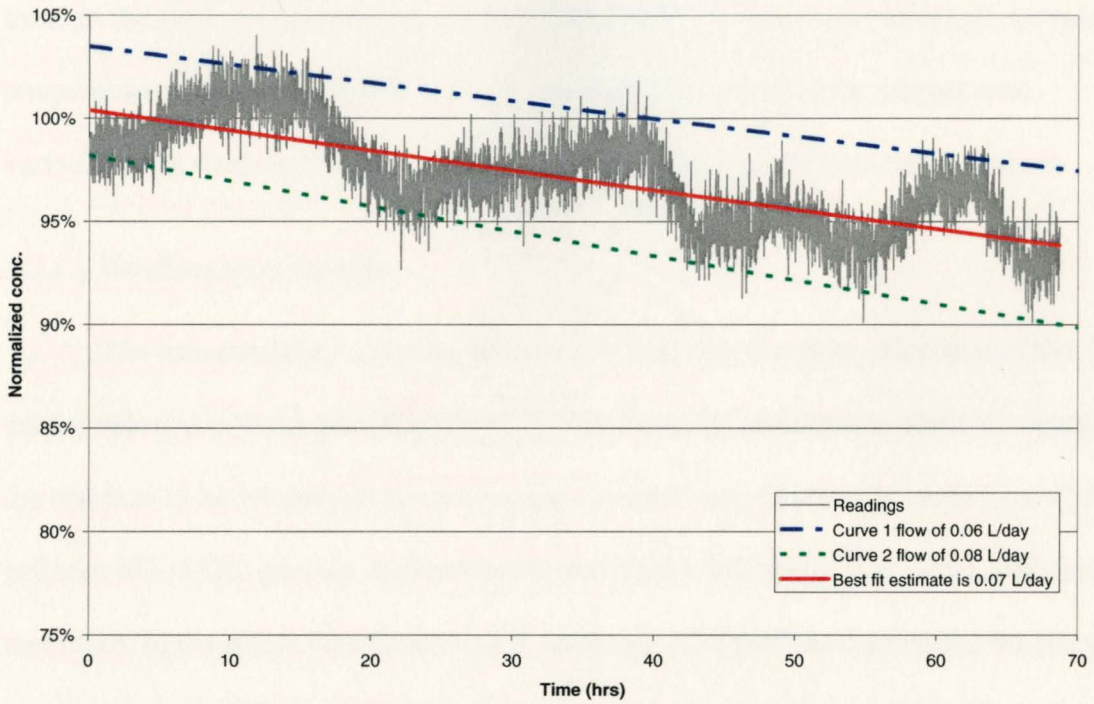

Figure 22: Least Dilution Results for SS-146

As an alternative to least squares regression, a type curve analysis can be used to best fit a curve to the data visually. Figure 22 also shows two additional curves. The slope of the first curve represents the lowest flow that can be reasonably fitted, visually, to the data. Similarly, the second curve shows the highest flow. Using type curve analysis one can quickly obtained a range of values that provide a simple and reasonably accurate method to analyze the data from a dilution test. The type curve analysis can also be used

to confirm the accuracy of the least squares regression. For the data in Figure 22, the type curve analysis and least squares analysis agrees quite well.

The error analysis used in the laboratory experiments was also applied to the results in Figure 22. Due to the large temperature variations in the data, this algorithm produced large errors. The fit of the maximum and minimum curves did not follow the trend in the data, and it was not possible to remove the temperature variations because the temperature of the spectrometer was not recorded. As a result of the temperature variations, the final error in the flow calculation is based on the type curve analysis.

5.3.1.2 Verification of Results

The measured flow rate was then used to calculate the production rate of the nearby recovery system (see Appendix D). Results of the calculations show that during the test (a very active period) the production system was producing 11 to 30 liters (3 to 8 gallons) of LNAPL per day. Unfortunately, the production rate of individual wells is not measured, so the actual production rate is unknown. The total production for the site prior to the test was 3400 liters (900 gal) per month or 111 liters per day (~30 gal/day). It seems reasonable that one recovery system could produce 10% and 25% of the total production.

A bail down test had been conducted at well SS-146 at similar initial fluid levels. By using the transmissivity calculated from the bail down test and the results of the dilution test, the LNAPL table gradient can be estimated. The calculations (see Appendix D) estimate the local LNAPL gradient to be between 0.0003 and 0.0007. This seems like a reasonable gradient near an active recovery well. Although there was insufficient site data to conclusively determine if the dilution method correctly estimated the LNAPL

flow, the estimated production rate and LNAPL gradient calculations are consistent with conditions at the time of the test.

5.3.2 Low Flow Test

The second test was conducted in well SS-115, which is located in the southwest corner of the former refinery. The recovery wells in this area are not active and it is thought the LNAPL is largely stable. The test began on October 22nd and was concluded on October 29th.

A least squared analysis of the data collected predicts a flow of less then 0.005 L/day through the well. Because of the extremely low flow combined with current limitations of the equipment and extreme temperature variations during the test, the data gathered does not follow a typical decay curve. The temperature variations are large compared to the change in fluorescent intensity, making any analysis challenging. A least squares regression performed on the later portion of the data set, when the temperature variations were less extreme, predicted a flow rate of 0.003L/day. However, due to the large errors and resulting poor fit, the slope of this curve and the resulting flow rate calculations are not significant. When type curves are visually fitted to the late time data, the resulting flow rates are estimated to be between zero and 0.005L/day. The results of this test suggest there is no flow through well SS-115 and the product in the area is stable. The results of this test are graphed in Figure 23.

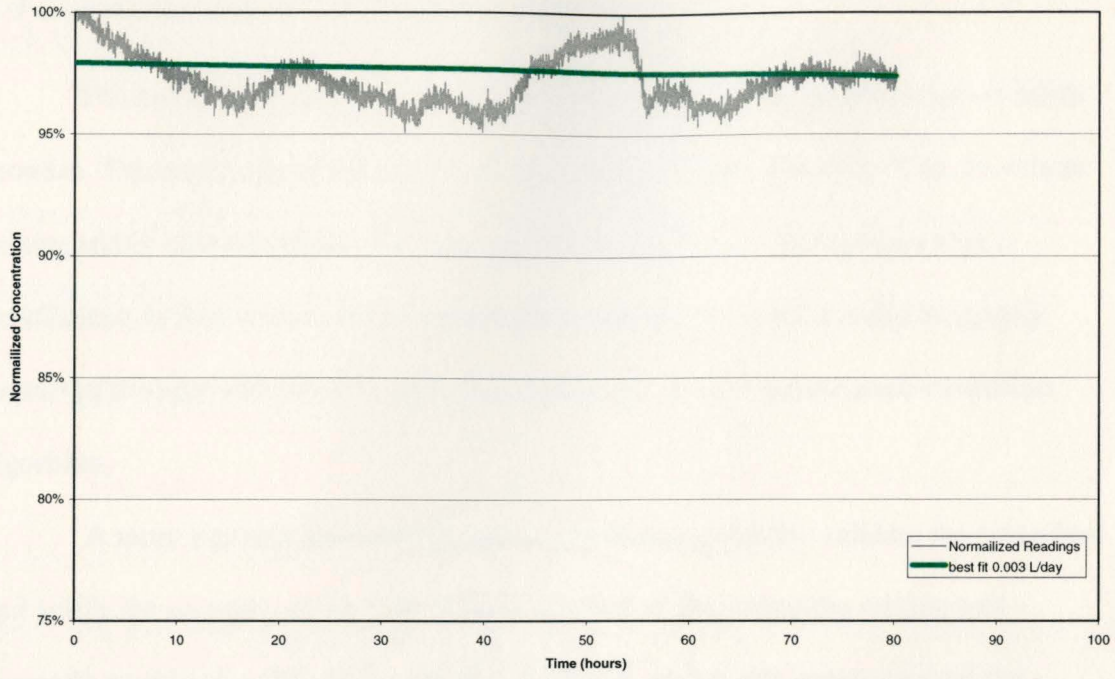

Figure 23: Dilution Results for Well SS-115

The error analysis developed for the laboratory studies was also performed on the data in Figure 23. The results confirm the error is large and varies from approximately 0.005 L/day to zero. The results of the time step analysis also developed for the laboratory experiments demonstrated that the solution did not converge; that is, the flow rate is a function of how much data is used in the regression analysis. The flow rate predictions' failure to reach a steady value suggests that more data is required to determine the flow rate accurately. Nonetheless, the data collected clearly demonstrate a near zero flow that is below the detection limit of the current method. In any case, the results of the second test clearly estimate a much lower flow than was measured in SS-146.

5.4 Conclusions from the Field Study

The initial field study successfully demonstrates that the dilution method holds promise. The sensitivity of the measurements can be greatly improved if the downhole mixing tool is sized properly. The current thermo-regulator in the spectrometer is insufficient; in future tests, the lower detection limit of the method could be greatly improved through additional temperature regulation, or via a temperature correction algorithm.

A more rigorous field test should be conducted to further validate the procedure and verify the accuracy of the tests already conducted. By sizing the mixing tool correctly, to minimize the active volume of LNAPL and to adequately control the temperature of the spectrometer, one can improve the resolution of this method.

6.0 Conclusions

Overall, the tracer dilution technique was determined to be an effective method to measure LNAPL flow rates. Through a review of the objectives and results, the following section presents conclusions.

6.1 Mathematical Developments

The mathematics for this thesis builds on previous work with the tracer dilution technique used to measure groundwater flow. In addition to presenting this previous work, this thesis develops a dimensionless analysis technique. The dimensionless analysis can be used to determine when data is due to tracer dilution alone and when the apparent tracer dilution is due to other processes. This thesis also provides a solution to calculate the diffusive losses based on an analog of a slug test. The diffusive solution demonstrates that the losses are relatively small compared to the LNAPL flow rates measured for this thesis. Finally, this thesis presents the necessary methods and equations to convert the tracer dilution data into LNAPL Darcy flux, average LNAPL seepage velocity, and average LNAPL conductivity.

6.2 Resolve the Applicability of the Tracer Dilution Technique

The tracer dilution technique has been studied and extensively applied to measuring flow rates of groundwater. Building on this work, a series of experiments were conducted to resolve the applicability of the tracer dilution technique to measure LNAPL flow rates. The results of these experiments indicate that the tracer dilution technique can measure *in situ* LNAPL flow rates from 7.2 $m^3/m/yr$ to less then 0.035 $m^3/m/yr$. The

tracer dilution technique provides a direct measure of LNAPL flow rates. This method does not require the complex and indirect measurements that are necessary to measure LNAPL flow via other common methods.

To understand and explore the potential of the tracer dilution technique to measure LNAPL flow rates, experiments were conducted both in the laboratory and the field. The preliminary laboratory experiments explored a variety of tracers and mixing devices. It was determined through the preliminary studies that the mixing technique used to maintain a uniform tracer concentration in the well is vital to obtaining accurate results.

Experiments were also conducted in a large tank, which simulated a field scale. These experiments rigorously tested the tracer dilution technique at LNAPL thicknesses of 9cm, 13cm, and 24cm over a range of LNAPL flow rates from 7.2 m^3/m/yr to 0.035 m^3/m/yr. The large tank studies demonstrated the ability of the tracer dilution technique to measure LNAPL flow rates repeatably, reliably and accurately.

Two field tests were conducted to validate the procedure at a field scale and refine the technology. The first experiment was conducted near an active recovery system and measured a flow rate of 0.1 m^3/m/yr to 0.3 m^3/m/yr. The second field test, conducted in a quiescent area, determined the flow rate of LNAPL was less then 0.009 m^3/m/yr. The field experiments further demonstrated that the tracer dilution technique is an accurate means to measure LNAPL flow rates. The field experiments also highlighted limitations of the method and revealed a number of avenues for improvements.

6.3 Develop the Technology to Apply Tracer Dilution Techniques

Through the efforts described in this thesis, the technology necessary to conduct tracer dilution tests in LNAPL has been developed and tested. First, a tracer which met the criteria presented in a previous section was identified. It was determined that a fluorescent tracer, BSL 715, met these criteria. BSL 715 is easily detectable at concentrations of less then 1 part per million, chemically stable, insoluble in water, and has a low toxicity relative to many compounds typically found in LNAPL bodies. A custom spectrometer and computer were selected to measure and record the concentration of the tracer through time.

In the small tank experiments, a mixing device was designed and tested. This mixing device utilizes a number of vertical diffuser tubes and manifolds to keep the tracer concentration uniform while not causing excessive tracer losses. This mixing system uses diffuser tubes to withdraw LNAPL and tracer from a number of points in the well and then mixes the samples internally. The uniform mixture then flows back to the well at a number of points via diffuser tubes. This system works by mixing the tracer internally, and not inducing significant flow within the well.

6.4 Future Work

To our knowledge, this thesis describes the first use of tracers in NAPL to resolve flow. The experiments conducted thus far demonstrate the ability of the tracer dilution technique to accurately measure LNAPL flow rates under typical conditions. Through additional experimentation and improvements to the technology, the usefulness of the tracer dilution technique can be expanded.

6.4.1 Additional Experiments

More work is necessary to understand the processes that govern the convergence of LNAPL flow about a well. An accurate determination of the convergence factor is vital to calculating the flow rate of LNAPL in the formation. Building on Ogilvi's equation, one finds that the convergence factor is proportional to the contrast in permeability between the well and the formation. For groundwater, this ratio can be fairly simple to determine; however, LNAPL conductivity varies vertically as a function of saturation. To further complicate the process, the type of well screen and the drilling technique can also affect the convergence. Future work in the area should consider the variable NAPL conductivity and should take into account different types of well screens. Future work should also consider the tendency for some well drilling techniques to smear a layer of fine material about the wellbore, which inhibits flow through the well.

Transient flow conditions should also be considered. The work completed for this thesis assumes the flow rate through the well is constant for the duration of the test. Through additional research, it should be possible to measure a varying flow rate via a tracer dilution test.

Unstable fluid levels were encountered during the field study, which complicated the analysis of the field tests. A better understanding of the processes which govern the tracer dilution during unstable water table conditions could provide guidance in determining when the tracer dilution test can accurately measure NAPL flow rates and when the tracer dilution is not related to the flow rate in the formation.

The lower detection limit of the tracer dilution technique has the potential to be greatly improved by quantifying the effects of the other loss mechanism. As a starting

point, the first order dilution curve could be modified to include the diffusion solution presented in Appendix B. The effects of other loss mechanisms could then be explored through addition experimentation or mathematical models.

A more rigorous error analysis algorithm should be investigated. The error analysis algorithm developed for this thesis quantified the error for the initial experiments. Additional effort should be given to improving this algorithm, and/or developing another measure of the uncertainty in the tracer dilution test.

This thesis has focused on measuring the flow rate of LNAPL. The same processes, procedures, and technology should be applicable to DNAPL flow. Although the mixing system will require some modification, the mixing concept should be applied. A series of experiments similar to those described in this thesis could then be conducted to verify the accuracy of the tracer dilution method to measure DNAPL flow rates.

Lastly, this thesis is one of the first known applications of tracer studies to evaluate LNAPL flow. The potential for other types of tracer tests to be applied to NAPL is significant. The development of other tracer tests may lead to a suite of tracer tests to characterize NAPL migration.

6.4.2 Improvements to the Technology

In the process of conducting the experiments, a number of opportunities to improve the technology were observed. During the field tests, it was determined that the thermo-regulator in the spectrometer was not sufficient because the temperature of the spectrometer greatly impacts the accuracy of the readings. For this method to be deployed in field applications, it will be necessary to improve the temperature regulation of the

spectrometer. By adequately controlling the temperature of the spectrometer, the accuracy of future field tests would be greatly improved.

Future mixing devices should also be constructed to minimize the active volume of the well during the tests. The large volume of LNAPL used in the field test reduced the rate of dilution and compromised the sensitivity. By minimizing the volume in the well the sensitivity to flow can be greatly increased.

Lastly, upgrades to the computer hardware and software could greatly expand the ability of the onsite computer. Customized software could be designed to not only record but process the data in real time. Customized software combined with a cellular connection would allow technicians to remotely view the status of the test in progress, including the estimated flow rate. The onsite computer could also be designed to alert users of any problems as they occur. These improvements to the computer would greatly increase the usefulness of the method and could reduce the cost of each test.

References

Brooks, R. H., Corey A.T., (1966), Properties of Porous Media Effecting Fluid Flow. ASCE journal of Irrigation and Drainage. IR2, v. 92, pp 61-88.

Charbeneau, R.J., Johns, R.T., Lake, L.W., McAdams, M.J., (1999), Free-Product Recovery of Petroleum Hydrocarbon Liquids. API publication 4682, June 1999.

Corey, A.T., (1990), Mechanics of Immiscible Fluids in Porous Media second edition,Water Resources Publications ISBN-0-918334-58-6.

Drost, W., Klotz, D., Koch, A., Moser, H., Neumaier, F. and Rauert, W. (1968), Point Dilution Methods of Investigating Ground Water Flow by Means of Radioisotopes. Water Resources Research 4, pp 125-146.

Edwards, C.H., Penney, D.E., (2000), Elementary Differential Equations (fourth edition).Prentice Hall, Upper Saddle River, NJ. 07458.

Farr, A.M., Houghtalen, R.J., McWhorter, D.B. (1989), Volume estimation of Light non-aqueous phase liquids in porous media. Journal of ground water, May 1989.

Freeze, R.A., Cherry, J.A., (1979), Groundwater. Prentice-Hall publishing company, Englewood Cliffs, NJ, 1979.

Gaspar, E. (1987), Modern Trends in Tracer Hydrology Vol. II. CRC press, Boca Raton, FL ISBN 0-8493-4321-6.

Halevy, E., Moser, H., Zellhofer, O., and Zuber, A., (1967), Borehole Dilution Techniques: a Critical Review. Proceedings of the 1966 symposium of the international atomic energy agency, pp 531-564.

Huntley, D., (2000), Analytic Determination of Hydrocarbon Transmissivity From Bail-down Tests. Groundwater, Vol 38 No. 1, January-Febuary, pp.46-52.

Lamontagne, S., Dighton, J., Ullman, W., (2002), Estimation of Groundwater Velocity in Riparian Zones Using Point Dilution Tests. CSIRO land and water technical report 14/02, May 2002

Marinelli, F., Durnford, D.S., (1996), LNAPL Thickness in Monitoring Wells Considering Hysteresis and Entrapment. Ground Water V34, No. 3, pp.405-414.

McWhorter, D.B., (1996) Processes Affecting Soil and Groundwater Contamination by DNAPL in Low-permeability Media. Oak Ridge National Laboratories, ORNL-27 (3-96).

McWhorter, D.B., and Sale, T., (2000), The Mobility of Liquid Hydrocarbon Below the Water Table. Unpublished document.

Sale, T., and Applegate, D., (1997), Mobile NAPL Recovery: Conceptual, Field, and Mathematical Considerations. Ground Water, vol. 35, No, 3 May-June 1997.

Sale, T., (2001), Methods for Determining Inputs to Environmental Petroleum Hydrocarbon Mobility and Recovery Models. API Publication 4711, July 2001.

Sale, T. (2003), Answers to Managing Frequently Asked Questions about Managing Risk at LNAPL Sites. API soil and groundwater research bulletin number 18, May 2003

VanGenuchton, M.T., (1980), A Closed-form Equation for Predicting the Hydraulic Conductivity of Unsaturated Soils. Soil sci. soc. Am J 44:892-898

Wilson, J.L., Conrad, S.H., Mason, W.R., Peplinski, W., Hafgan, E., (1990), Laboratory Investigations of Residual Liquid Organics from Spills, Leaks, and the Disposal of Hazardous Wastes in Groundwater. EPA/600/6-90/004. April.

Appendix A: Experimental Results

This Appendix presents the data acquired for all of the large tank experiments. Depending on the experiment, there is anywhere from 1,500 to upwards of 10,000 data points, at four wavelengths, for each experiment. To print this data in text format is not practical. All of the data are therefore presented graphically.

Each of the following pages of this appendix present the information for one experiment. First, the tank parameters are presented followed by experiment labels, LNAPL thicknesses, pump settings and comments about the experiment. Below the settings are four graphs. The first graph presents all of the data recorded and highlights the start point for the regression with an arrow. The second graph then presents the regression. The third graph shows the error analysis of the data; finally, the dimensionless analysis of the selected data is plotted and the slope of the data shown on the graph. Below the graphs, if necessary, is a brief description of the experiment and an explanation of how the start point for the regression was selected.

Experiment #	A3		
Integration time	2500ms	Time and date	12:30p 5-15-03
Thickness in formation	9cm	Start time of logging	12:35p
Flow rate of pump	2.1ml/min	Thickness in well	20.5cm
Reading #	4	Time of injection	12:40p
Concentration of dye	10%	Volume of dye	.8ml

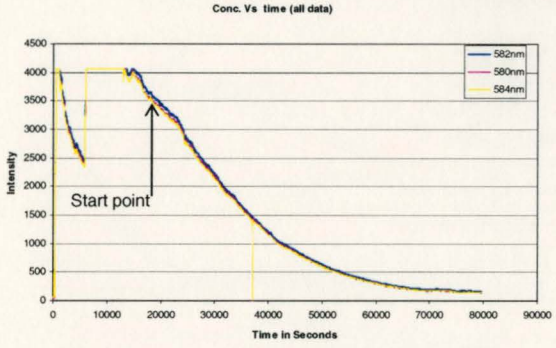

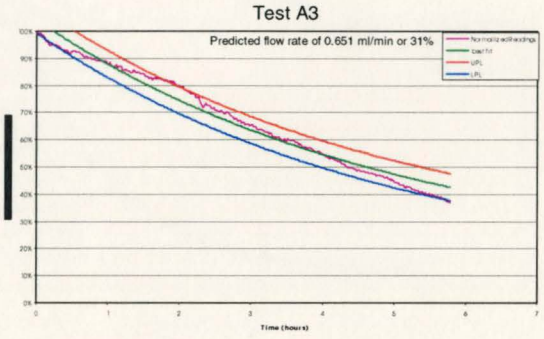

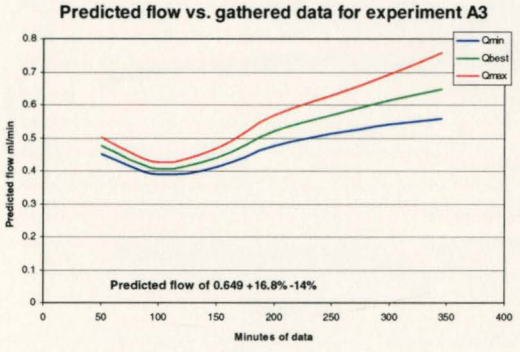

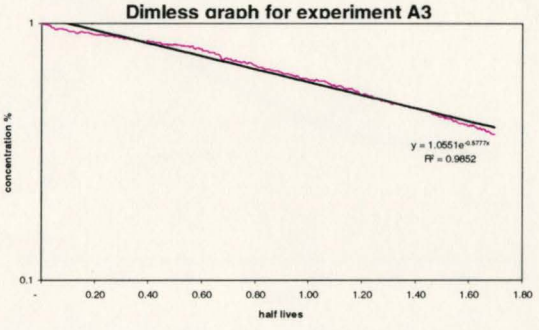

The integration time was changed at ~100,000 seconds and the spectrometer maxed out at 4000 counts. The start time was selected shortly after the curve started to decline.

Experiment #	A3B		
Integration time	3000	*Time and date*	5-16-03 11:15am
Thickness in formation	9cm	*Start time of logging*	11:15am
Flow rate of pump	2.1ml/min	*Thickness in well*	21.5cm
Reading #	0	*Time of injection*	None
Concentration of dye	None	*Volume of dye*	None

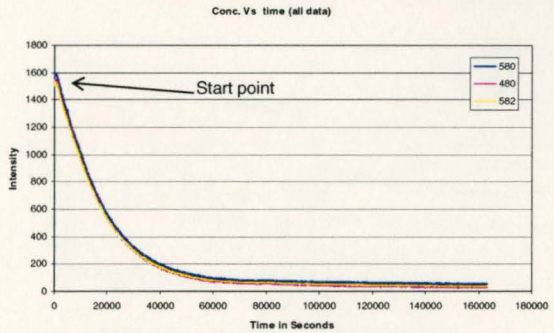

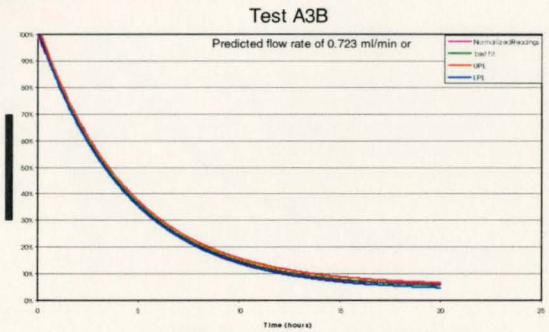

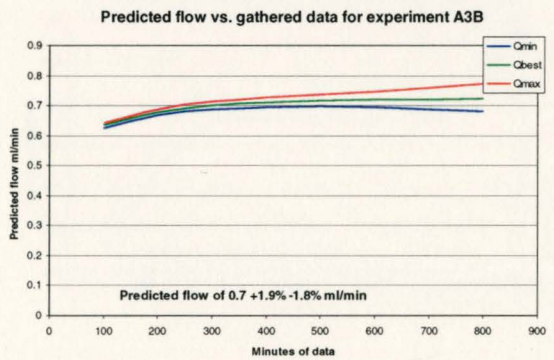

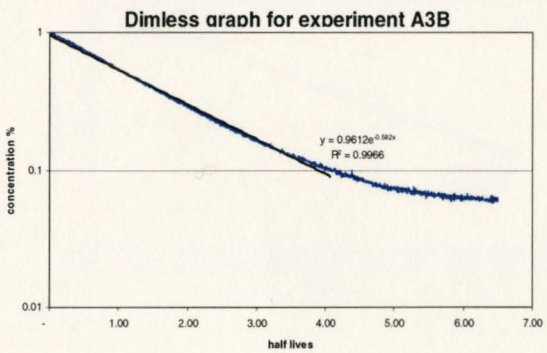

Before the start of this test, the tracer was already mixed, so the start point was selected as the first data point recorded.

Experiment #	A4		
Integration time	2000	***Time and date***	5-19-03 12:15pm
Thickness in formation	9cm	***Start time of logging***	12:10pm
Flow rate of pump	2.0ml/min	***Thickness in well***	20.5cm
Reading #	8	***Time of injection***	12:25pm
Concentration of dye	10%	***Volume of dye***	.5ml

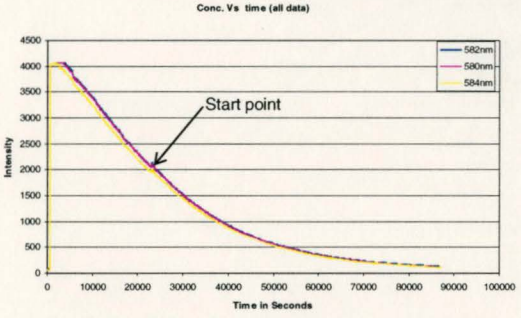

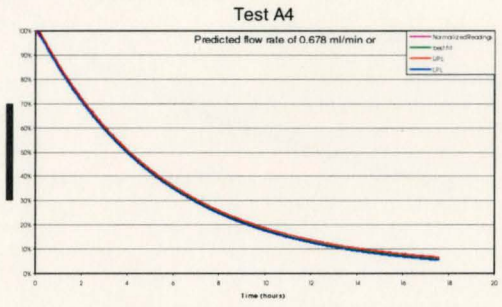

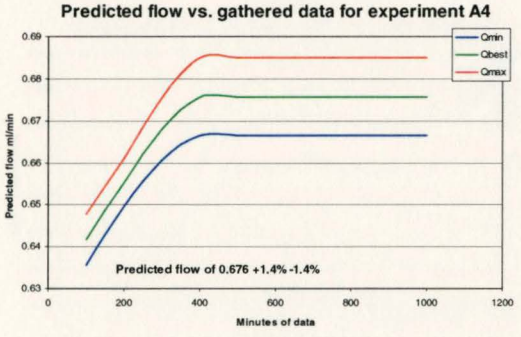

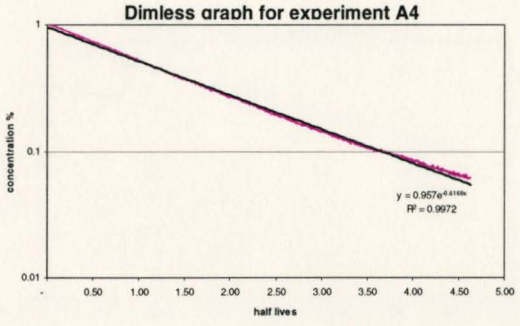

The start point for this experiment can be seen just after the jump in the data; this was due to someone turning lights on during the experiment. Starting the experiment after the lights were turned off made the results more accurate.

Experiment #	A5		
Integration time	1650	Time and date	5-29-03 12:21pm
Thickness in formation	10cm	Start time of logging	12:21pm
Flow rate of pump	0.5ml/min	Thickness in well	16.5cm
Reading #	5	Time of injection	12:30
Concentration of dye	10%	Volume of dye	.4ml

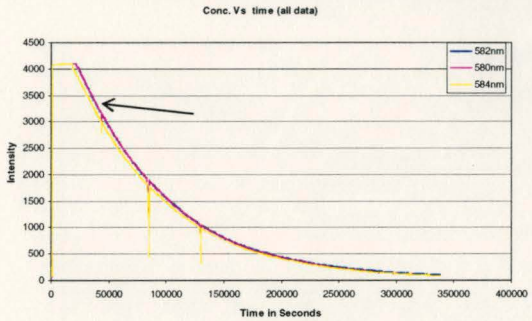

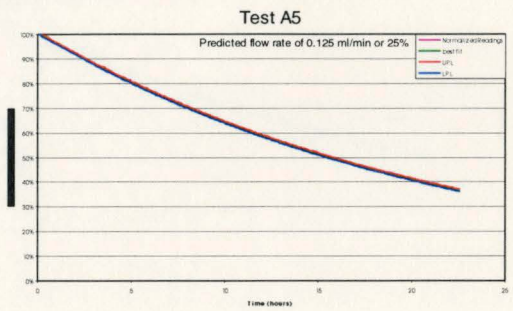

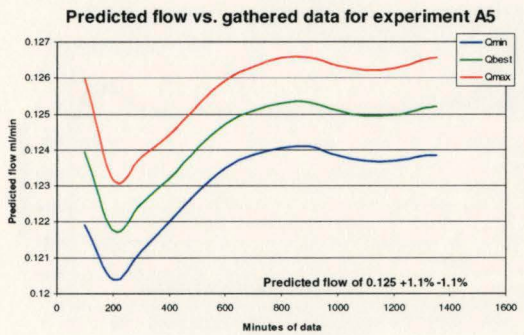

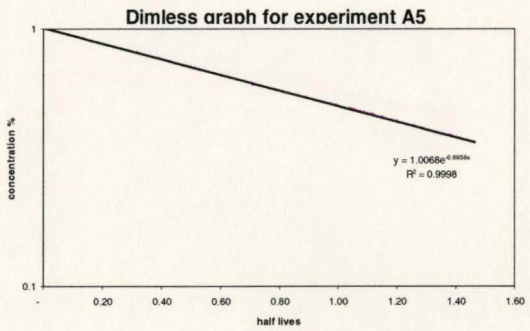

The start point was selected shortly after the decay curve started. The points that are much lower than the curve are a result of brief power failures during the test. These points were not removed from the analyzed data as one or two points out of thousands makes very little difference.

Experiment #	A6		
Integration time	1400ms	***Time and date***	6-9-03 10:00am
Thickness in formation	9cm	***Start time of logging***	10:00am
Flow rate of pump	0.05ml/min	***Thickness in well***	15.5cm
Reading #	3	***Time of injection***	10:20
Concentration of dye	10%	***Volume of dye***	0.35ml

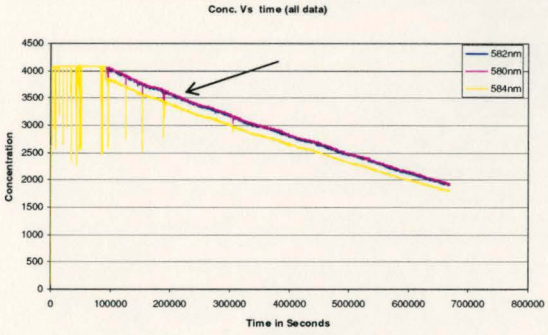

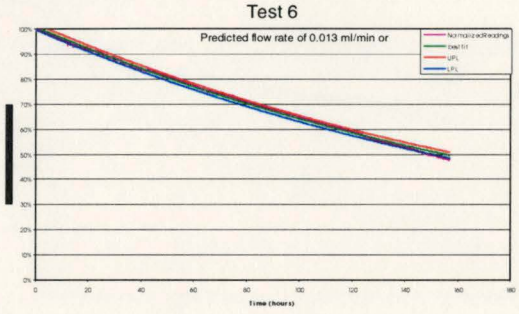

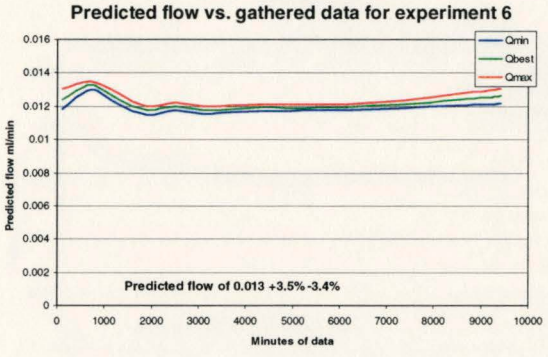

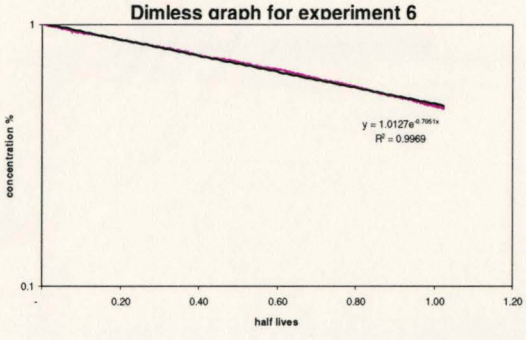

Early in the experiment, the light source intensity varied with very unstable power, and a small battery backup. The start point was selected as soon as the power became reliable.

Experiment #	A6B		
Integration time	2000	***Time and date***	6-17-03
Thickness in formation	9cm	***Start time of logging***	3:15pm
Flow rate of pump	0.05ml/min	***Thickness in well***	15.5cm
Reading #	0	***Time of injection***	None
Concentration of dye	None	***Volume of dye***	None

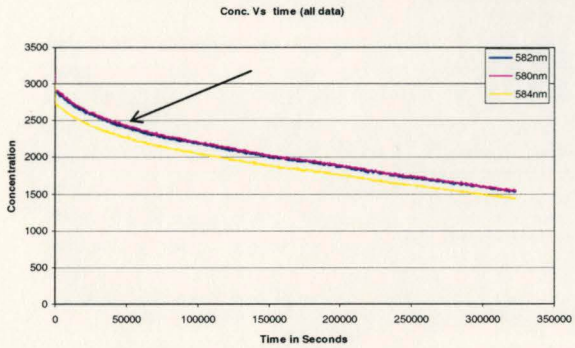

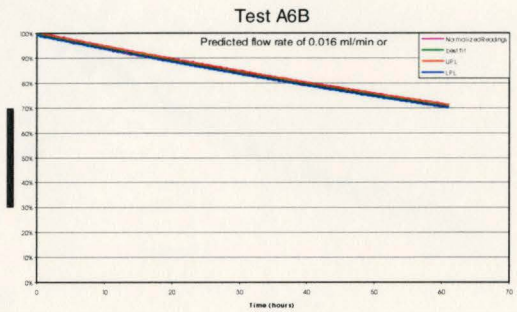

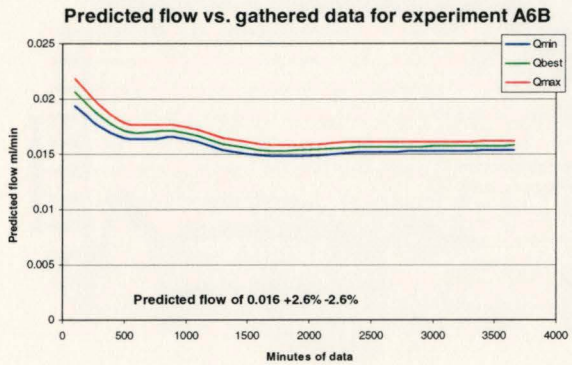

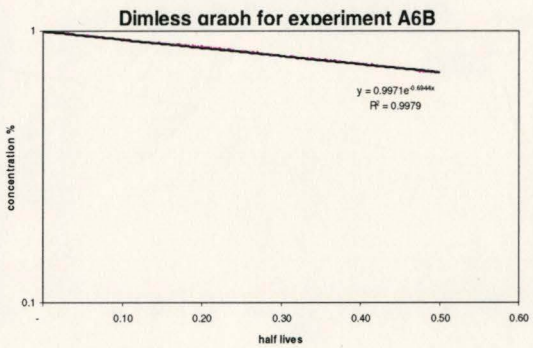

The start point for this experiment was selected at 55,000 seconds into the data collection after the mixing had occurred and the mixing rate slowed down.

Experiment #	A7		
Integration time	1300ms	Time and date	6-29-03 12:30pm
Thickness in formation	9cm	Start time of logging	12:48pm
Flow rate of pump	+- 0.009ml/min	Thickness in well	16cm
Reading #	1	Time of injection	12:52pm
Concentration of dye	10%	Volume of dye	0.35ml

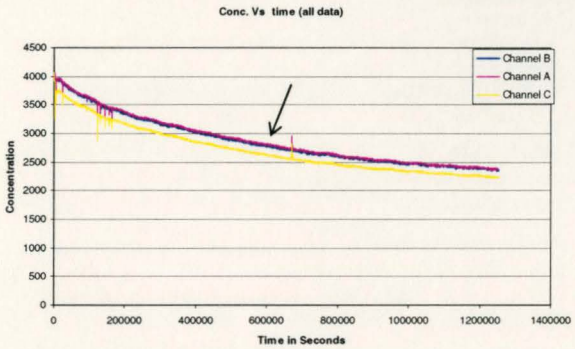

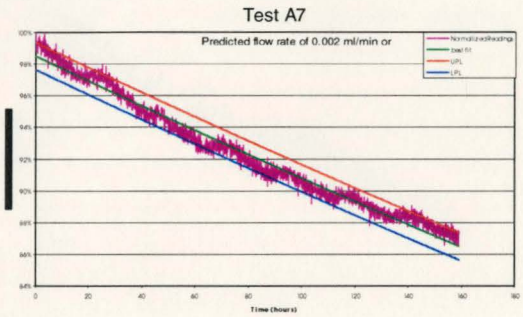

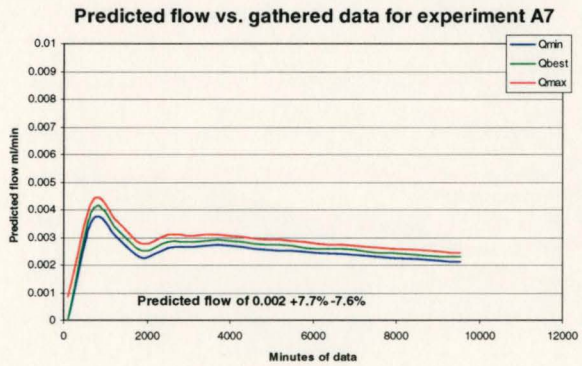

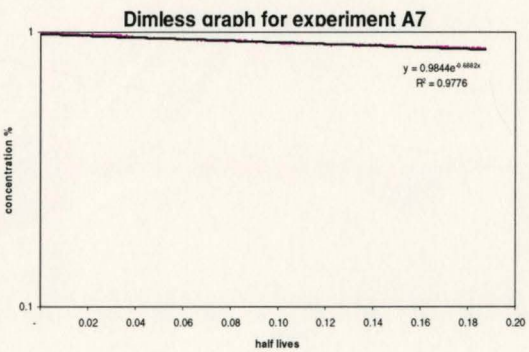

The start point for this experiment occurred later than the others. It is likely that because the flow rate in the tank was initially higher, the experiment started too soon. The point selected, just before the spike, was determined, via the dimensionless analysis, as the point where the data fit a straight line.

Experiment #	B1		
Integration time	1100ms	***Time and date***	11-3-03 10:10am
Thickness in formation	15cm	***Start time of logging***	10:17am
Flow rate of pump	0.013ml/min	***Thickness in well***	24.5cm
Reading #	0	***Time of injection***	None
Concentration of dye	None	***Volume of dye***	None

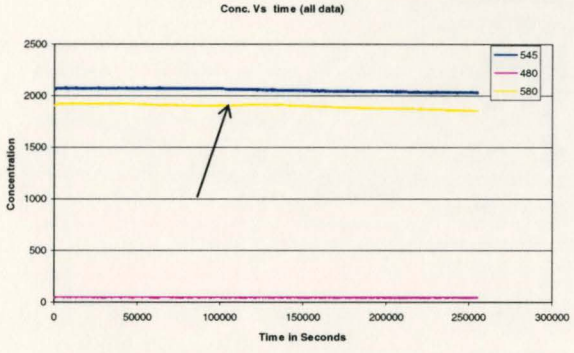

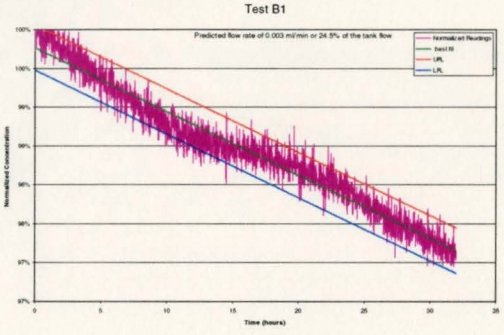

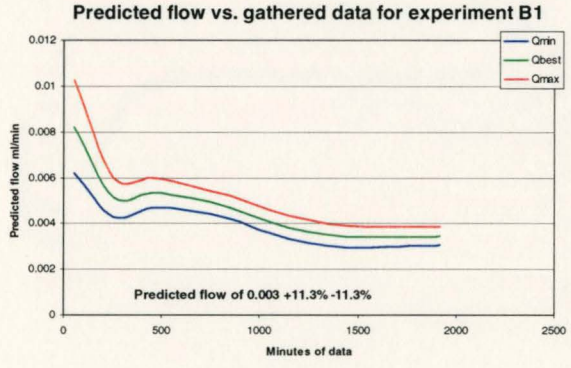

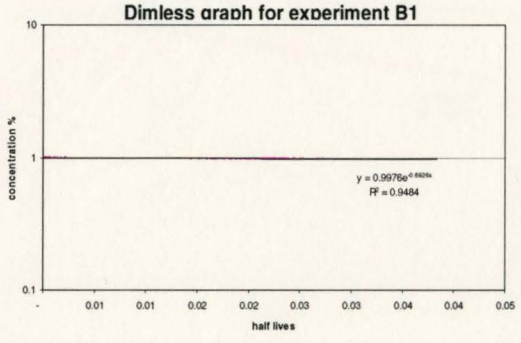

The experiment was started just in time for the pumps to fail. The start point was selected as the point when the pumps were fixed and the flow rate through the tank reestablished.

Experiment #	B2		
Integration time	3000ms	Time and date	11-17-03 10:25am
Thickness in formation	13cm	Start time of logging	10:25am
Flow rate of pump	0.3ml/min	Thickness in well	24cm
Reading #	2	Time of injection	10:27am
Concentration of dye	1%	Volume of dye	.4ml

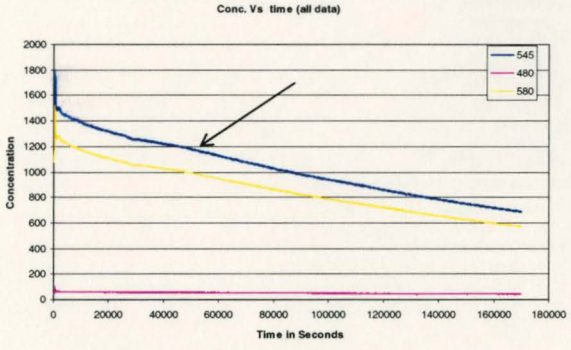

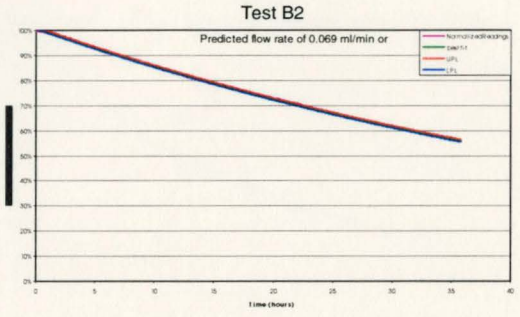

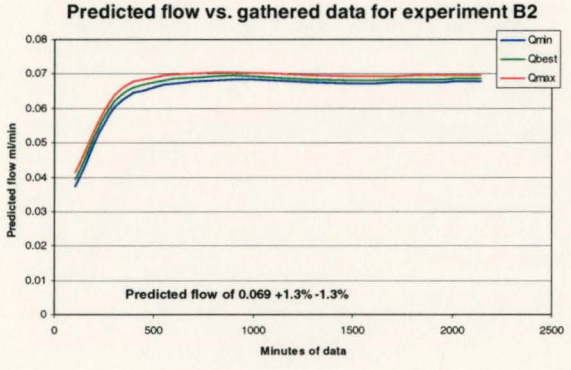

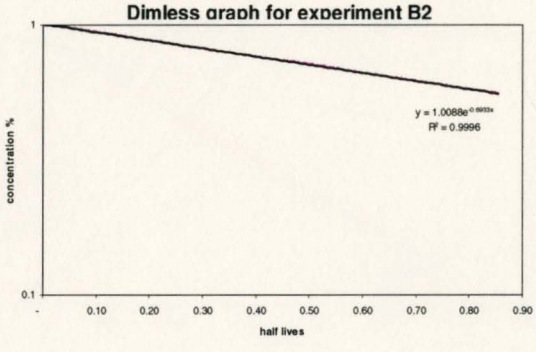

Again, there were some problems with the pumps early in the experiment. The start point was selected after the flow rate had been reestablished.

Experiment #	B3		
Integration time	1100ms	*Time and date*	11-20-03
Thickness in formation	13cm	*Start time of logging*	10:13am
Flow rate of pump	2.9ml/min	*Thickness in well*	24.5cm
Reading #	0	*Time of injection*	10:13am
Concentration of dye	100%	*Volume of dye*	.2ml

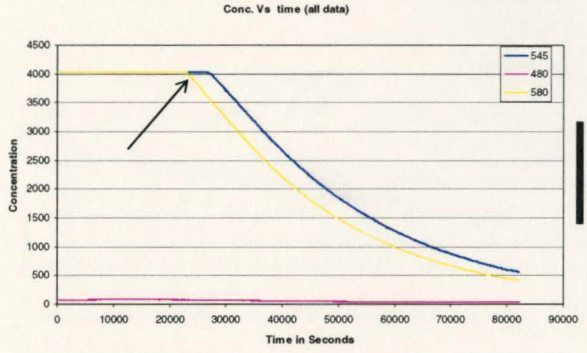

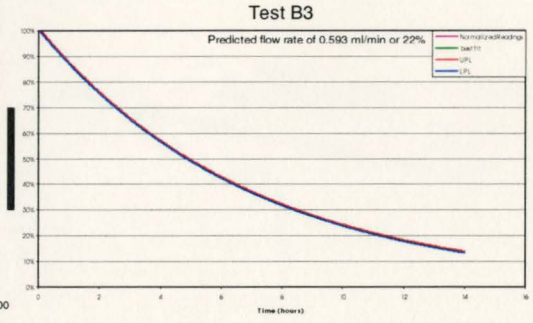

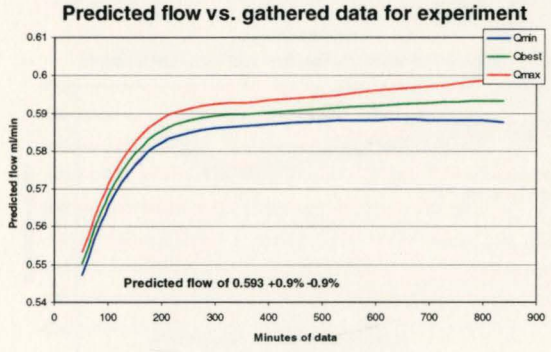

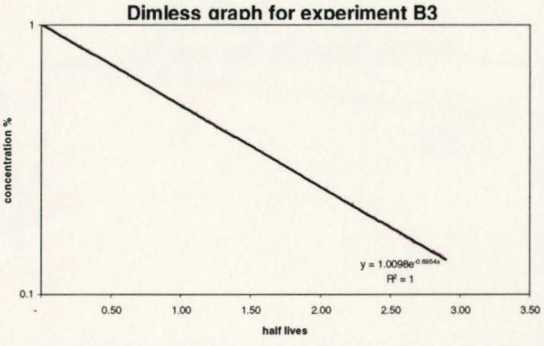

The start point for this experiment was established shortly after the decay began.

Experiment #	C1		
Integration time	3000ms	Time and date	1-16-04
Thickness in formation	24cm	Start time of logging	4:00pm
Flow rate of pump	0.1ml/min	Thickness in well	34cm
Reading #	0	Time of injection	None
Concentration of dye	None	Volume of dye	None

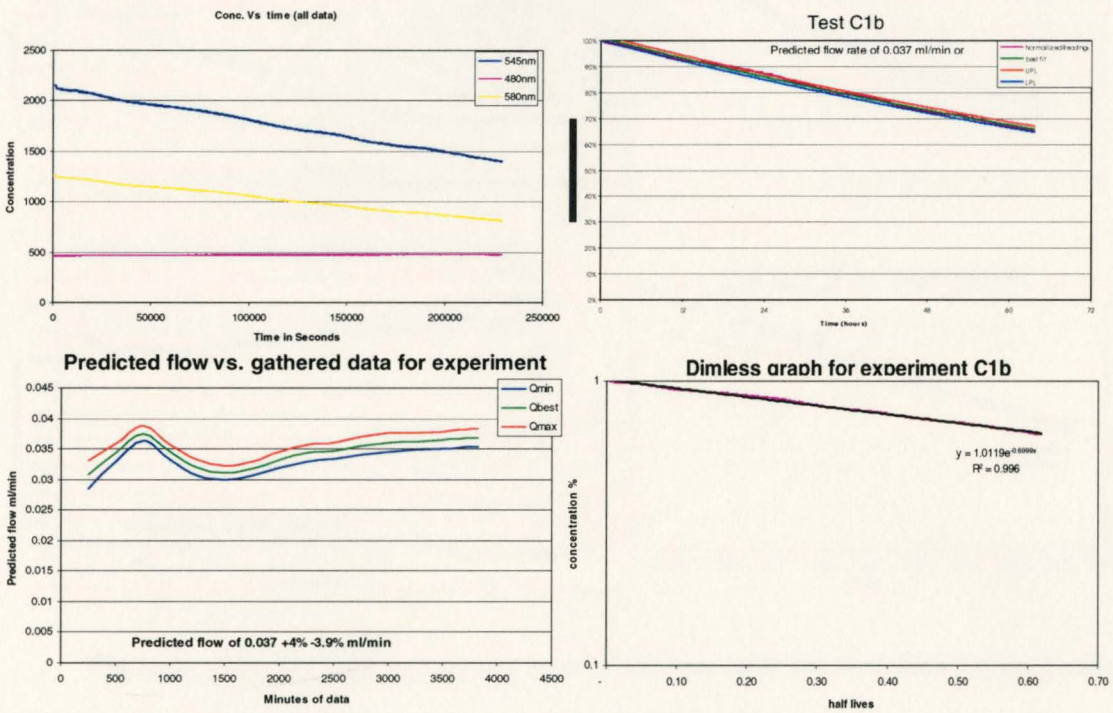

This test was challenging due to the large volume of LNAPL in the tank and pumping rates which were not stable. All of the data shown above was used in the regression. It was not necessary to add any tracer at the start of this test because there was already tracer in the well from a previous attempt. The results of this analysis predict a higher percentage of the tank flow than previous experiments. It is likely that the flow in the tank was higher than the flow measured from the pumps.

Experiment #	C2		
Integration time	2000ms	*Time and date*	12-10-03 11:00am
Thickness in formation	24cm	*Start time of logging*	11:23am
Flow rate of pump	.5ml/min	*Thickness in well*	34cm
Reading #	14	*Time of injection*	11:30am
Concentration of dye	1%	*Volume of dye*	4ml

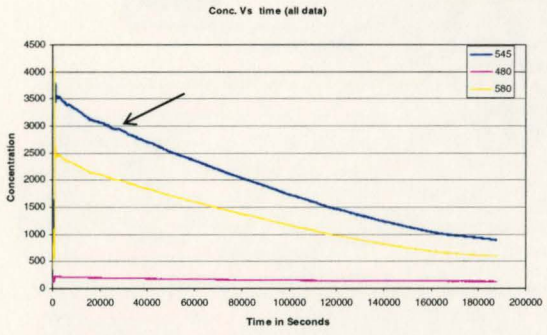

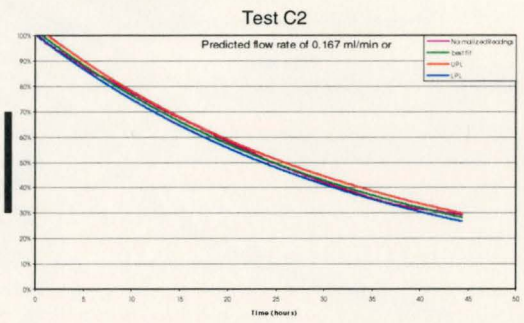

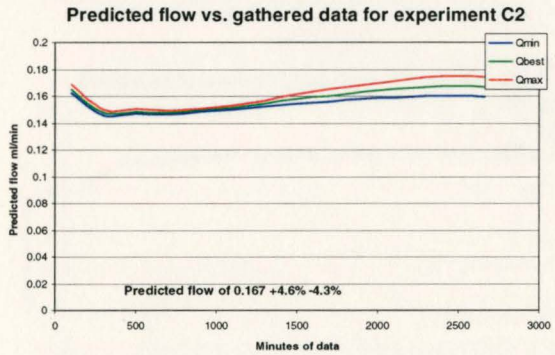

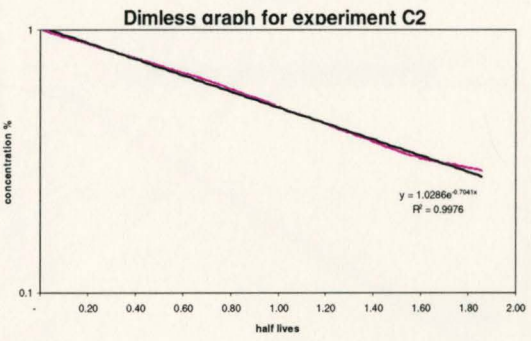

The start point for this experiment was 28,000 seconds into the data logging, after the tracer had been mixed and the mixing pump slowed down.

Experiment #	C3		
Integration time	1500ms	Time and date	12-16-03 10:00am
Thickness in formation	24cm	Start time of logging	10:15am
Flow rate of pump	2.0ml/min	Thickness in well	34cm
Reading #	0	Time of injection	10:15am
Concentration of dye	1%	Volume of dye	4.5ml

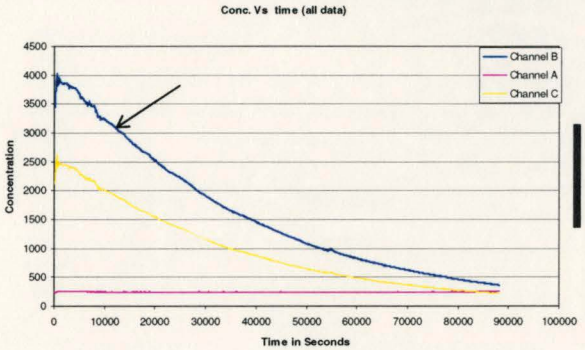

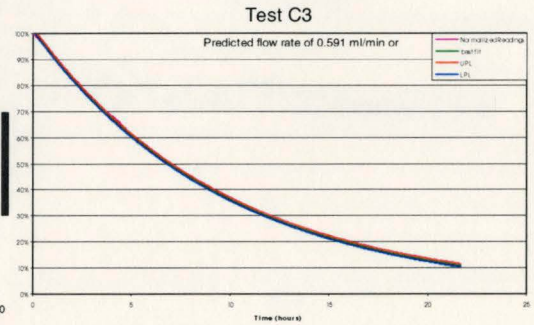

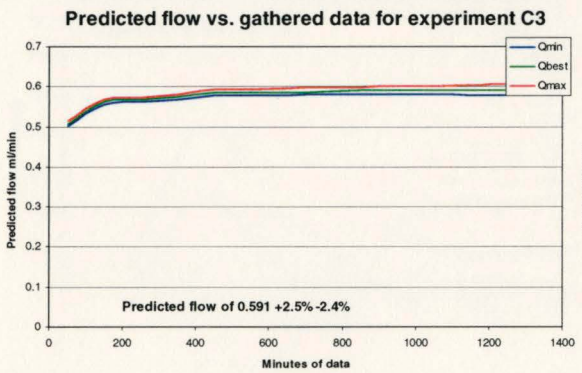

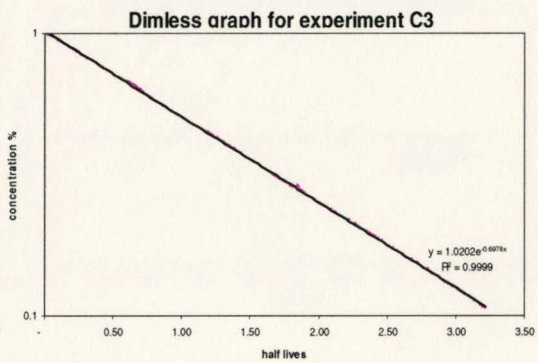

Experiment #	Static Test		
Integration time	1100ms	***Time and date***	10-11-03 3:45pm
Thickness in formation	14cm	***Start time of logging***	3:51pm
Flow rate of pump	0	***Thickness in well***	24cm
Reading #	0	***Time of injection***	3:48pm
Concentration of dye	100%	***Volume of dye***	0.01mL

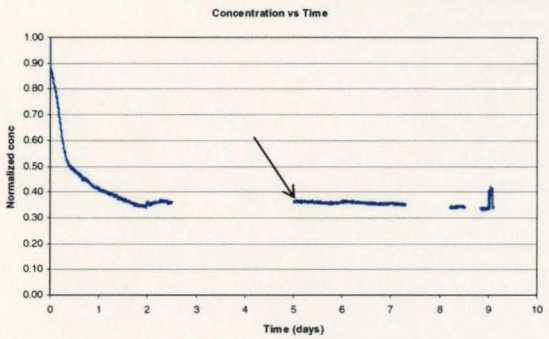

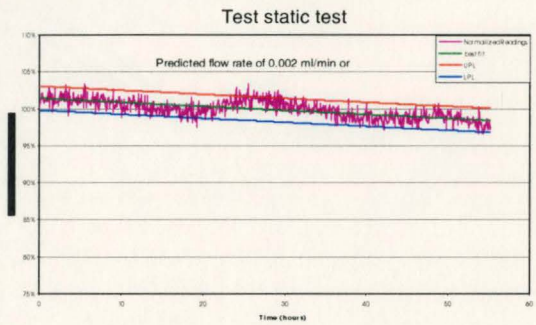

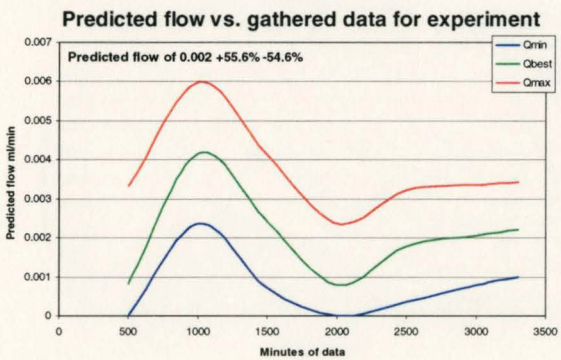

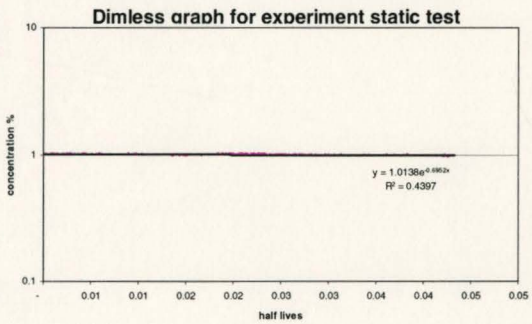

The data gaps were caused by the computer software crashing. By rebooting the computer and noting the start time, it was possible to generate the graph above. The start point was selected as the reboot point. This made the analysis fairly easy; it seems to be representative of the steady portion of the data.

Experiment #	Field test SS-146		
Integration time	3000ms	***Time and date***	9-19-03
Thickness in formation	N/A	***Start time of logging***	12:00pm
Flow rate of pump	N/A	***Thickness in well***	0.96ft
Reading #	0	***Time of injection***	Done on 9-16
Concentration of dye	XXXX	***Volume of dye***	XXX

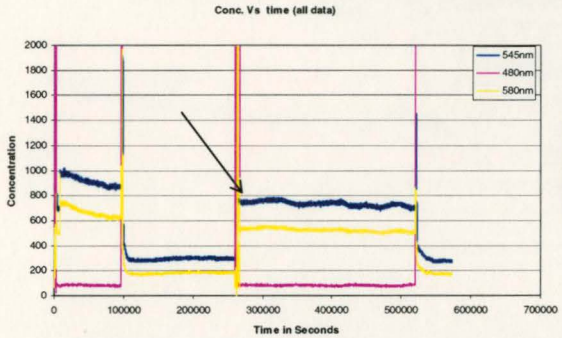

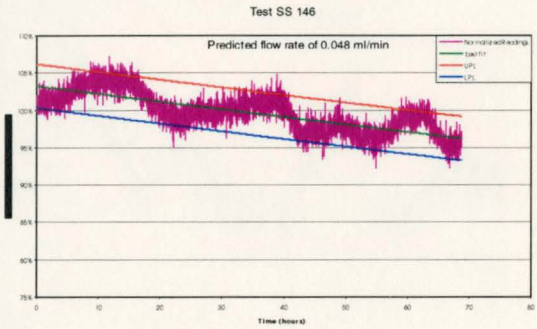

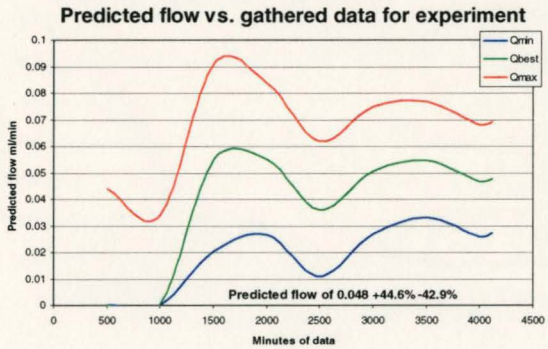

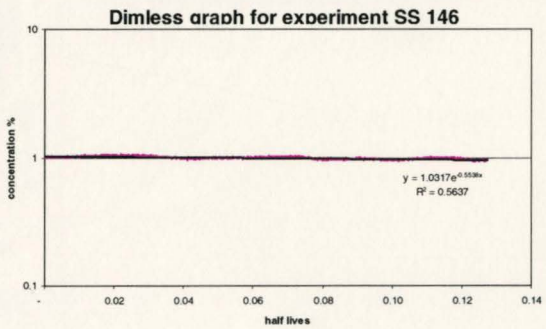

Due to falling fluid levels, it was hard to obtain consistent readings. The start time was selected where the longest duration of valid data was recorded.

Experiment #	Field test SS-115		
Integration time	30000	Time and date	10-29-03
Thickness in formation	N/A	Start time of logging	3:15 am
Flow rate of pump	N/A	Thickness in well	0.77ft
Reading #		Time of injection	3:15pm
Concentration of dye	100%	Volume of dye	1.5ml

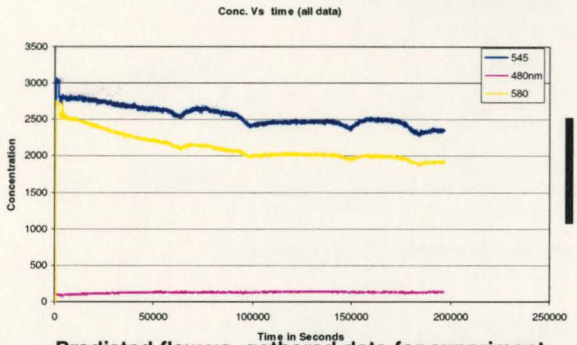

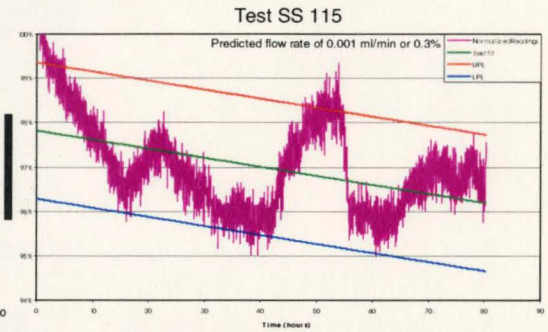

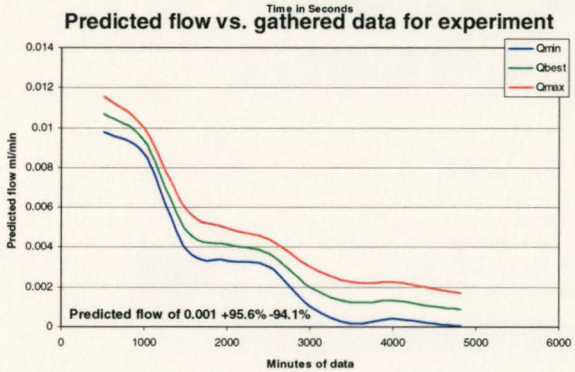

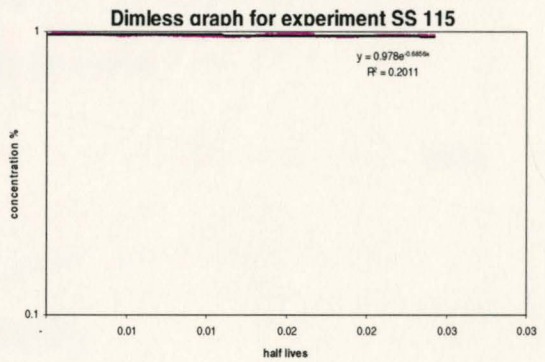

Appendix B: Calculations of Diffusion from a Well

From Jacob et al. (1967), Equation B1 predicts the height of water in a well after a volume of water has been instantaneously injected or removed.

$$H(t) = \frac{8H_o\alpha}{\pi^2}\int_0^{\infty}\frac{e^{-\beta u^2/\alpha}}{u\cdot\Delta u}du \qquad \text{(B1)}$$

Where:

H(t)= Height of water in the well at time t

H_o= The initial height of water immediately after the injection

$$\alpha = \frac{r_s^2 S}{r_c} \qquad \text{(B2)}$$

Where:

r_s= Radius of the well screen

r_c= Radius of the well casing

S= Coefficient of storage of the aquifer

$$\beta = \frac{Tt}{r_c^2} \qquad \text{(B3)}$$

Where:

T= Transmissibility of the aquifer

t= Time

$$\Delta u(u) = \left[u\cdot J0(u) - 2\alpha\cdot J1(u)\right]^2 + \left[u\cdot Y0(u) - 2\alpha\cdot Y1(u)\right]^2 \qquad \text{(B4)}$$

This problem is analogous to instantaneously introducing a tracer to the well, which creates a concentration gradient. For this analogy the coefficient of storage (S) becomes the volume of LNAPL and can be written as:

$$S = S_n \phi \tag{B5}$$

Where:

S_n= LNAPL saturation

ϕ= Formation porosity

The transmissibility of the aquifer is analogous to the effective diffusivity of the tracer in the LNAPL and can be written as:

$$T = \phi \cdot S_n \cdot \tau \cdot D \tag{B6}$$

Where:

D= Diffusivity of the tracer in the LNAPL

$$\tau = \phi^{1/3} S_n^{7/3} \tag{B7}$$

The graph below shows the diffusive losses that would be expected from a 5 cm (2in) well under typical conditions (ϕ=0.3, D=7.5x10^{-10} m^2/sec). The five curves show that diffusive losses increase at higher saturations but are small compared to all the dilutions measured for the experiments in this thesis.

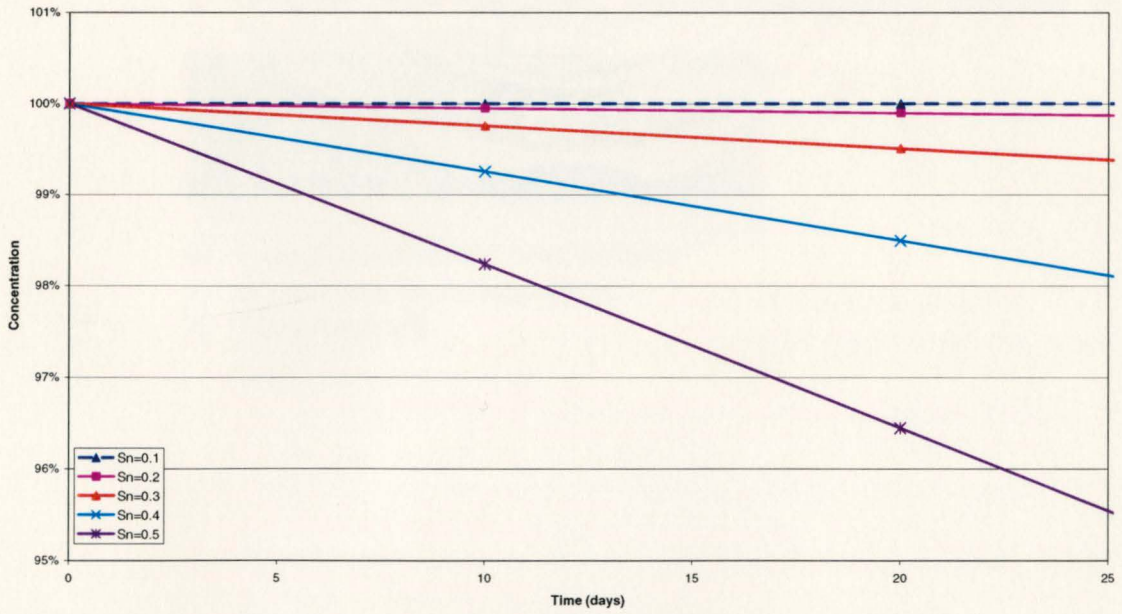

Figure B1: Graph of Diffusive Losses Under Typical Condition

Appendix *C:* Field Procedures

Procedure to sample background fluorescence:

1) Hook up cables to equipment
    a. Power supply (inverter or line) and turn on power supply
    b. Fiber optic probe (both to light source and to spectrometer)
        i. Untie twist ties only, and feed probe end through the hole in box (from inside to out) until the yellow tape then hooks up to spectrometer.
        ii. Be extremely careful not to bend fiber sharply; the fiber can easily be broken
    c. It is not necessary to replace rubber in connection hole (at this time)
2) Start the computer
    a. Verify that both power and USB cables are plugged in securely.
    b. Turn computer on; allow to boot
3) Open and configure Optics software package "OOI base32" (Icon is on desktop)

    a. Go to the "Time Acquisition," pull down menu, select "configure" > "configure acquisition"

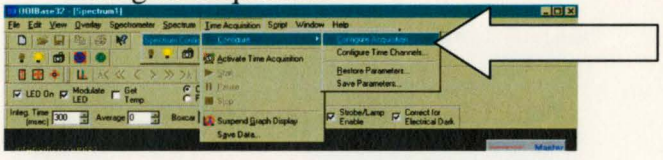

    b. Change test name to "well samples"
    c. Select "save every acquisition"
    d. Then select OK

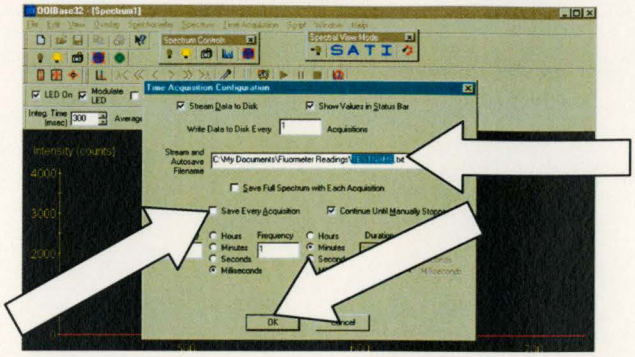

e. Again, pull down the "time acquisition" menu; this time select "activate time acquisition"
f. Finally from the "time acquisition" menu select "start"

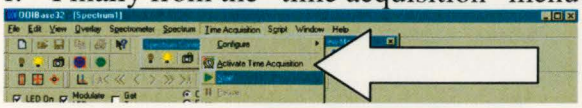

4) Test Spectrometer
   a. Turn on light source; a bright blue light should emanate from end of probe. (Once tested, the light can be shut off until the test is ready)
   b. Verify Temp setting. LED on front of spectrometer should be lit green
      i. If red, wait to begin sampling
      ii. If extremely hot or cold, the set point temp can be adjusted
   c. Check signal input.
      i. The graph on the OOI32 program should change as the probe is pointed toward, or away, from light sources
5) When ready, begin testing
   a. Verify Green LED on spectrometer is lit. (If not, wait to begin sampling)
   b. Turn on light source
   c. Set integration time to ~1500ms (adjust as necessary to maintain good signal strength)

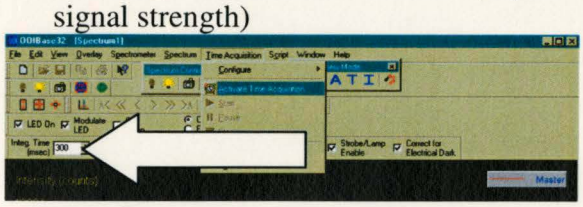

   d. Carefully lower probe down well (do not bend cable sharply)
   e. When close to oil, slowly lower cable; watch signal to determine when probe has contacted oil
      i. When probe is close to oil, there will be a spike at 480nm
      ii. As the probe gets closer to the oil, the spike will increase
      iii. As soon as probe is immersed, 480 spike will disappear
      iv. And the fluorescence from the oil can be observed
   f. Adjust integration time until a strong signal can be seen (only adjust integration time on the first test)
   g. Finally record numbers from Channels A through D on log sheet

h. Remove probe and clean with paper towel
i. For successive wells, repeat steps D through F (do not adjust integration time)

Procedure to begin recording a dilution test:

NOTE: if the instrument has been set up for background testing, some of these steps may already be complete; if so, they may be skipped.

1) Hook up cables to equipment box
    a. Power supply
    b. Fiber optic probe (both to light source and to spectrometer)
        i. Untie twist ties only, and feed probe end through the hole in box (from inside to out) until the yellow tape; then hook up to the spectrometer.
        ii. Be extremely careful not to bend fiber sharply; the fiber can easily be broken
    c. Hook up drive cable (drive motor is located under fan)
        i. Find the rib inside the drive cable
        ii. Turn motor shaft to align the groove in the shaft with the rib on the cable
        iii. Insert motor end of cable through hole in box
        iv. Turn motor back and forth slowly until the rib and slot slide together
        v. Secure screw to hand tight
        vi. Install rubber washer to seal box
2) Start the computer
    a. Turn on power supply
    b. Verify that both power and USB cables are plugged in securely.
    c. Turn computer on, allow to boot (power button is located on side)
    d. Verify that red/green light on spectrometer is lit
        i. If not, reboot computer (this will reinitialize the USB port)
    e. Once spectrometer light is on, open and configure Optics software package "OOI base32" by double clicking on the icon (on desktop)

    f. Go to the "Time Acquisition," pull down menu, select "configure" > "configure acquisition"

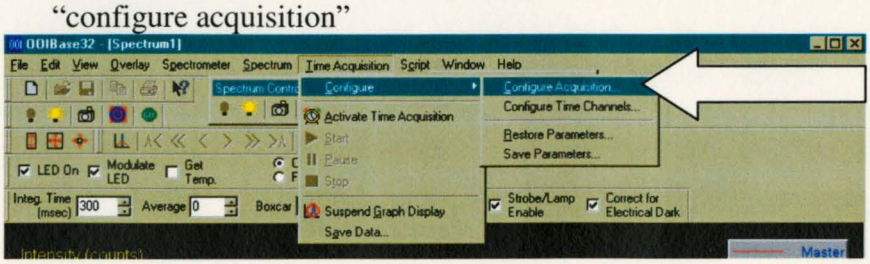

g. **Change test name to "well XX" (where xx is the well number)**
h. Save acquisitions every 1 minute
i. Then select OK

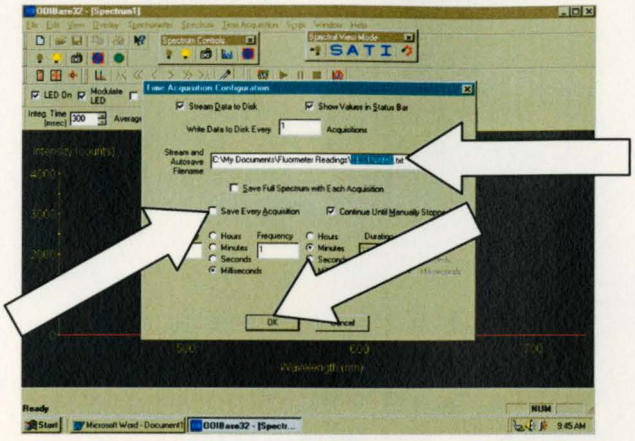

3) Test Spectrometer
    a. Turn on light source; a bright blue light should emanate from end of probe. (Once tested, turn light off)
    b. Check signal input.
        i. The graph on the OOI32 program should change as the probe is pointed toward, or away, from light sources
4) Hookup cables to downhole mixer
    a. Remove pump housing
    b. Feed cables through the top of the loose pump housing
        i. Drive cable
        ii. Fiber optic probe cable
        iii. Support cable and hanging bracket (remove AND SAVE the two small screws from hanging bracket)
        iv. DO NOT feed the plastic tracer cable
    c. Align and hook up pump drive cable; screw should be slightly more than hand tight, use pliers.
    d. Secure the hanging bracket in place
    e. Insert and secure the fiber optic cable into the probe
        i. Nut should be hand tight
        ii. Cable should be firmly in place
        iii. This may require jiggling the cable to get nut tight
5) Test / Secure connections
    a. Switch motor control to forward
    b. Set speed to ~7
    c. Use flashlight to verify pump is turning in the downhole mixer
    d. Turn on spectrometer light; verify a spike occurs at ~480nm
    e. Check and secure all screws and connections
    f. Secure pump housing in place (two screws from hanging bracket)
    g. Via rubber bands, secure tracer hose to outside of tool
        i. Outlet of hose should be located at first diffuser hole 3" below manifold

6) Obtain Well Parameters (if not already measured)
    a. Use oil water probe to measure depth from top of casing to depth of oil
    b. And depth to water
7) Prepare to lower mixer
    a. Set cable clamp on hanging cable such that the distance from lower face of the cable clamp to the bottom of the manifolds is 1" to 1 ½" less than the measured depth to oil. (see picture below)

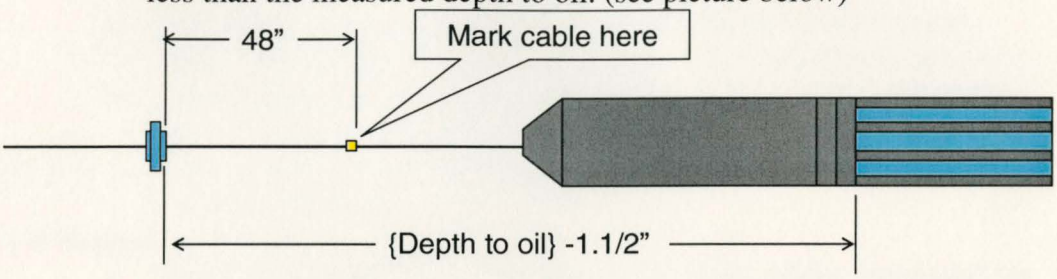

    b. Mark cable 4' down from cable clamp with tape or marker (see picture above)
    c. Prime tracer tube with tracer solution
        i. amount of tracer depends on oil thickness (see tracer chart)
    d. Once tracer tube has been primed, pull 1 to 2 ml of air into bottom of tube to keep tracer away from end of tube
    e. Do a final check to make sure everything looks secure, no loose parts etc.
8) Lower mixer
    a. Carefully lift and insert mixer into well (do not bend cables sharply) until top of mixer is 2 to 3 inches below top of well casing.
    b. While holding mixer by the hanging cable, install piece A of the well casing cap. (Be careful to insert the cables in the proper order (as shown on the cap)
    c. With piece "A" of the cap installed, slowly lower mixer to the mark on cable, making sure not to crimp or tangle cords at the surface.
    d. Remove mark (if necessary) and lower the last 4 feet of cable extremely slowly until the cable clamp encounters the well casing cover
    e. Install well casing cover, part B.
    f. Secure remaining cables at the surface, as straight at as possible
9) Priming mixing pump/ beginning data collection
    a. Turn on spectrometer light source, verify spike at 480 nm
    b. Switch mixing motor direction, switch to forward
    c. Increase mixing motor speed to ~8
    d. Observe spectrum to verify pump is working
        i. As oil gets close to the probe the 480nm spike will increase
        ii. When the oil contacts the probe the 480nm spike will disappear and the oil's fluorescent spectrum will be present
        iii. Adjust integration time, as necessary, such that the maximum fluorescence is between 100 and 500 counts

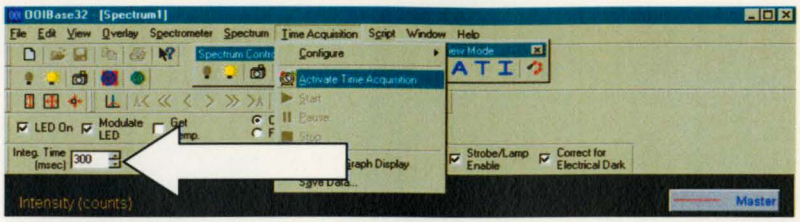

e. Slow mixer motor to ~6 minimum speed where it is still turning
f. Select "activate time acquisition" from the time acquisition menu
g. Select "start" from the time acquisition pull-down menu, and make note of the time on log sheet
h. Allow tool to set and the formation to equilibrate (Tom says over lunch is sufficient)

10) Beginning the test
   a. Verify Green LED on spectrometer is lit. If not, adjust "set temp", or wait for green light
   b. Verify spectrometer is reading the oil fluorescence
   c. Note the time and reading number on computer on log sheet
   d. Set mixing motor speed to 10 if product thickness is over 6 in otherwise set to <7
   e. Inject tracer
      i. Inject all of the tracer
      ii. Inject 5 to 10ml of air to clear line.
      iii. Cycle oil in and out of tube to clean base, and mix tracer at least 5 times.
      iv. Inject 5ml more air to clear line.
   f. Fill out test form, and make any necessary notes
   g. Allow mixer to mix for 15 min for every 6in of product in well.
   h. Observe spectrum peaks
      i. 580mn (channel C) should be 2000 to 3000 counts
      ii. Reading should be stable
      iii. If peaks are low, more tracer can be added and step F repeated.
      iv. If peak values are changing, allow mixing to continue.
   i. When peak values are constant and strong, slow mixing pump to 2/3 of previous setting. (note time on log sheet)
   j. Close laptop screen
   k. Secure equipment box
   l. Check readings every 24 hours until peak values have decayed to background levels

11) Conclusion of test
   a. Shut down equipment
      i. Select "stop" from time acquisition menu
      ii. Close the spectrometer program
      iii. Shut down computer via start menu
      iv. Turn off spectrometer light source (on spectrometer)
      v. Turn off mixing motor
   b. Drain and extract mixing tool

i. Lift mixing tool, via hanging cable ~4 feet and secure via cable clamp
ii. Allow to hang for ~5 minutes.
iii. Turn on mixing pump to full speed for 2 min,
iv. Reverse flow of pump for 2 min.
v. Allow to hang for another 5 min
vi. Retrieve mixing tool case (2"pipe) and secure one end
vii. Using hanging cable to pull tool to surface
viii. Remove well casing cap and extract mixing tool; place in case
ix. Remove pump cover of mixing tool and remove cables
    1. Tracer injection hose
    2. fiber optic cable
    3. pump drive cable
    4. lastly, remove hanging cable bracket
x. Reinstall pump cover (no screws), insert stopper, and secure top of container

c. Equipment box shut down
i. Turn off power supply switch
ii. Unplug power supply
iii. Remove cables
    1. Pump drive cable
    2. Fiber optic cable
iv. Roll up cables and secure. Place in metal box

Appendix D: Field Test SS-146 Calculations

Well ss146 Dilution Method Calculations

Setting:

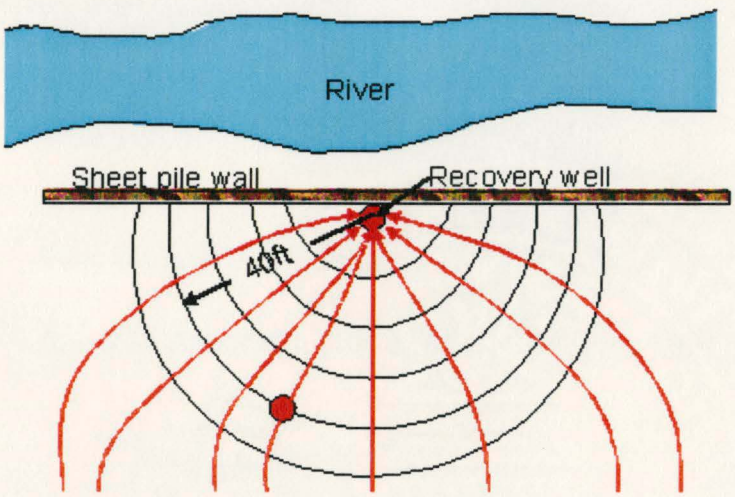

Goal: Use the dilution test data, and the test wells proximity to an active recovery system to determine the recovery rate of the well.

$L := \frac{40ft \cdot 2 \cdot \pi}{2}$ Distance perp. to flow over which the flow occurs (at the well)

$Qw_{min} := 2.5 \frac{mL}{hr}$ $Qw_{max} := 3.5 \frac{mL}{hr}$ Flow rate measured through the well from dilution test

$\alpha_{min} := 1$ $\alpha_{max} := 2$ Well convergence factor

$D := 4in$ Well screen diameter

Volumetric flow rate per unit width of LNAPL body perpendicular to flow is:

$$Qf_{min} := \frac{Qw_{min}}{\alpha_{max} \cdot D} \qquad Qf_{min} = 1.161 \frac{ft^2}{yr}$$

$$Qf_{max} := \frac{Qw_{max}}{\alpha_{min} \cdot D} \qquad Qf_{max} = 3.25 \frac{ft^2}{yr}$$

Based on the volumetric flow rate per unit width of LNAPL body, the recovery system is recovering:

$$Q_{rec.min} := Qf_{min} \cdot L \qquad Q_{rec.min} = 3 \frac{gal}{day}$$

$$Q_{rec.max} := Qf_{max} \cdot L \qquad Q_{rec.max} = 8 \frac{gal}{day}$$

Next the LNAPL gradient can be estimated, since the LNAPL transmissivity has been calculated via a baildown test:

From baildown test: $T_{baildown} := 0.0008946 \frac{ft^2}{min}$

From the mathmatics section of this thesis: $Qf = T \cdot I$ so $I = \frac{Qf}{T}$

So, using the minimum and maximum values the gradient (I) can be calculated as:

$$I_{min} := \frac{Qf_{min}}{T_{baildown}} \qquad I_{min} = 0.0025$$

$$I_{max} := \frac{Qf_{max}}{T_{baildown}} \qquad I_{max} = 0.007$$

Appendix E: Equipment Design Details

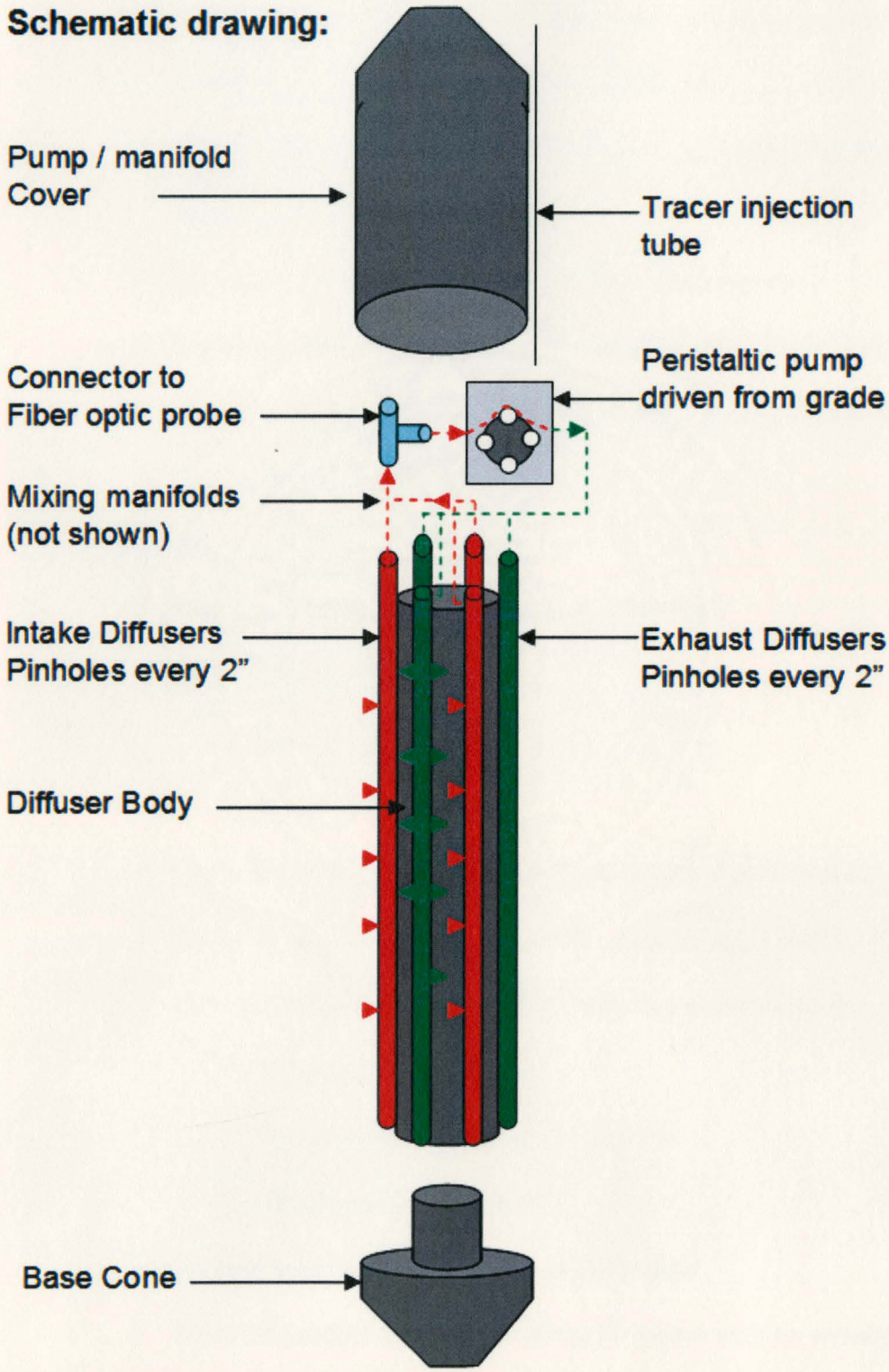

Diffusive Style Mixer Schematic Drawing

Design Objective of the Mixing Device:

The requirements for the downhole tool are:

- Capable of mixing the contents of the wellbore quickly, and maintaining a well mixed volume throughout the experiment
- The process of mixing must not introduce any gradients to the well that could increase the tracer dilution
- Providing a platform to reliably measure fluorescence
- Capable of fitting down a 2" well, and sufficiently robust for field work
- Constructed of materials which will not degrade in the LNAPL environment

Features:

- Constructed from chemically resistant materials
    - Stainless Steel
    - Viton
    - Glass
- Pump driven from grade; therefore, no downhole electronics
- Diffusers minimize in well gradients while mixing LNAPL
- Hollow tool body isolates product, reducing active volume
    - Requires less tracer
    - Decreases time required for each test
    - Minimizes displacement
- Tapered ends to slide in and out of well easily
- Works in product thicknesses of 6 to 36 inches with no adjustments

How the Mixer Works:

Six diffuser tubes (small tubes with pinholes in them) are secured around a 1" diameter body. Then, a peristaltic pump driven by a motor at the surface pumps LNAPL in through three of the six diffuser tubes, mixing the LNAPL in the diffusers and manifolds, then passing the LNAPL past the fiber optic probe. Finally, the mixed LNAPL is returned to the well via the remaining three diffuser tubes. The diffusers work in LNAPL between 6 and 36 inches thick.

Pictures of the Mixer and Surface Equipment

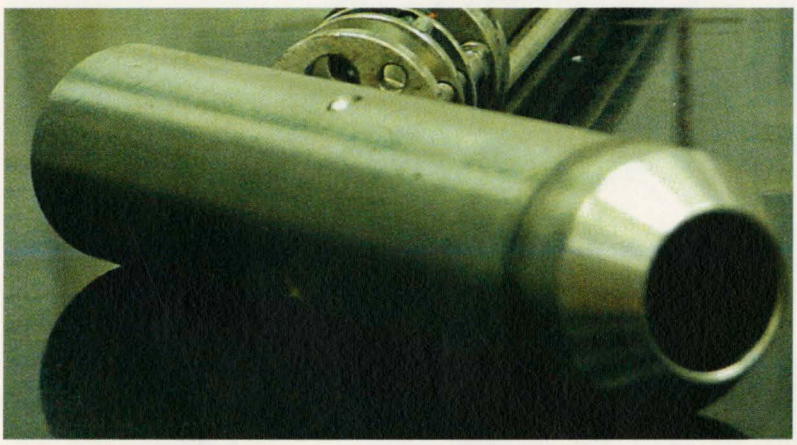

Pump Housing Cover

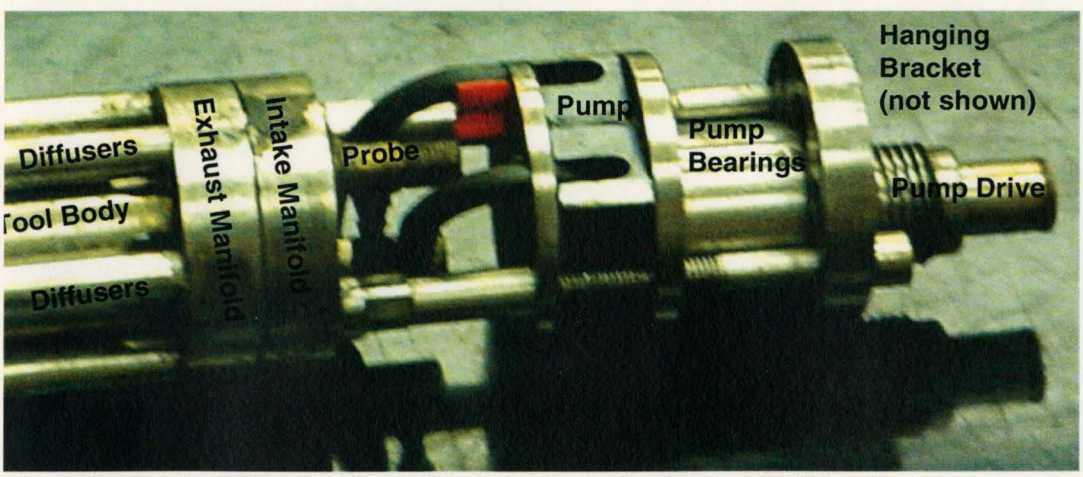

Upper Portion Including the: Pump, Manifold, Probe Connection, and Hanging Bracket

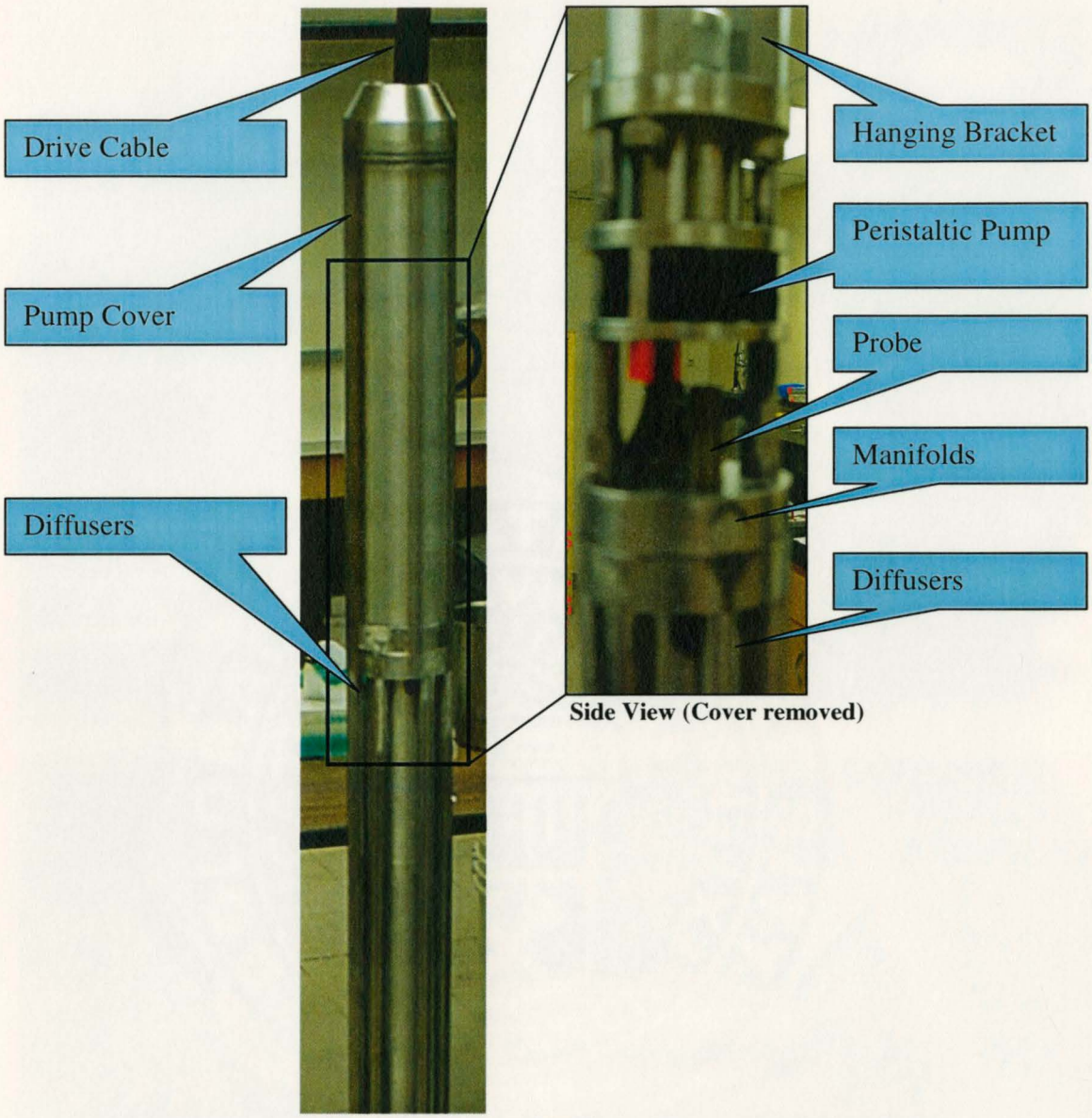
Drive Cable
Pump Cover
Diffusers
Hanging Bracket
Peristaltic Pump
Probe
Manifolds
Diffusers
Side View (Cover removed)
Side view

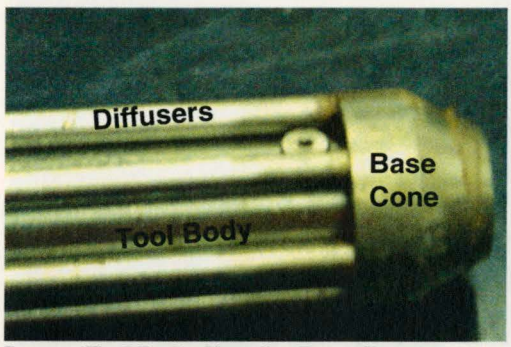

Lower End Including the Base Cone

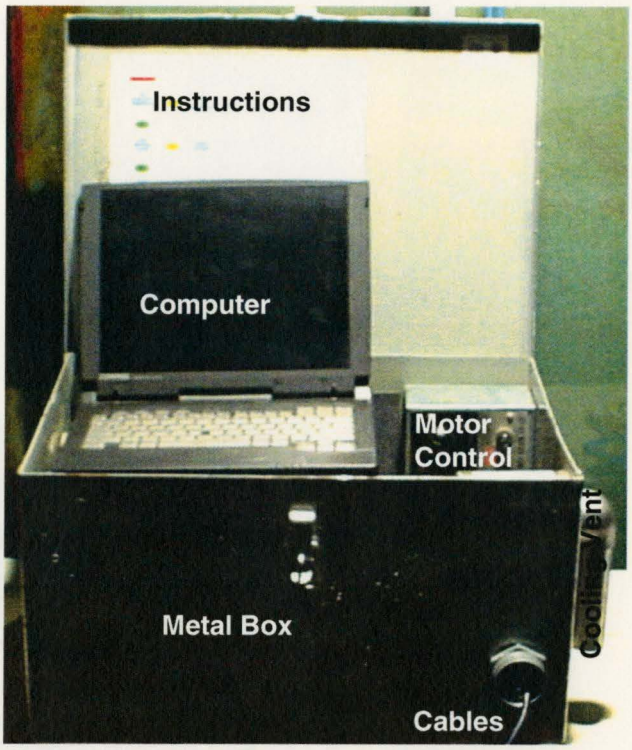

Surface Equipment Box

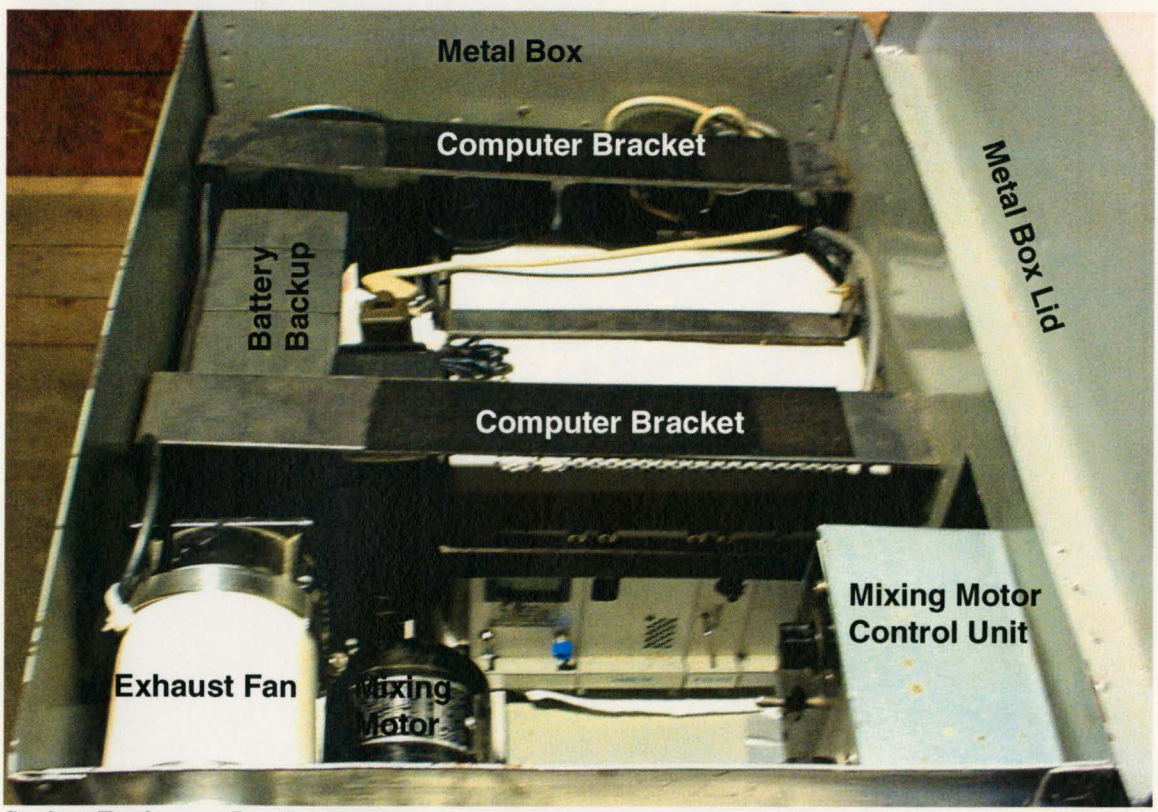

Surface Equipment Box Interior

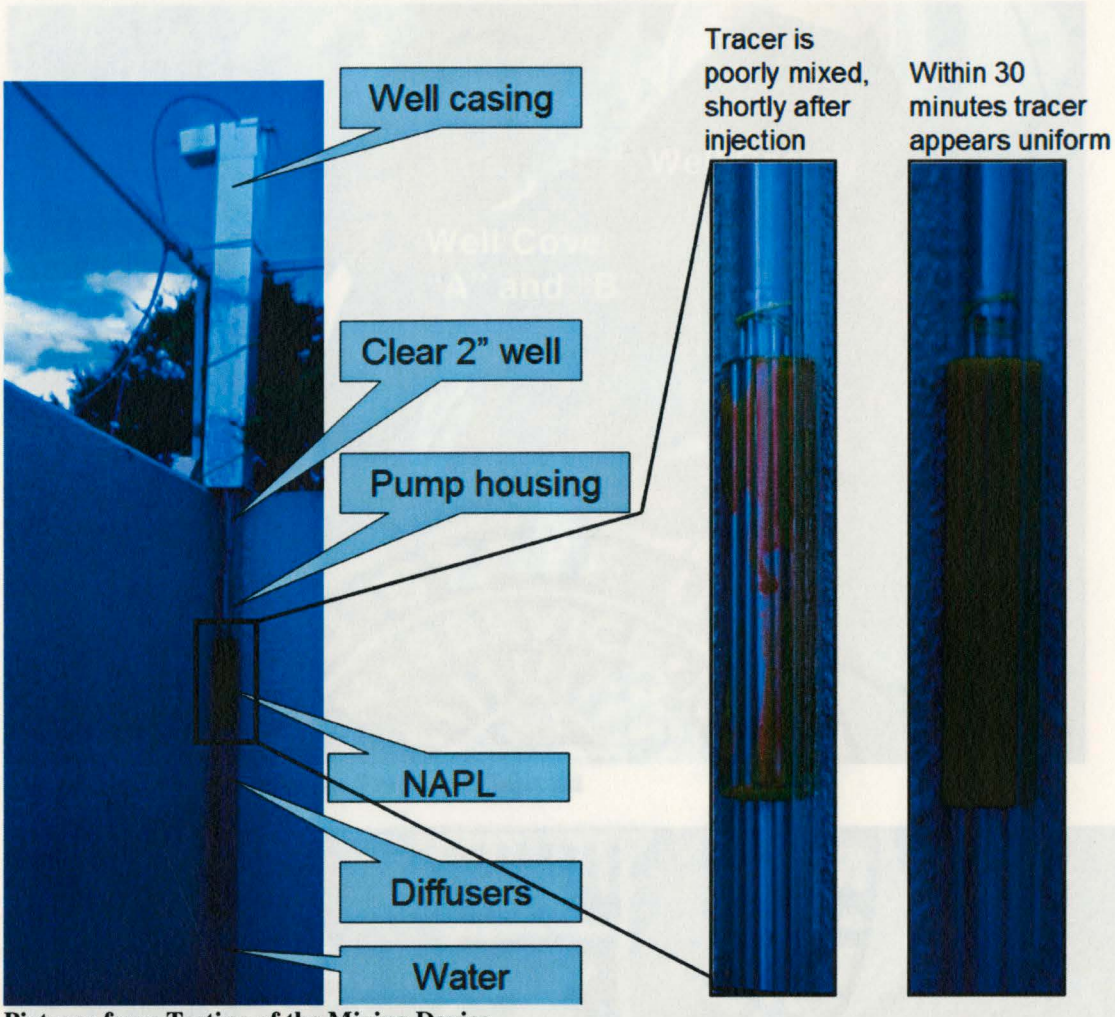

Pictures from Testing of the Mixing Device

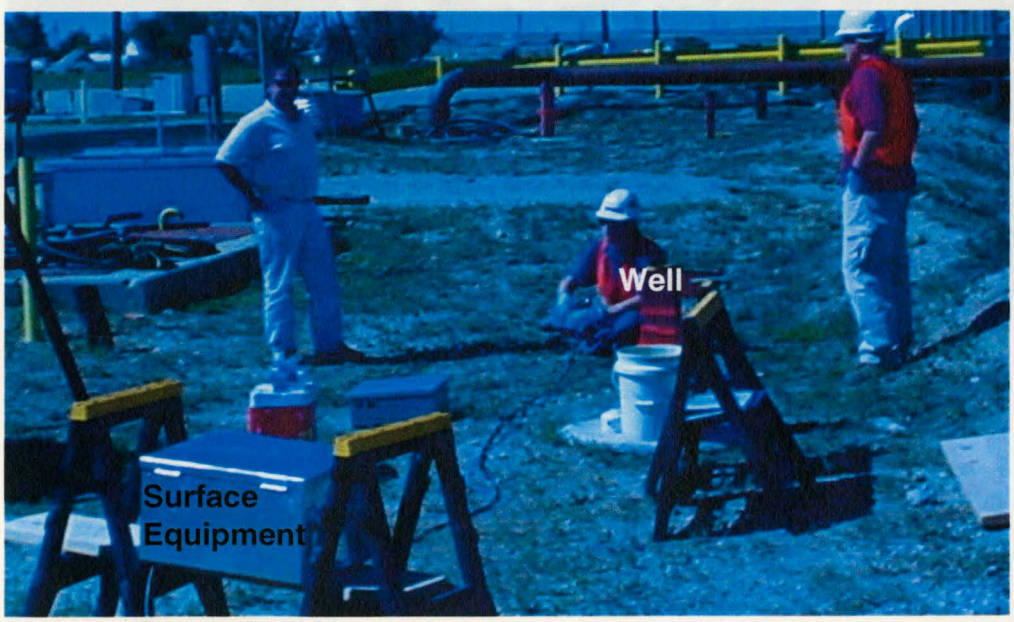

Equipment Setup in the Field